OPTICAL PROPERTIES OF RADIOGALAXIES IN THE VLA-VVDS SURVEY +zCOSMOS

Sandro Bardelli
INAF-OABo


VVDS survey
VVDS
zCOSMOS survey
COSMOS
Cosmic Evolution Survey
z-COSMOS
40’000 VLT redshifts
for COSMOS

The VVDS Collaboration

, D. Bottini[2], B. Garilli[2], V. Le Brun[1], **O. Le Fèvre P.I.**[1], D. Maccagni[2], R. Scaramella[4,13], M. Scodeggio[2], L. Tresse[1], G. Vettolani[4], A. Zanichelli[4]
, C. Adami[1], S. Arnouts[23,1], S. Bardelli[3], M. Bolzonella[3], A. Cappi[3], S. Charlot[8,10], P. Ciliegi[3], T. Contini[7], S. Foucaud[21], P. Franzetti[2], I. Gavignaud[12], L. Guzzo[9], O. Ilbert[20], A. Iovino[9], F. Lamareille[7], H.J. McCracken[10,11], B. Marano[6], C. Marinoni[18], A. Mazure[1], B. Meneux[22,24], R. Merighi[3], S. Paltani[15,16], R. Pellò[7], A. Pollo[14,17], L. Pozzetti[3], M. Radovich[5], D. Vergani[2], G. Zamorani[3], E. Zucca[3]
, U.Abbas[1], M. Bondi[4], A. Bongiorno[22], J. Brinchmann[19], O. Cucciati[9], S. de la Torre[1], L. de Ravel[1] Memeo[2], E. Pérez-Montero[7], Y. Mellier[10,11], P. Merluzzi[5], S. Temporin[9], and C.J. Walc

[1] 1) Laboratoire d'Astrophysique de Marseille, UMR 6110 CNRS-Université de Provence, BP8, F-13376 Marseille C
[2] 2) IASF-INAF, Via Bassini 15, I-20133, Milano, Italy
[3] 3) INAF-Osservatorio Astronomico di Bologna, Via Ranzani 1, I-40127, Bologna, Italy
[4] 4) IRA-INAF, Via Gobetti 101, I-40129, Bologna, Italy
[5] 5) INAF-Osservatorio Astronomico di Capodimonte, Via Moiariello 16, I-80131, Napoli, Italy
[6] 6) Università di Bologna, Dipartimento di Astronomia, Via Ranzani 1, I-40127, Bologna, Italy
[7] 7) Laboratoire d'Astrophysique de Toulouse-Tarbes, Université de Toulouse, CNRS, 14 av. E. Belin, F-31400 France
[8] 8) Max Planck Institut für Astrophysik, D-85741, Garching, Germany
[9] 9) INAF-Osservatorio Astronomico di Brera, Via Brera 28, I-20021, Milan, Italy
[10] 10) Institut d'Astrophysique de Paris, UMR 7095, 98 bis Bvd Arago, F-75014, Paris, France
[11] 11) Observatoire de Paris, LERMA, 61 Avenue de l'Observatoire, F-75014, Paris, France
[12] 12) Astrophysical Institute Potsdam, An der Sternwarte 16, D-14482, Potsdam, Germany
[13] 13) INAF-Osservatorio Astronomico di Roma, Via di Frascati 33, I-00040, Monte Porzio Catone, Italy
[14] 14) The Andrzej Soltan Institute for Nuclear Studies, ul. Hoza 69, 00-681 Warszawa, Poland
[15] 15) Integral Science Data Centre, ch. d'Écogia 16, CH-1290, Versoix, Switzerland
[16] 16) Geneva Observatory, ch. des Maillettes 51, CH-1290, Sauverny, Switzerland
[17] 17) Astronomical Observatory of the Jagiellonian University, ul Orla 171, PL-30-244, Kraków, Poland
[18] 18) Centre de Physique Théorique, UMR 6207 CNRS-Université de Provence, F-13288, Marseille, France
[19] 19) Centro de Astrofísica da Universidade do Porto, Rua das Estrelas, P-4150-762, Porto, Portugal
[20] 20) Institute for Astronomy, 2680 Woodlawn Dr., University of Hawaii, Honolulu, Hawaii, 96822, USA
[21] 21) School of Physics & Astronomy, University of Nottingham, University Park, Nottingham, NG72RD, UK

VVDS

~50 people
24 Institutes

Deep wid
with CFH

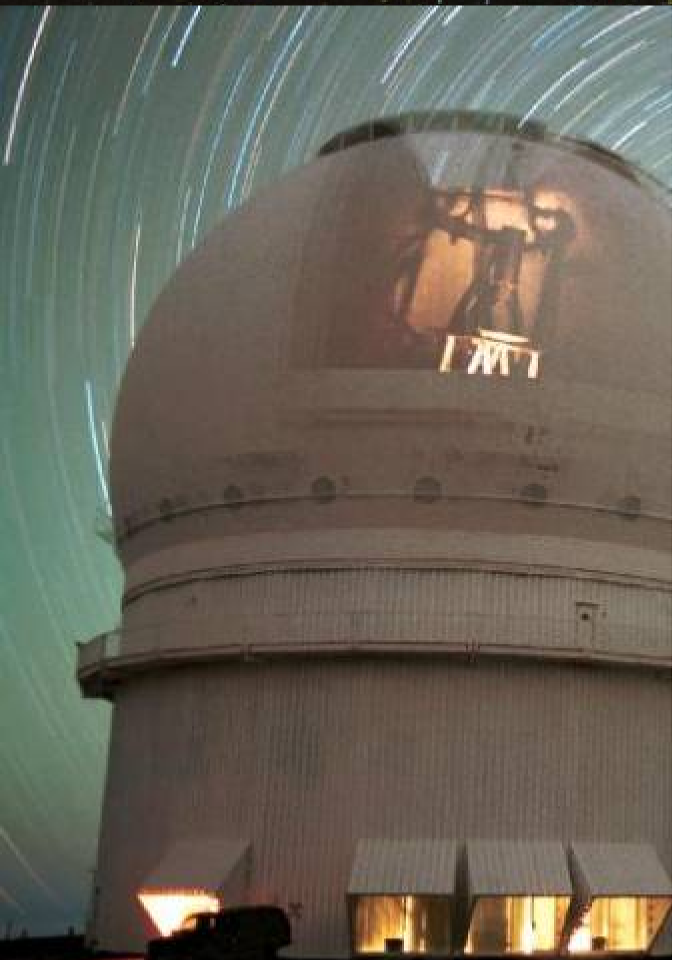

CFHT telescop

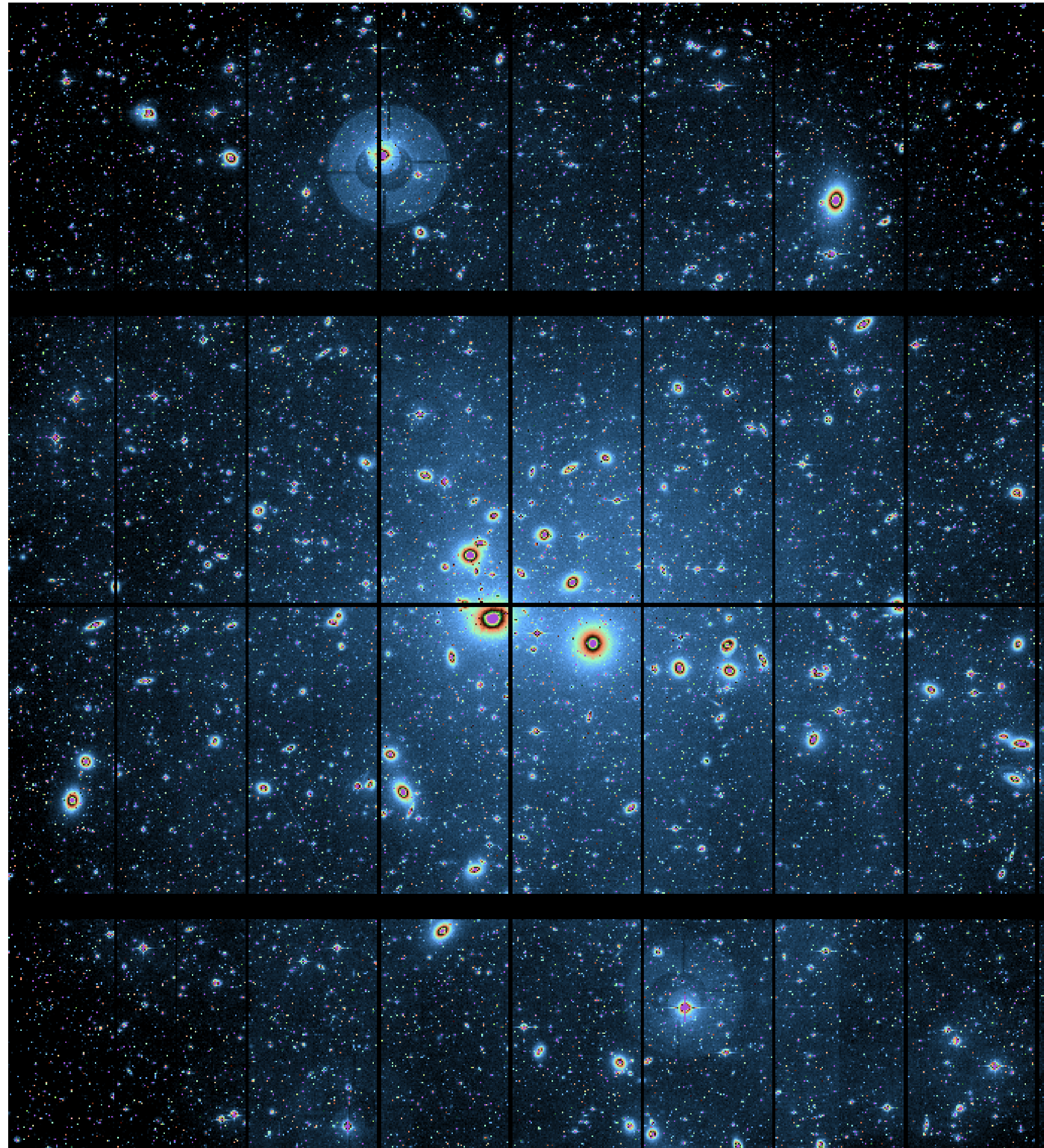


One square degree
BVRI -12 k camera
u* g’ r’ I’ z’ MEGACAM Legacy Survey
J K NTT data
K UKIDSS

VIMOS -VLT-UT3

A highly efficient high redshift machine in operations since 2002 on the VLT

Multi-slit mode

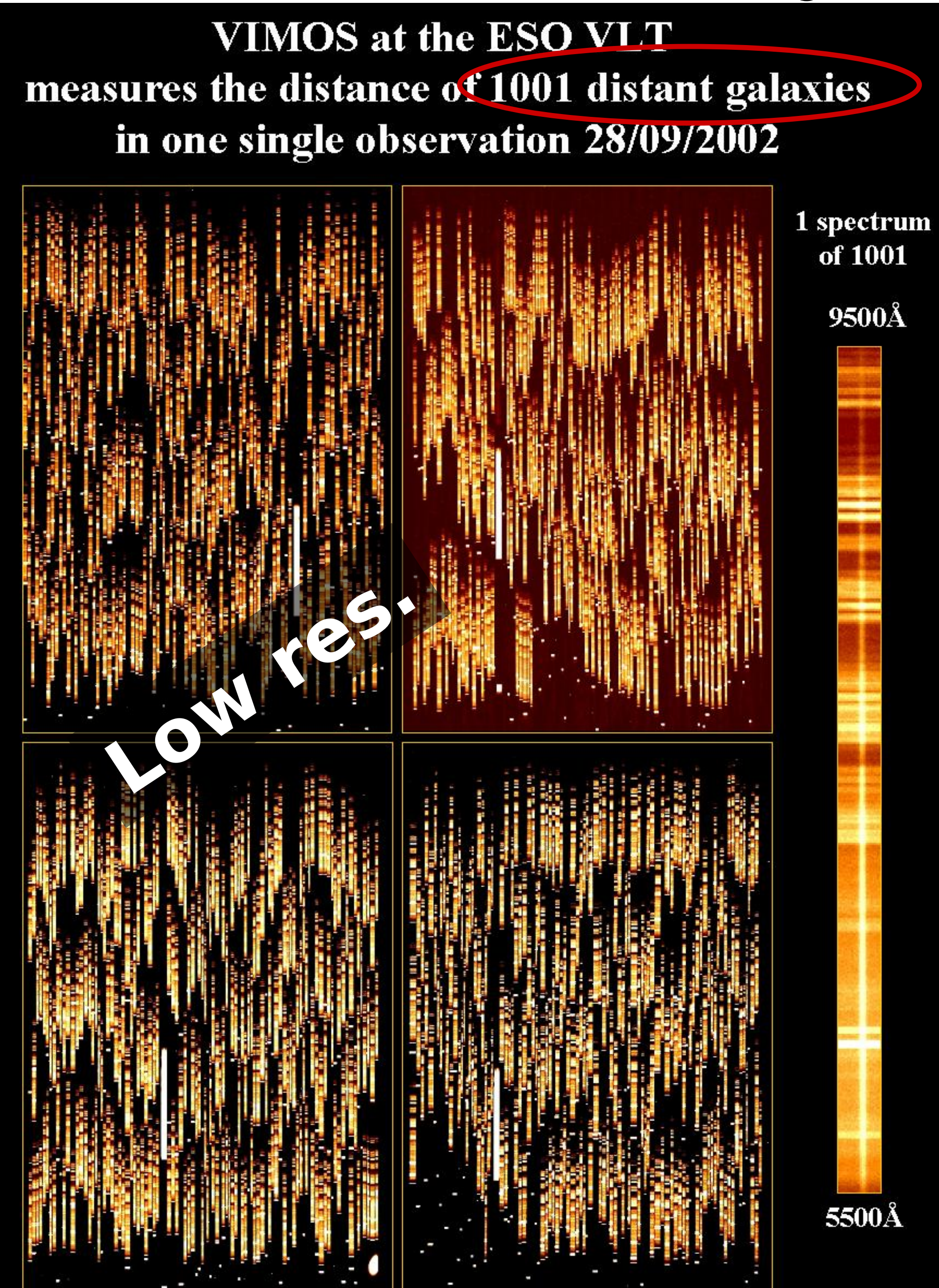

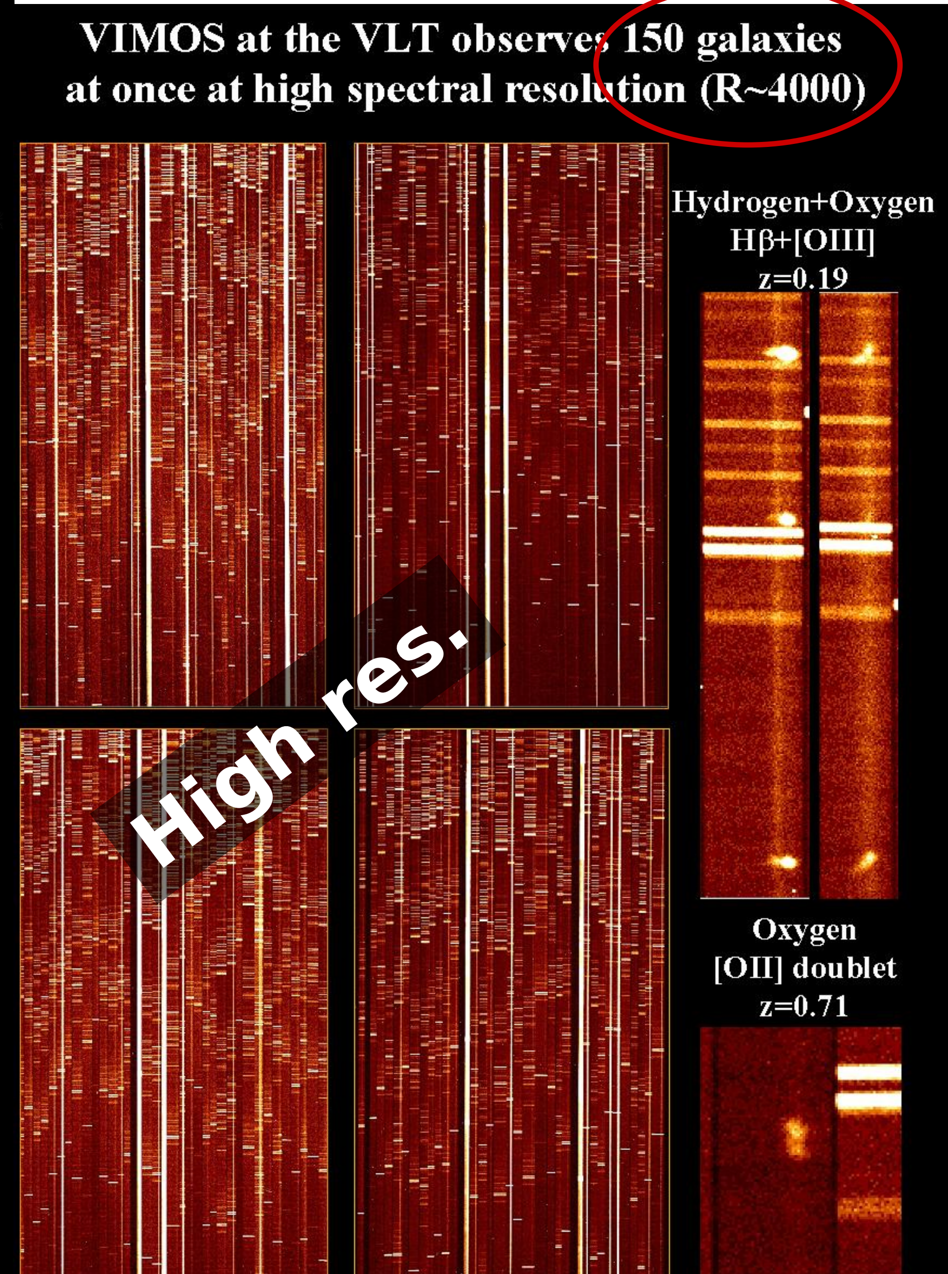

VIMOS VLT Deep Survey

Field	I_{AB}<22.5 WIDE 16+ deg^2	I_{AB}<24 DEEP 1deg^2	I_{AB}<24.75 Ultra-Deep 600 arcmin^2
0226-04		~14000 *9000 Public*	*1000 (on-going)*
1000+03	~5000		
1400+05	~11000		
2217+00	~15000 (~10000 on-going)		
CDFS		~1600 *Public*	
Total	~35000	~15500	~1000
GOAL	***100000***	***20000***	***1000***

Deep Field
I<24

- R~230, 5500-9300Å
- **~50000 spectra today**
- Goal >20000 Deep and 100000 Wide

VVDS-Deep Field $I_{AB} \leq 24$

Magnitude selection only: complete census of the population, minimize apriori selection bias

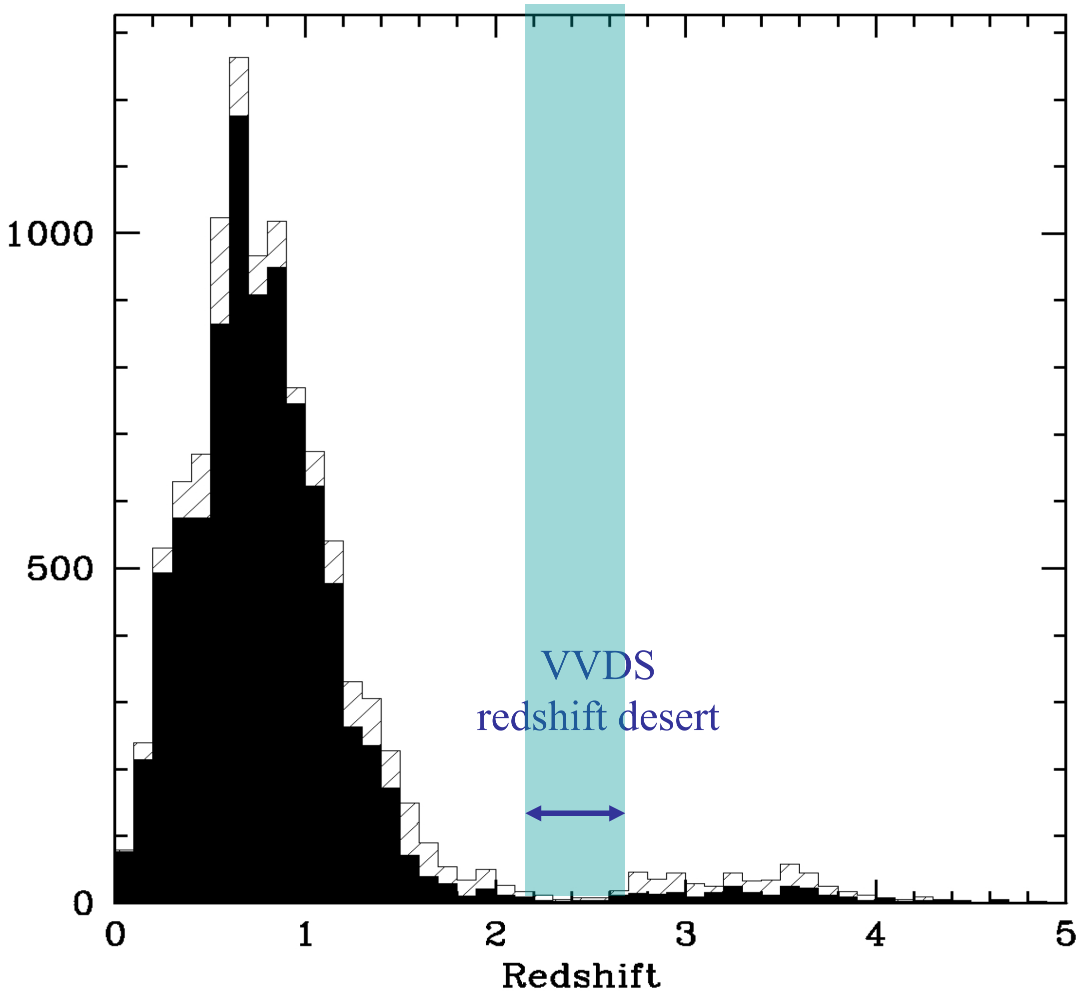

$I_{AB} \leq 24$

$<z>=0.75$

High redshift tail to z~4-5

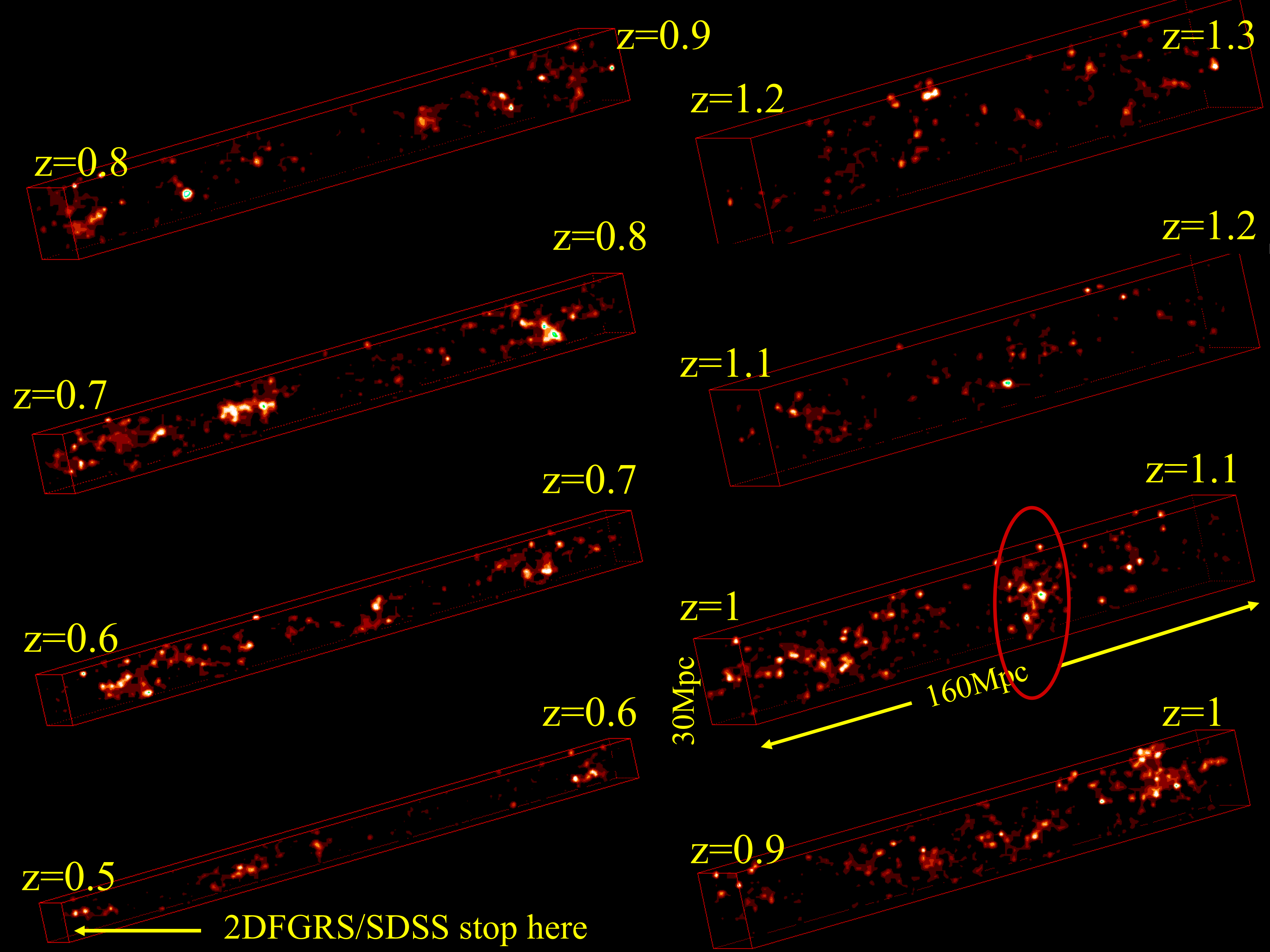

z=0.9
z=0.8
z=0.8
z=0.7
z=0.7
z=0.6
z=0.6
z=0.5
2DFGRS/SDSS stop here
z=1.3
z=1.2
z=1.2
z=1.1
z=1.1
z=1
30Mpc
160Mpc
z=1
z=0.9

Spectrophotometric Classification

We used CWW templates
to define 4 classes.
Assuming the redshift,
The class is given by the
template which gives the best
to the mutli-band photometry

TYPE	CWW	$M_B - M_I$ (AB)
1	Ell	1.3 - $+\infty$
2	Sbc	0.95 - 1.3
3	Scd	0.68 - 0.95
4	Im+SB	$-\infty$ - 0.68

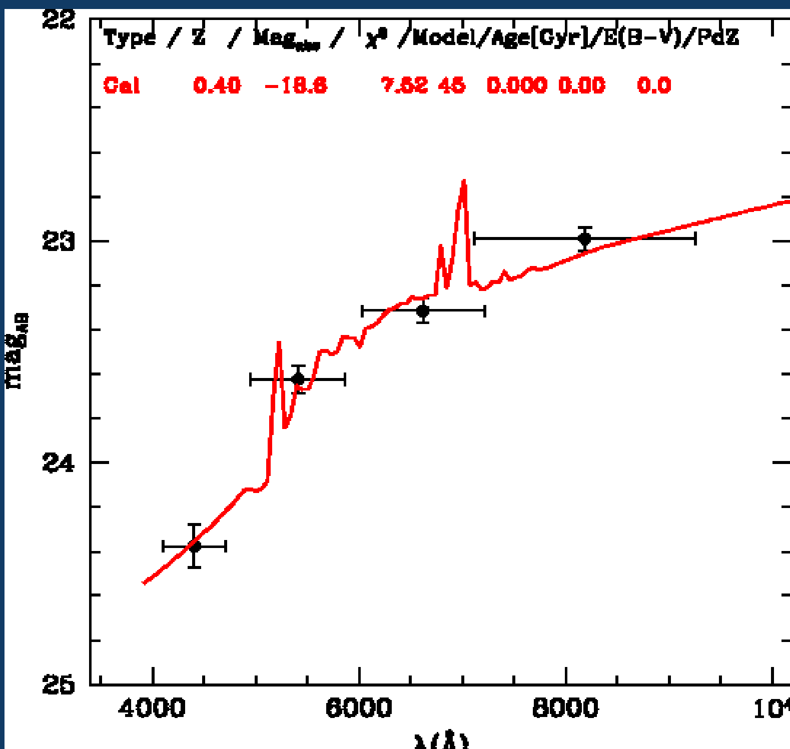

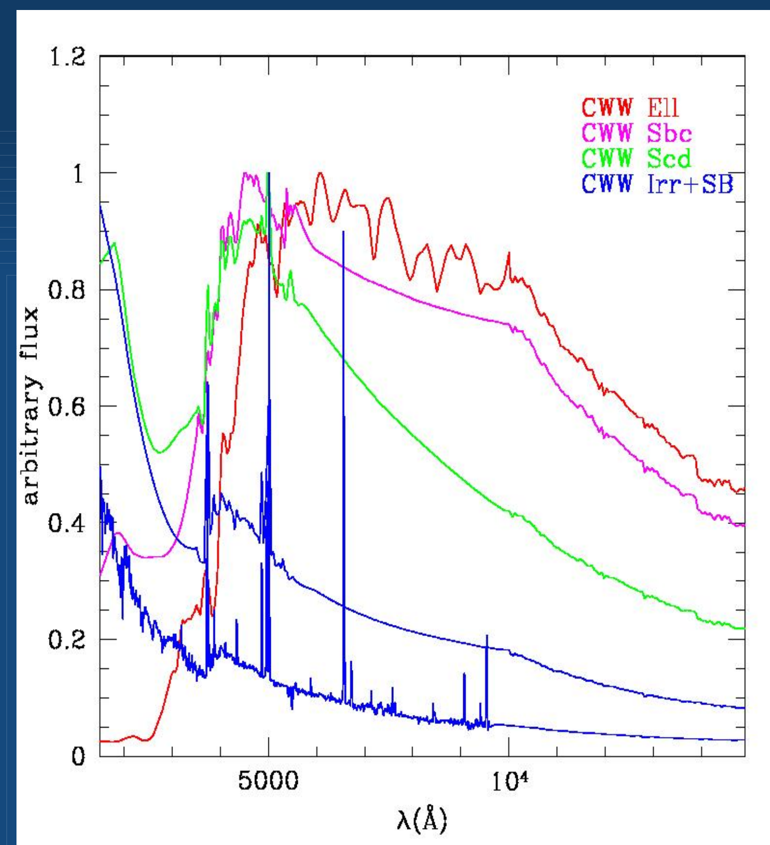

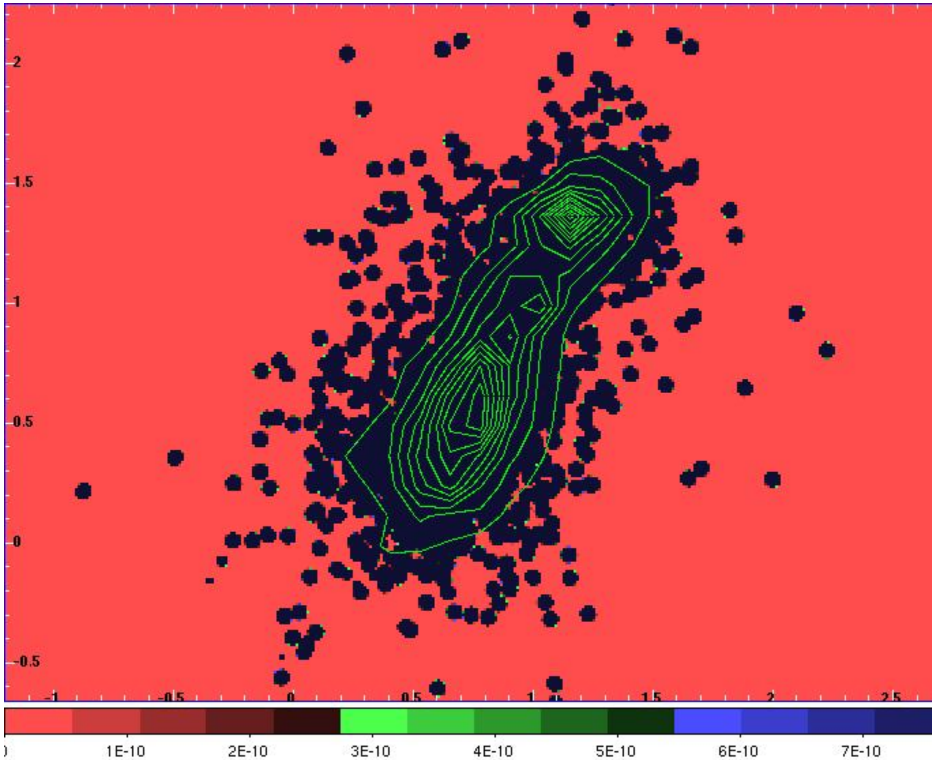

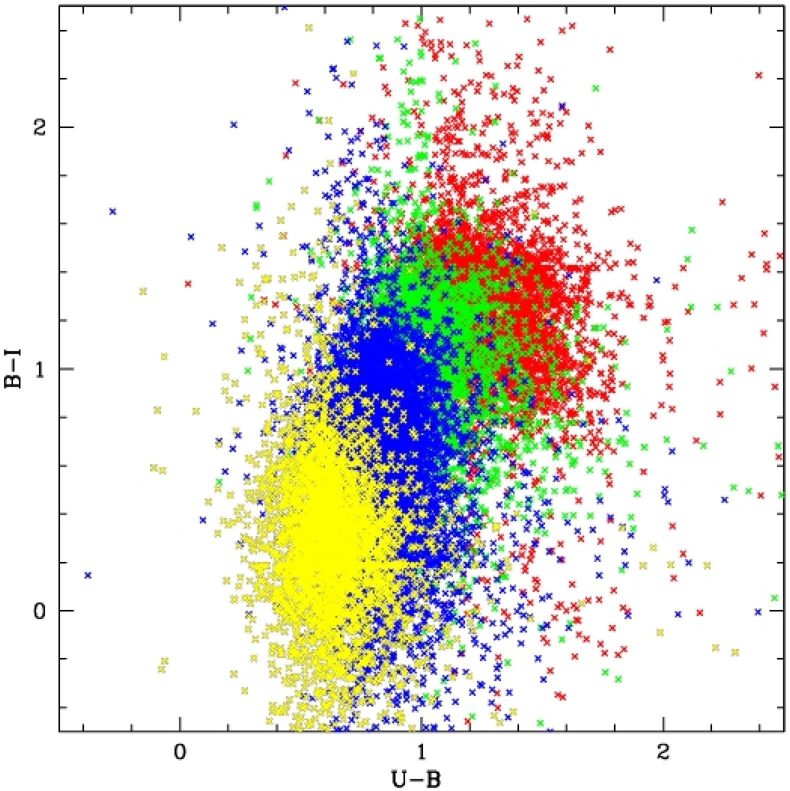

Good correlation between bimodality and types

Red:type 1(early)
Green:type 2 (Sbc)
Blue :type 3(Scd)
Yellow:type 4 (Irr)

0.0 -.0.2

0.6 -0.8

0.8 -1.0

Redshift ranges

Type 1 galaxies (~ellipticals)

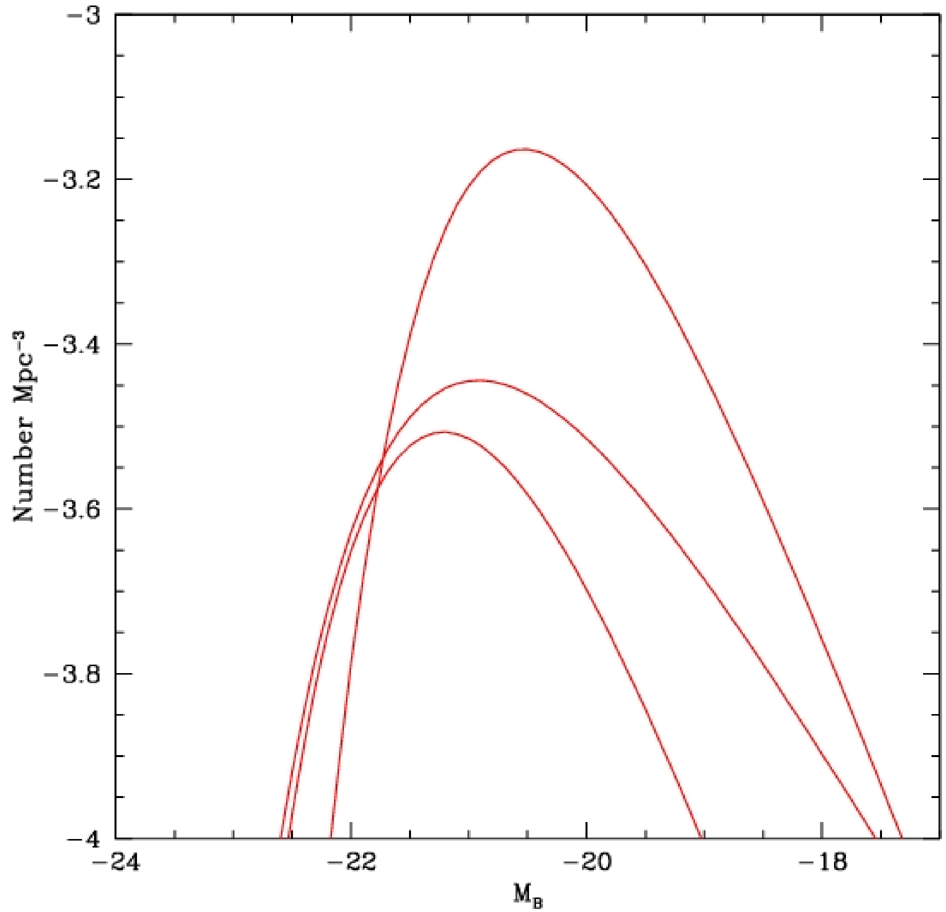

Little evolution , 0.2 mag of brightening, decreases in number of objects

Zucca, Ilbert, Bardelli et al. (2006)

0.2 -.0.4 ←

0.4 -0.6 ←

0.6 -.0.8 ←

0.8 -1.0 ←

1.0 -1.2 ←

redshift ranges

Type 3+4 galaxies (late type spirals)

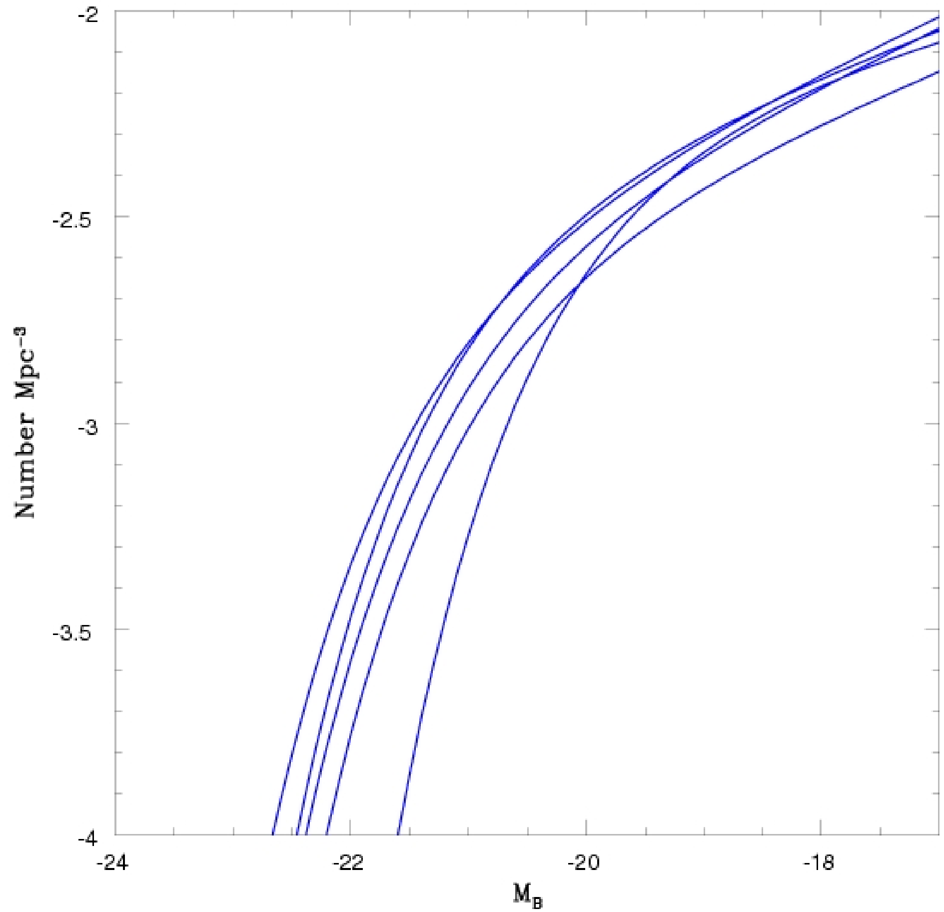

Steepening of the luminosity function and one magnitude of brightening

Zucca, Ilbert, Bardelli et al. (2006)

VLA-VVDS Deep Field

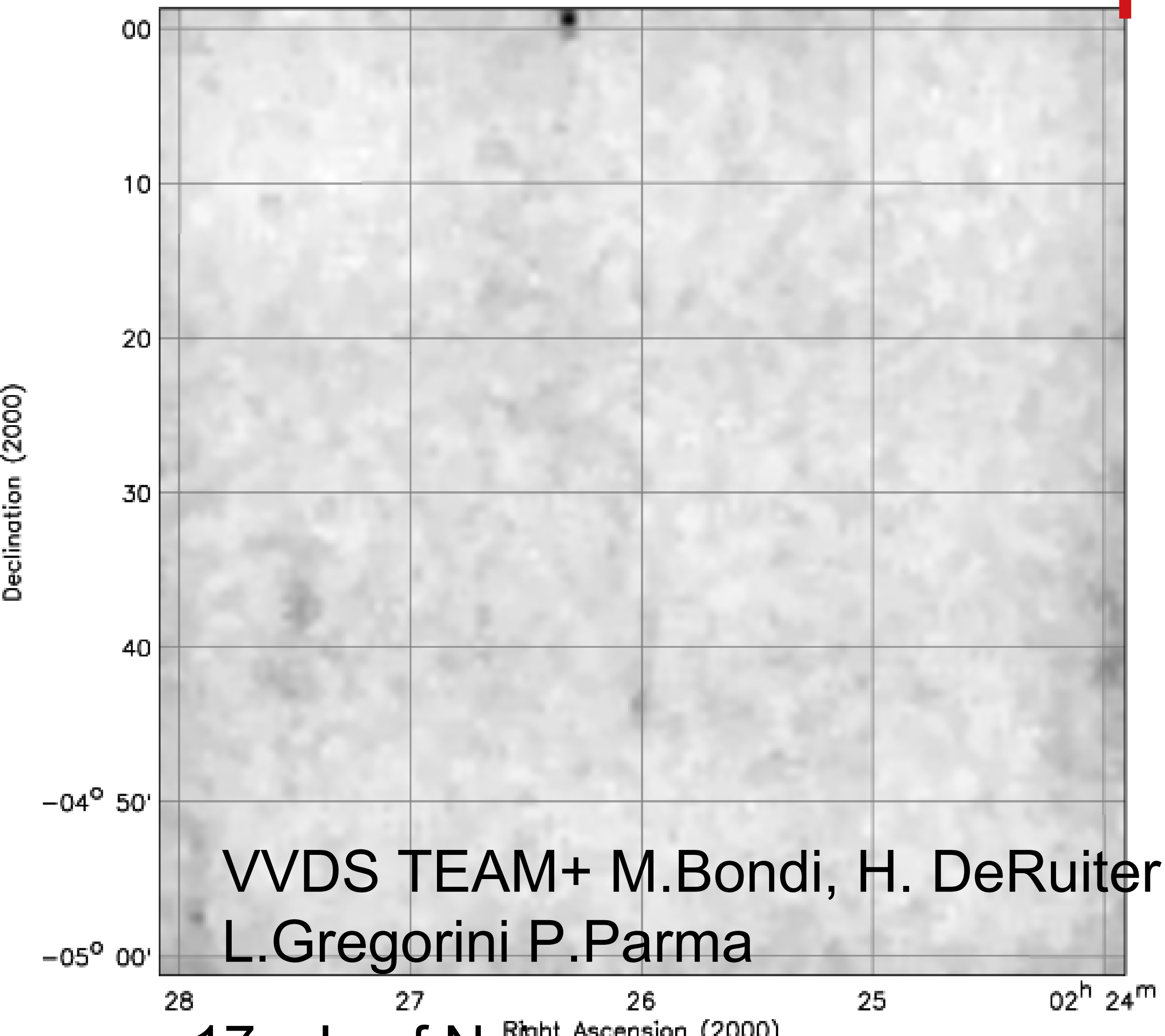

1.4 GHz
1 Sq Degree

VLA
B-Configuration
Primary beam of 31 arcmin FWHM

9 pointings separated by 23 Arcmin
6 hours of exposure time

VVDS TEAM+ M.Bondi, H. DeRuiter
L.Gregorini P.Parma

17 µJy of Noise

Bondi et al. (2003) Ciliegi et al. (2005)

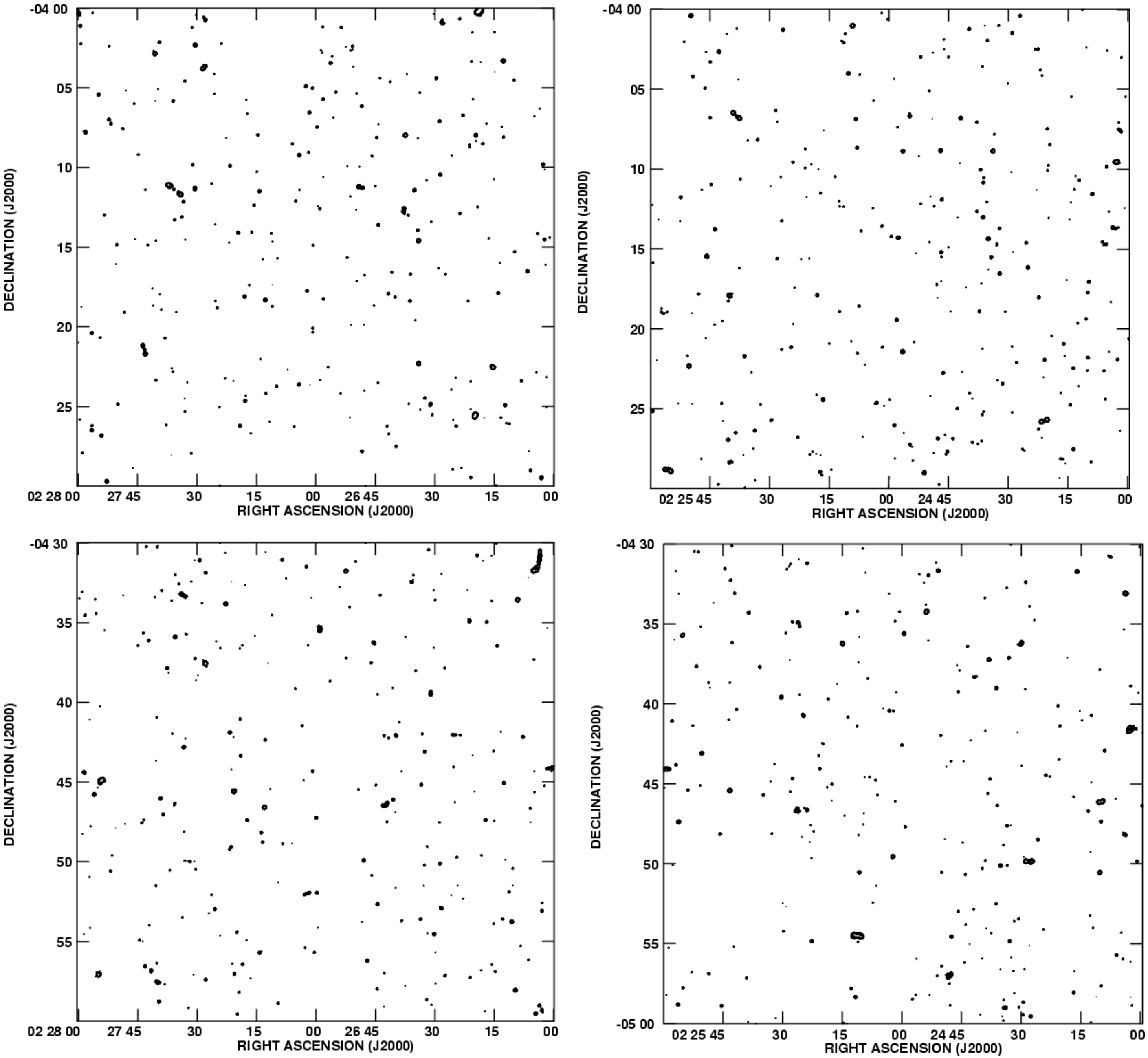

1054
Sources
To
~80 μJy
(5 σ)

718
with
optical
counterpart

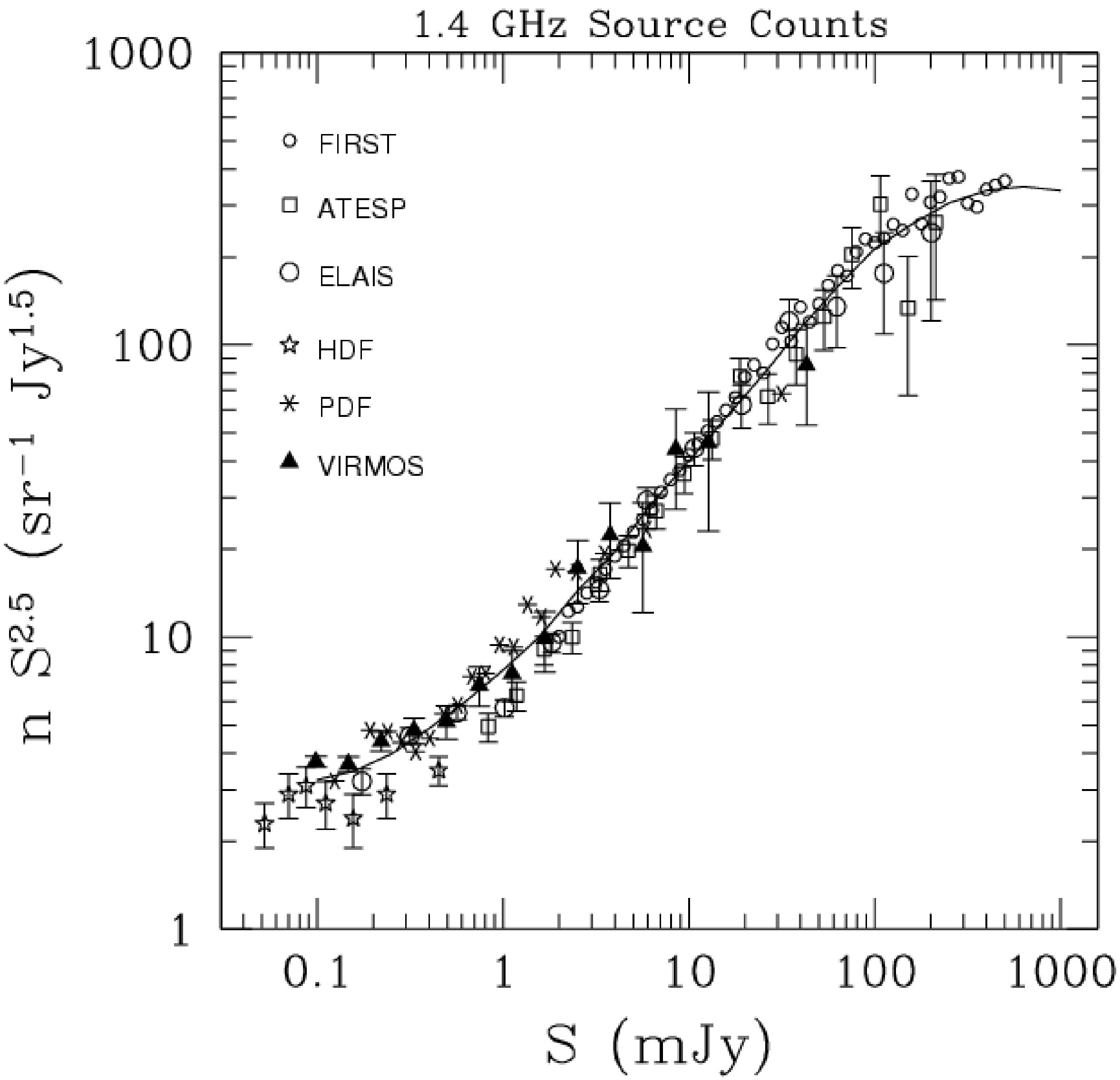

Bondi et al. (2003)

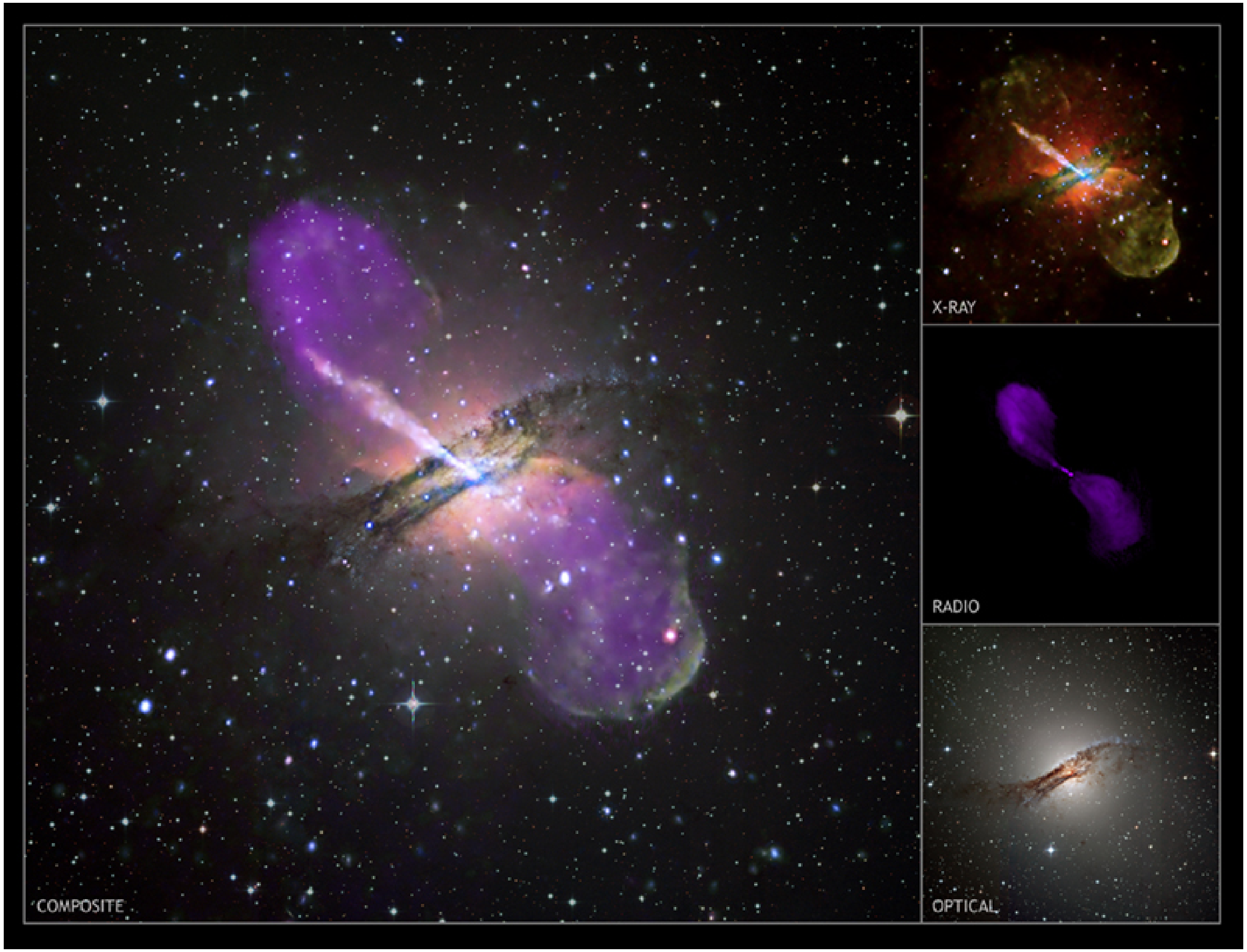

AGN emission associated to early type galaxies

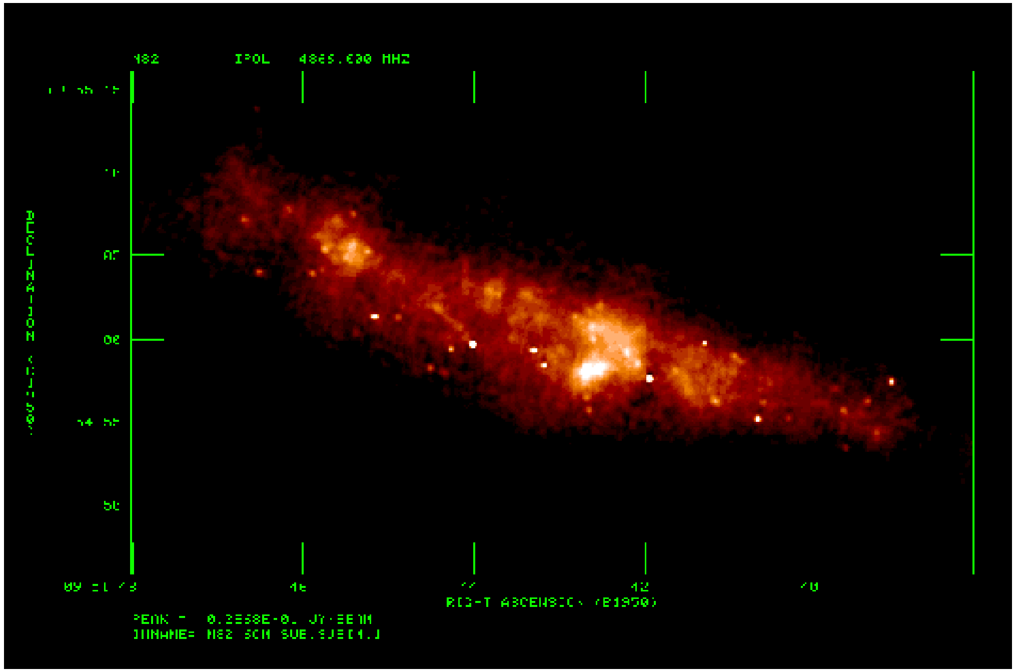

A 6cm MERLIN/VLA image of nearby starburst galaxy M82.
The discrete sources are mostly supernova remnants with ages less than 1000 years and compact HIIregions.
The non-thermal extended background is mainly due to relativistic electrons generated by older remnants M>8 M0 time ~10**8 yrs

Radio emission associated to late type galaxies

Aim of this work

study the properties of radio galaxies
knowing a priori optical behaviours

because.....

Evolution in Radio band is due to

changes of the probability for an optical galaxy to be radio emitter

A) changes of the radio-optical ratios

B) changes in the global number of optical galaxies

Recepies

0) All properties of radiogalaxies have to be compared with those of all optical galaxies (within each morphological Class)
i.e. define a Control sample

1)Use Rest Frame Quantities

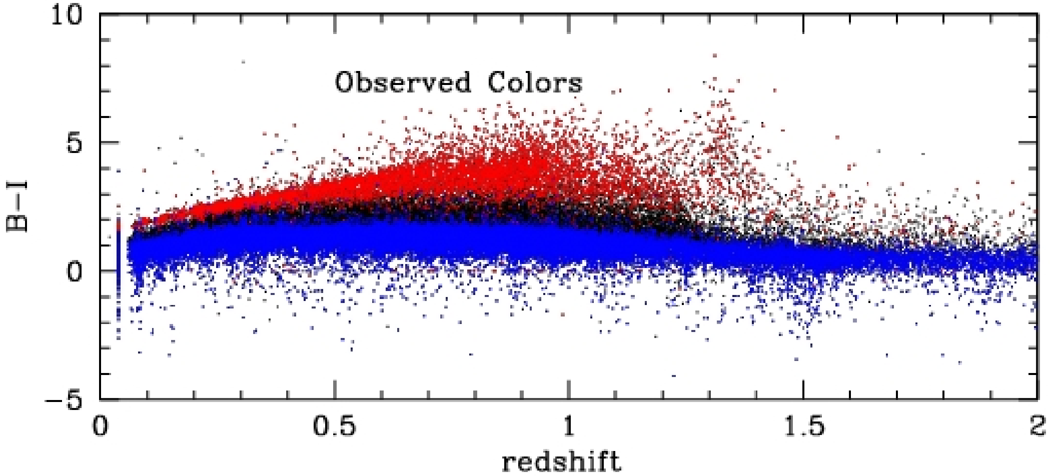

B-I at z=0
means
R-J at z=0.5
Z-H at z=1.0

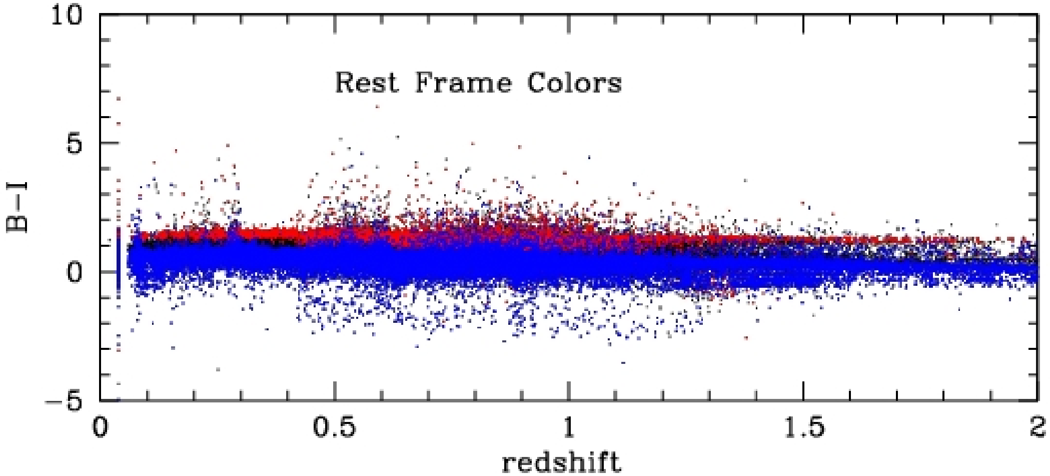

What is the meaning of the radio-optical ratio?

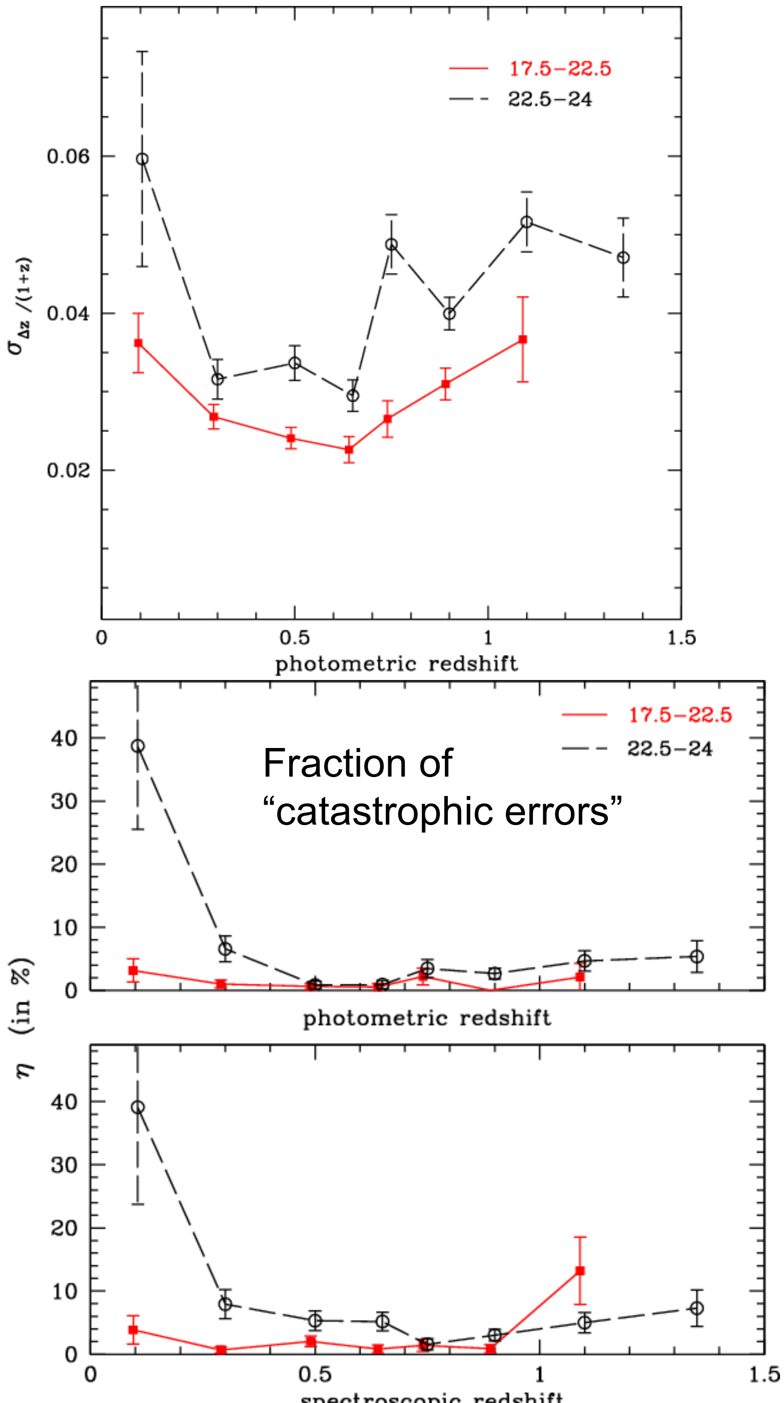

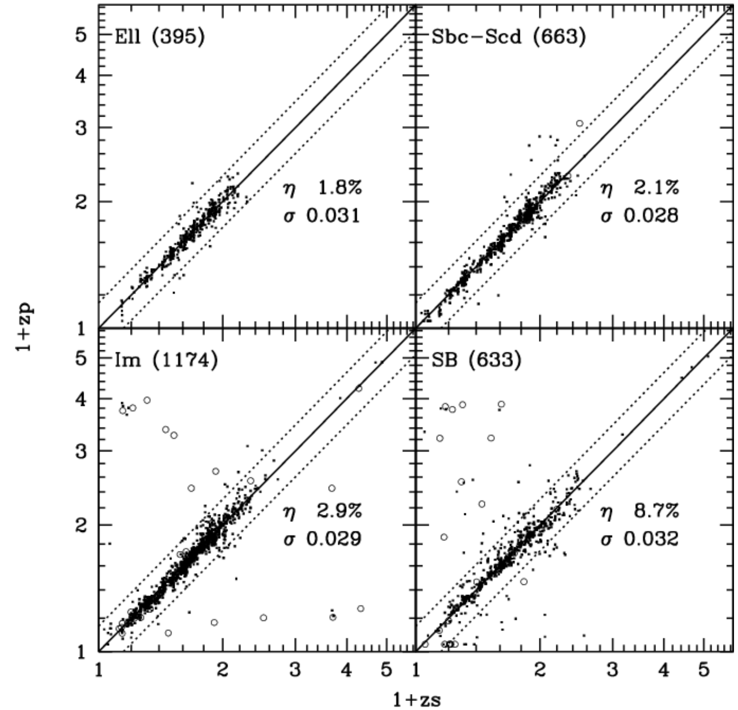

Ilbert et al. (2006)

2) Use accurate photometric redshifts

3) Take into account different depths

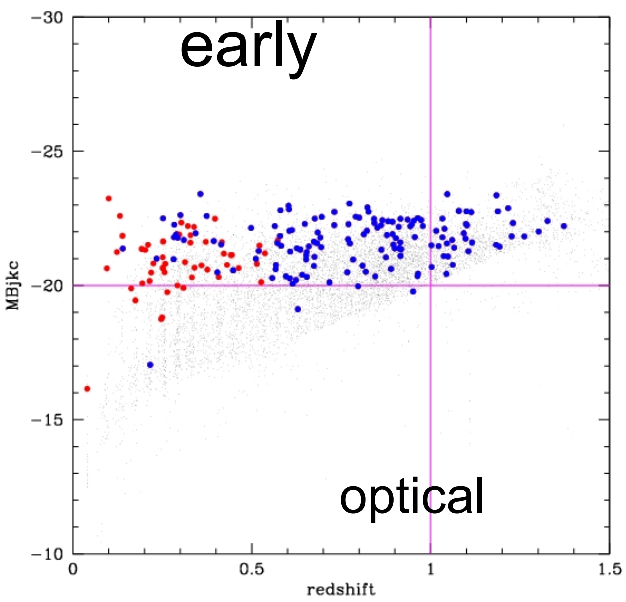

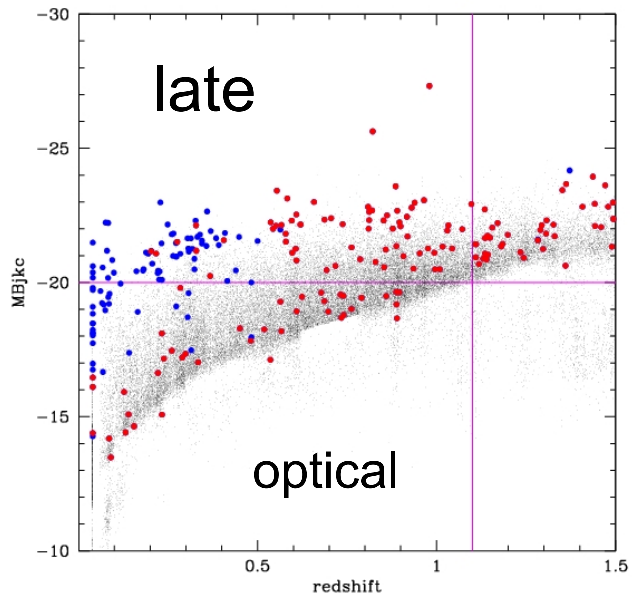

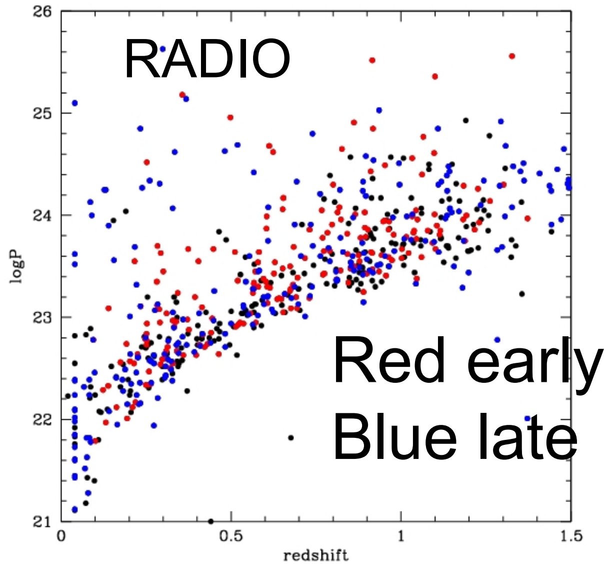

Red log P>23
Blue log P<23

Cut at
M_B<-20
z<1.0 (early) 1.1 (late)

The used sample

+4)

COMPLETE

(optical)

Type 1 (ellip

Type 2

Type 3+4 (la

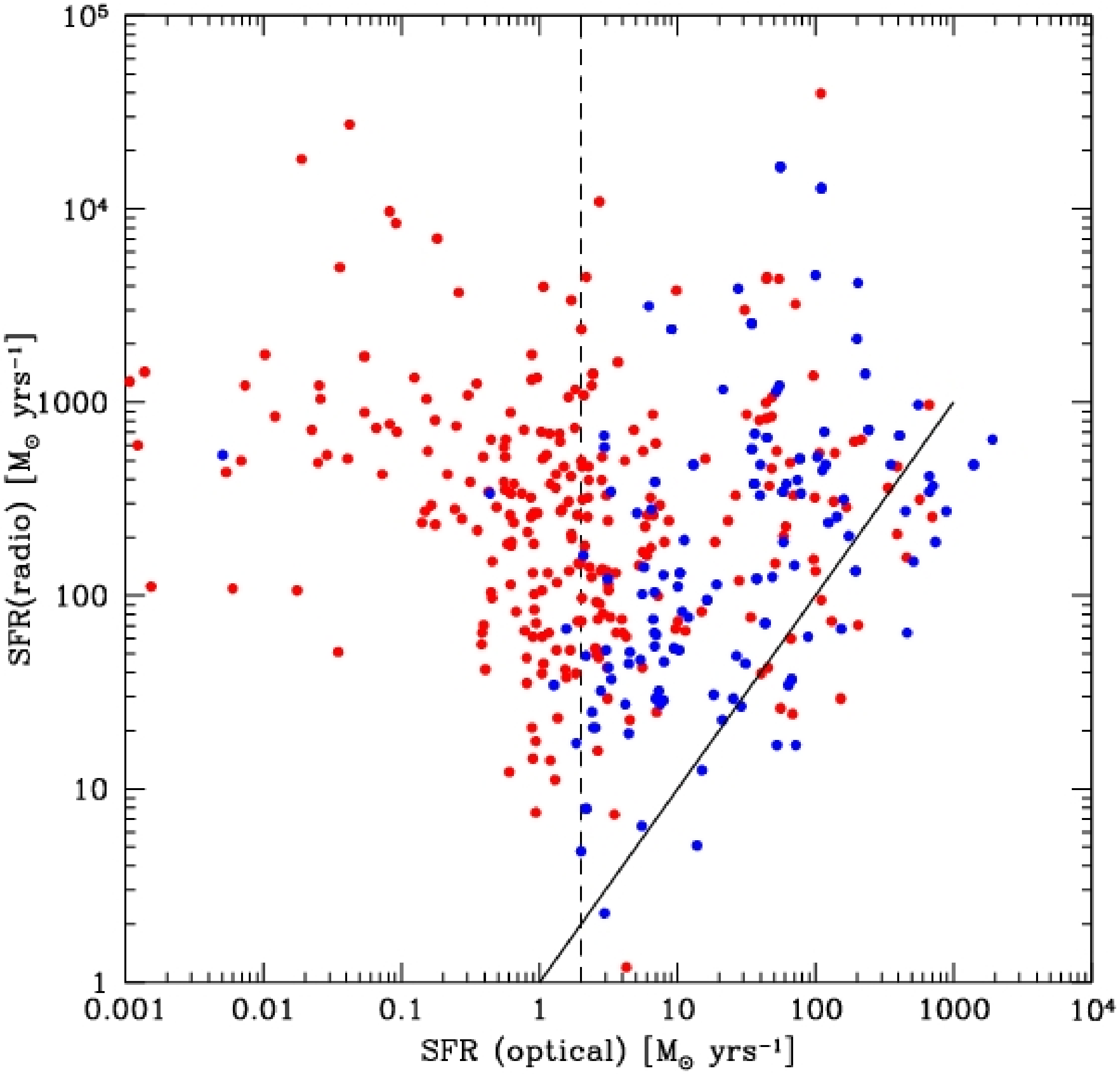

Effect of our cuts

Lost objects:
133 M_B>-20
154 M_B<-20 but z>1.1

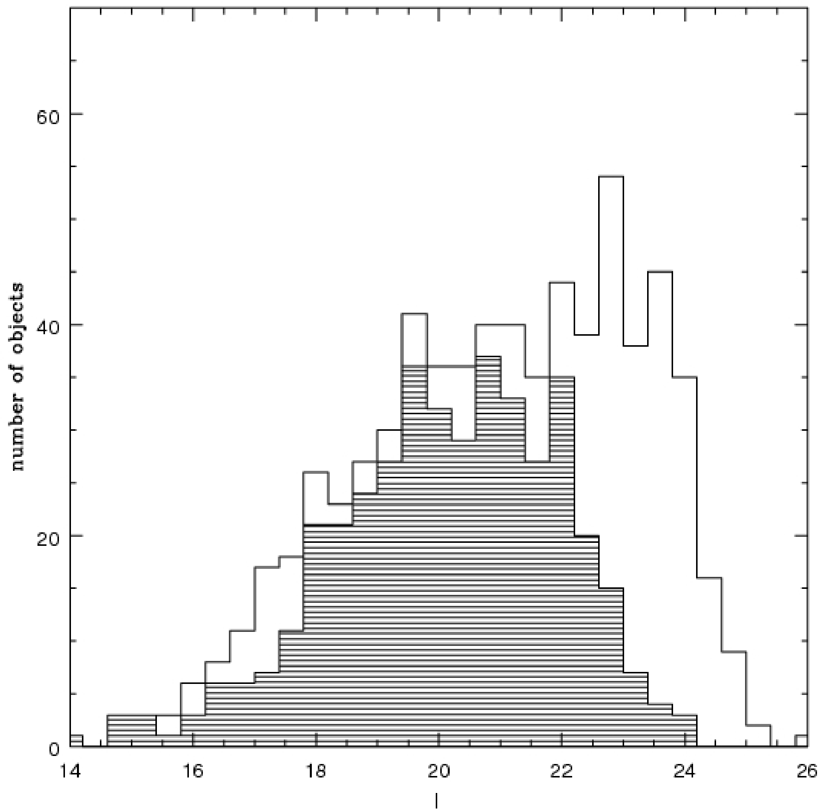

No trend of morphological mix with 1.4 GHz flux

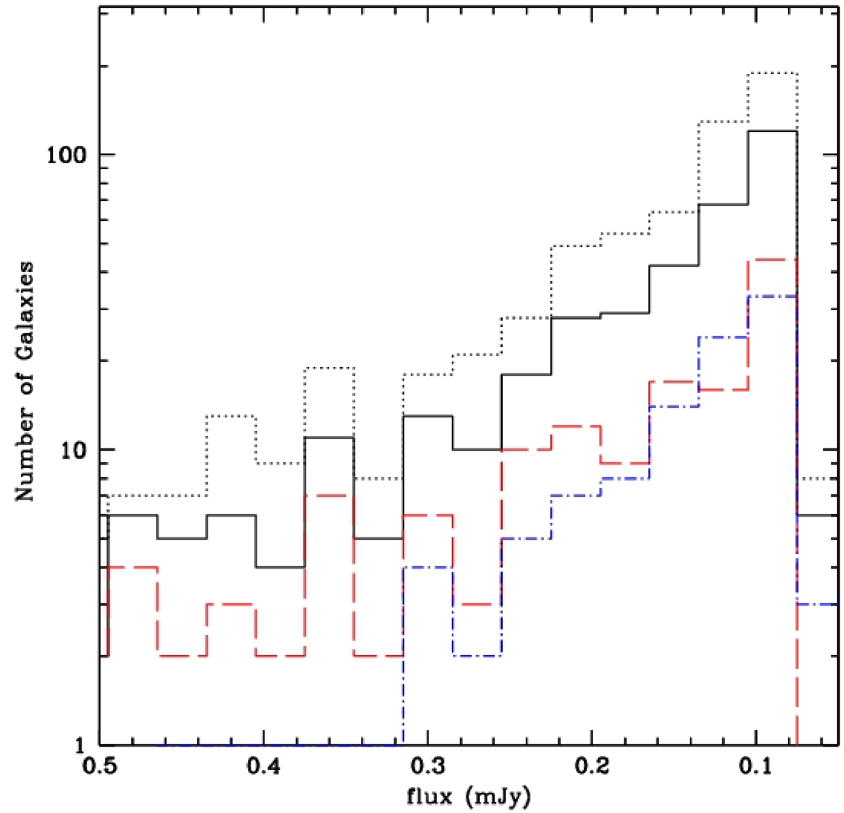

Redshift Distribution

Red: Control Sample

Black: radio galaxies

Type 1
(early type)

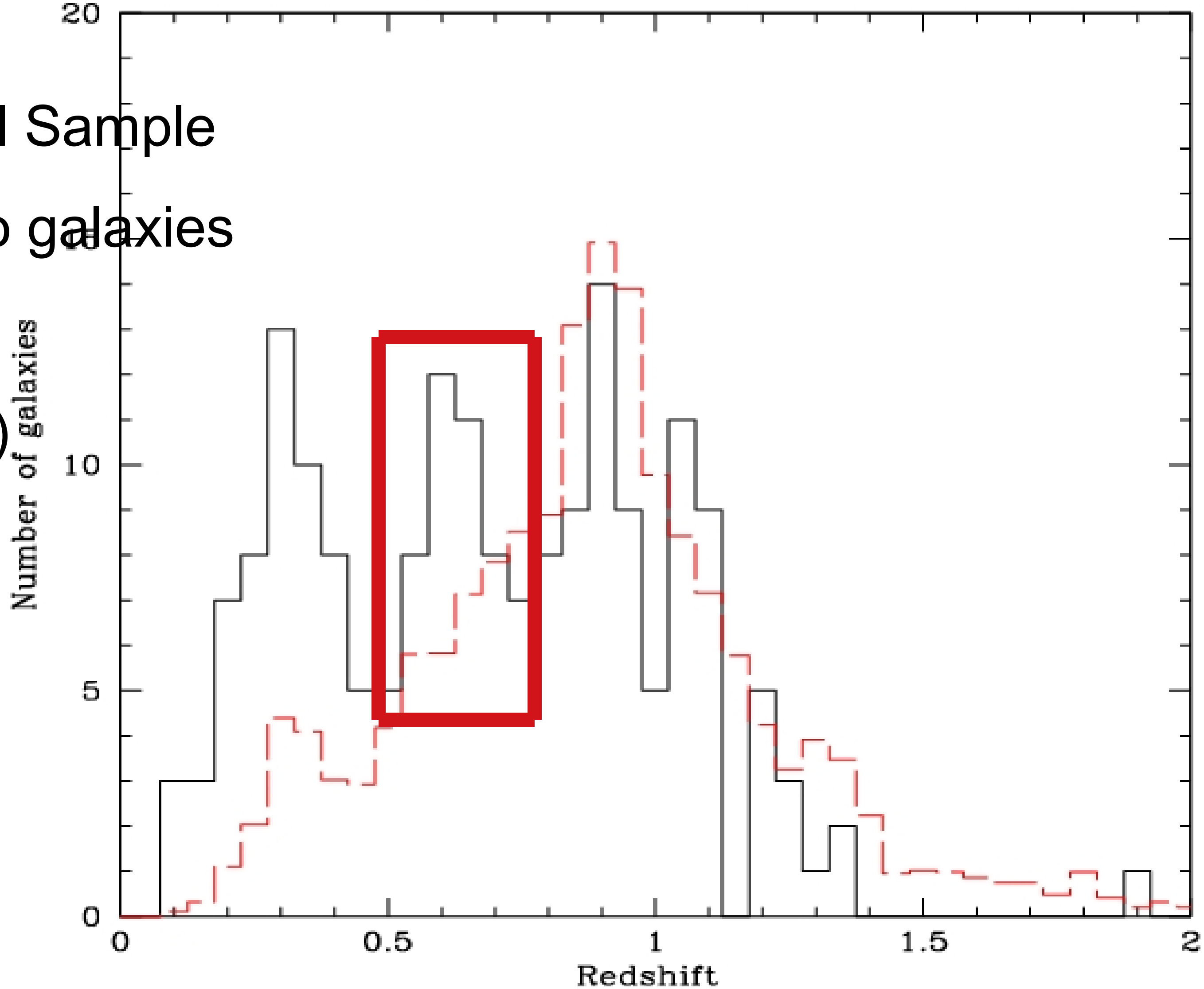

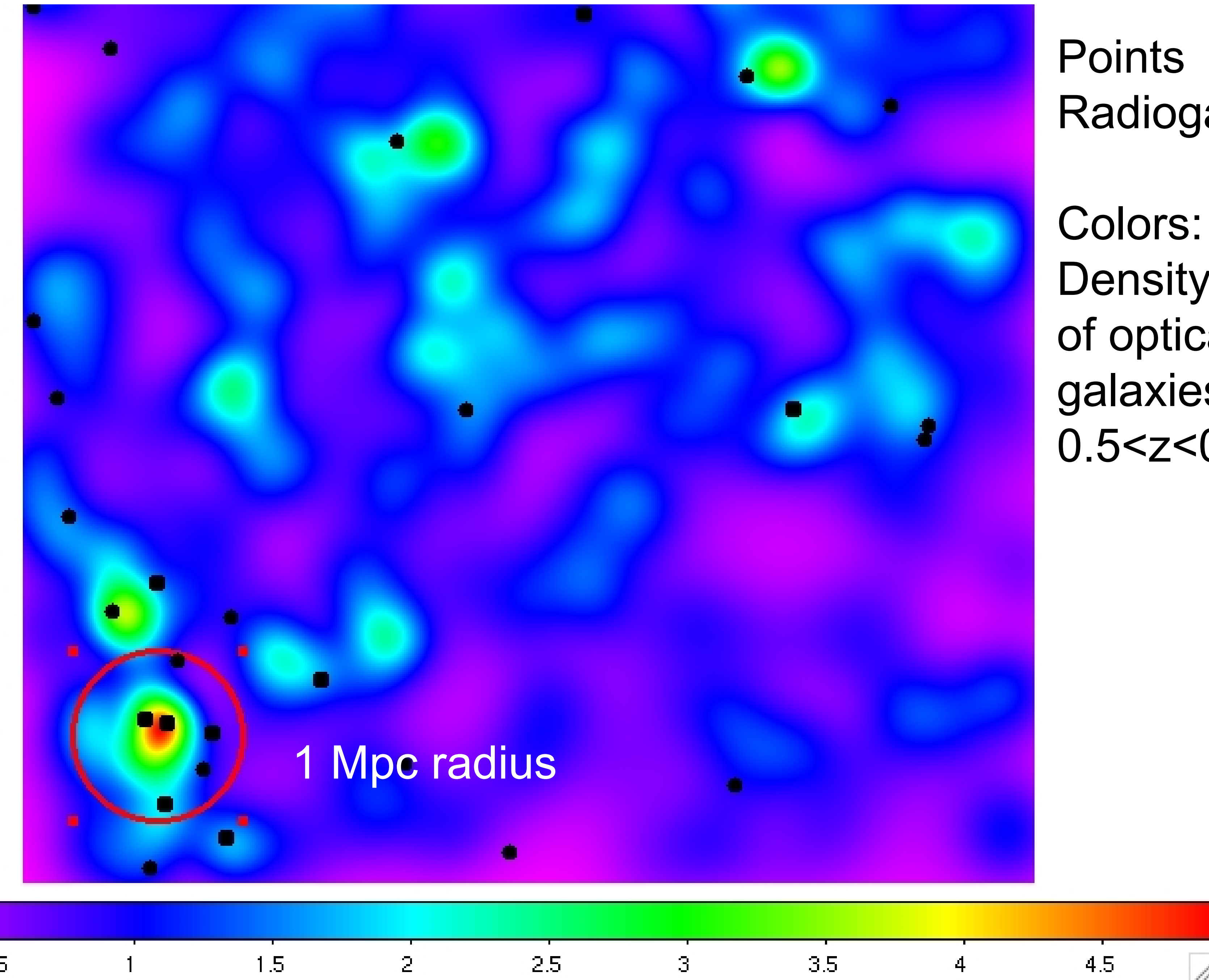

Points
Radiogalaxies

Colors:
Density map of optical galaxies 0.5<z<0.65

COLORS DISTRIBUTION

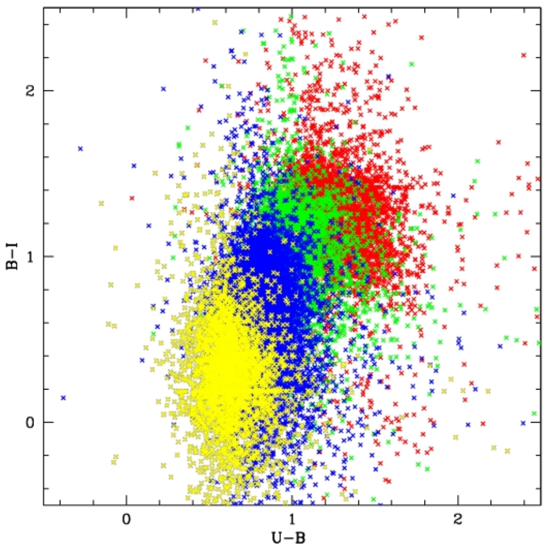

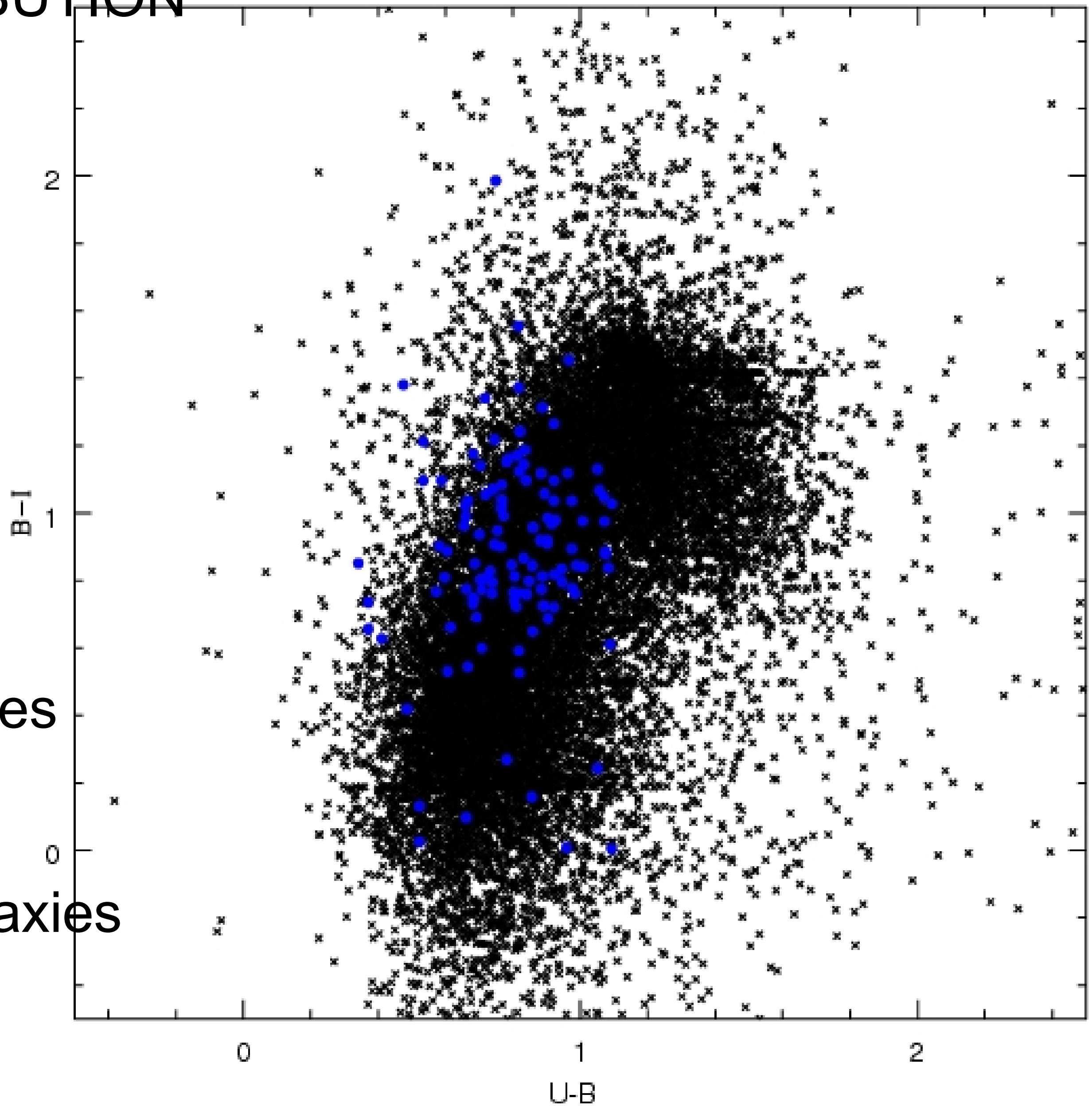

Red points:
Type 1 radiogalaxies

Blue points:
Type 3+4 radiogalaxies

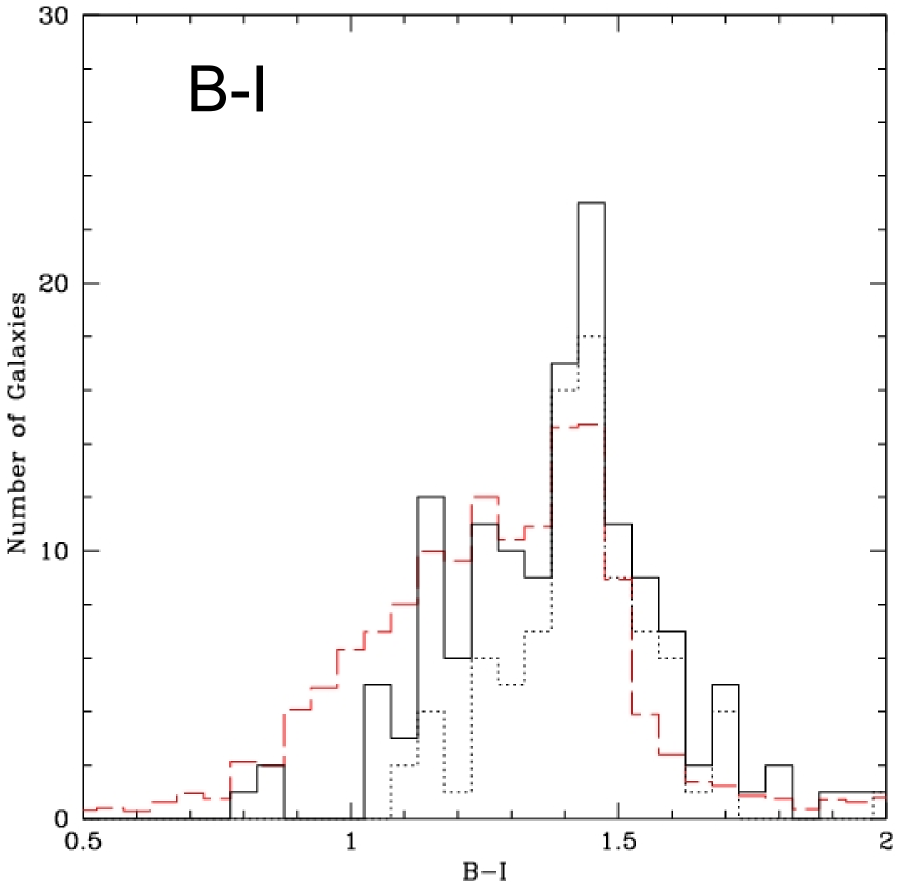

B-I peak most evident for radio faint galaxies (log<23)

Type 1

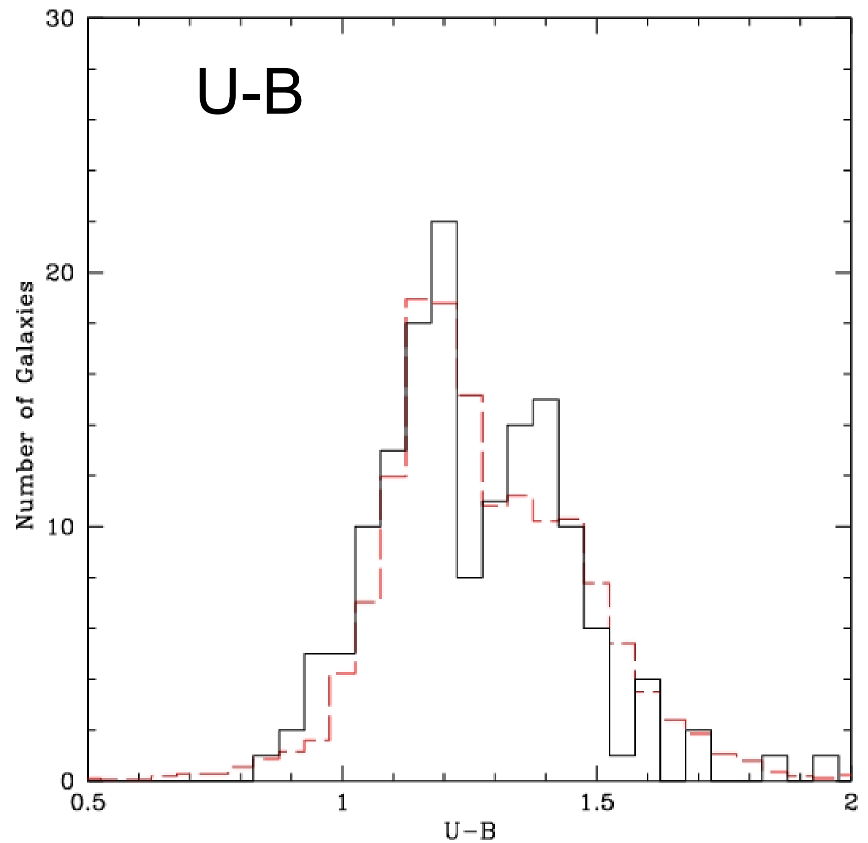

Radio bright (logP>23) show no difference with control sample

Type 3+4

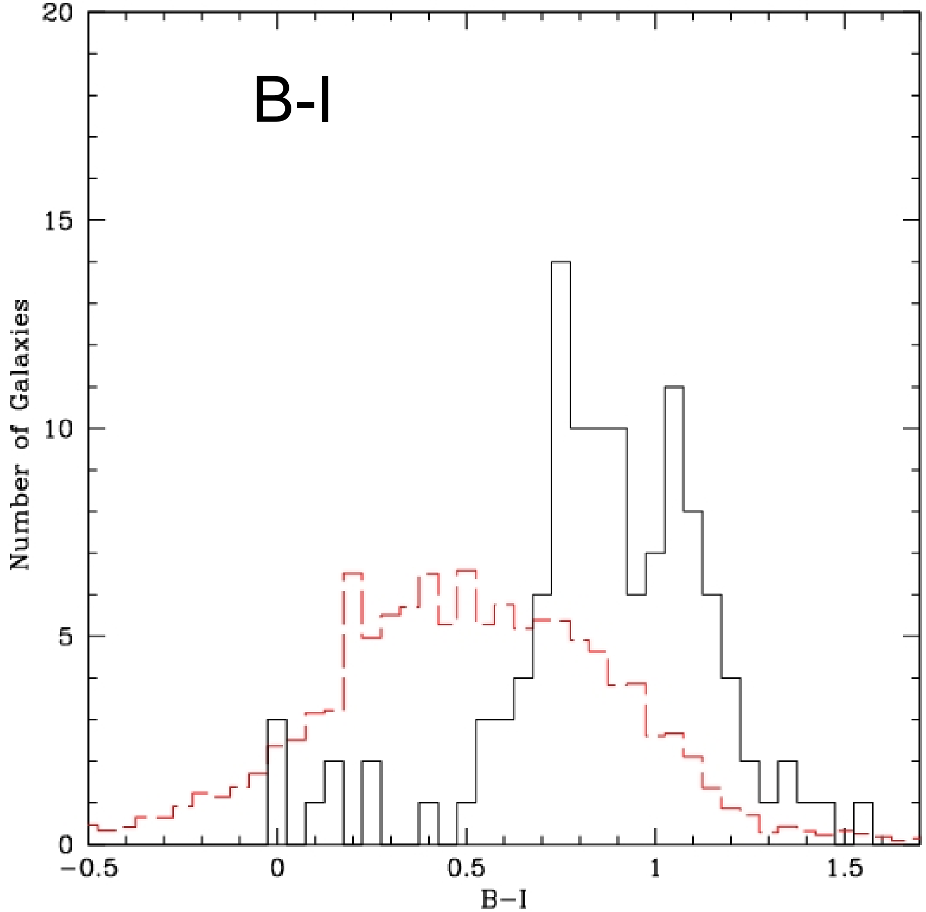

EFFECT of DUST?

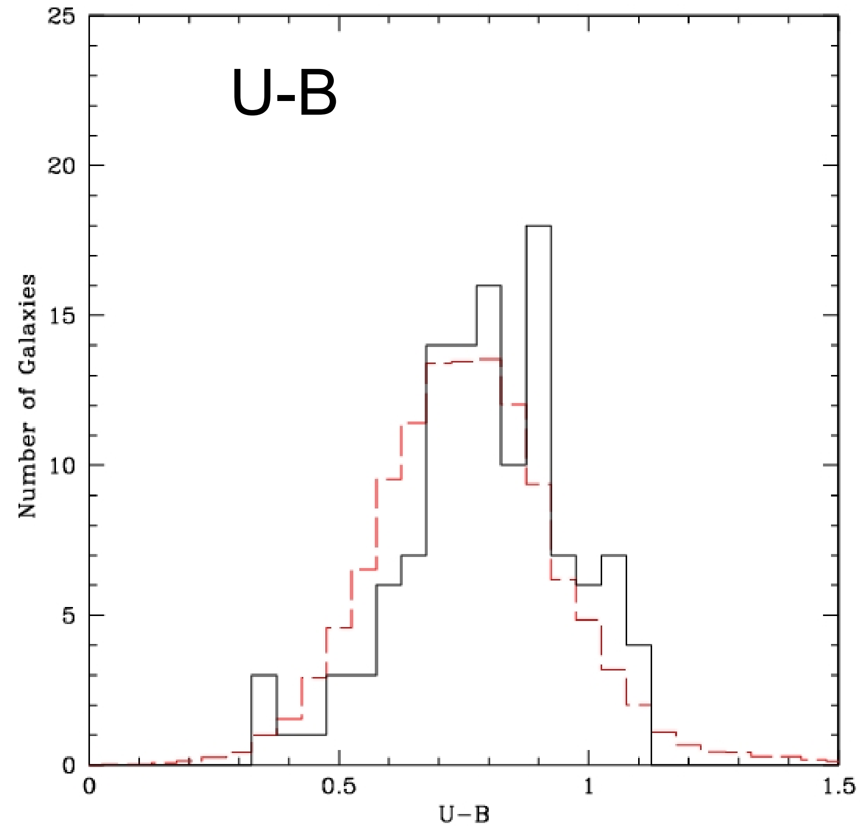

LUMINOSITY FUNCTIONS

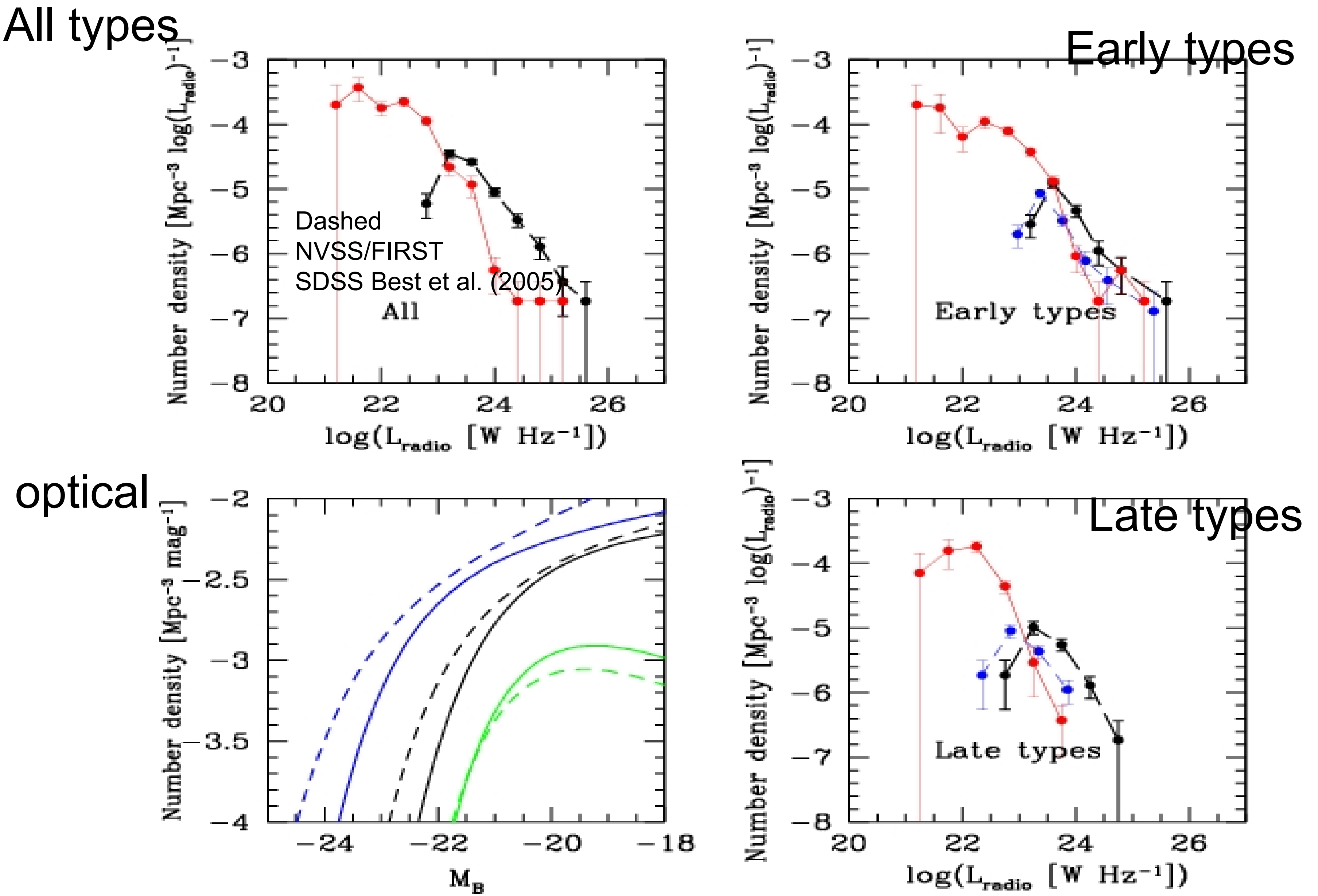

LUMINOSITY FUNCTIONS

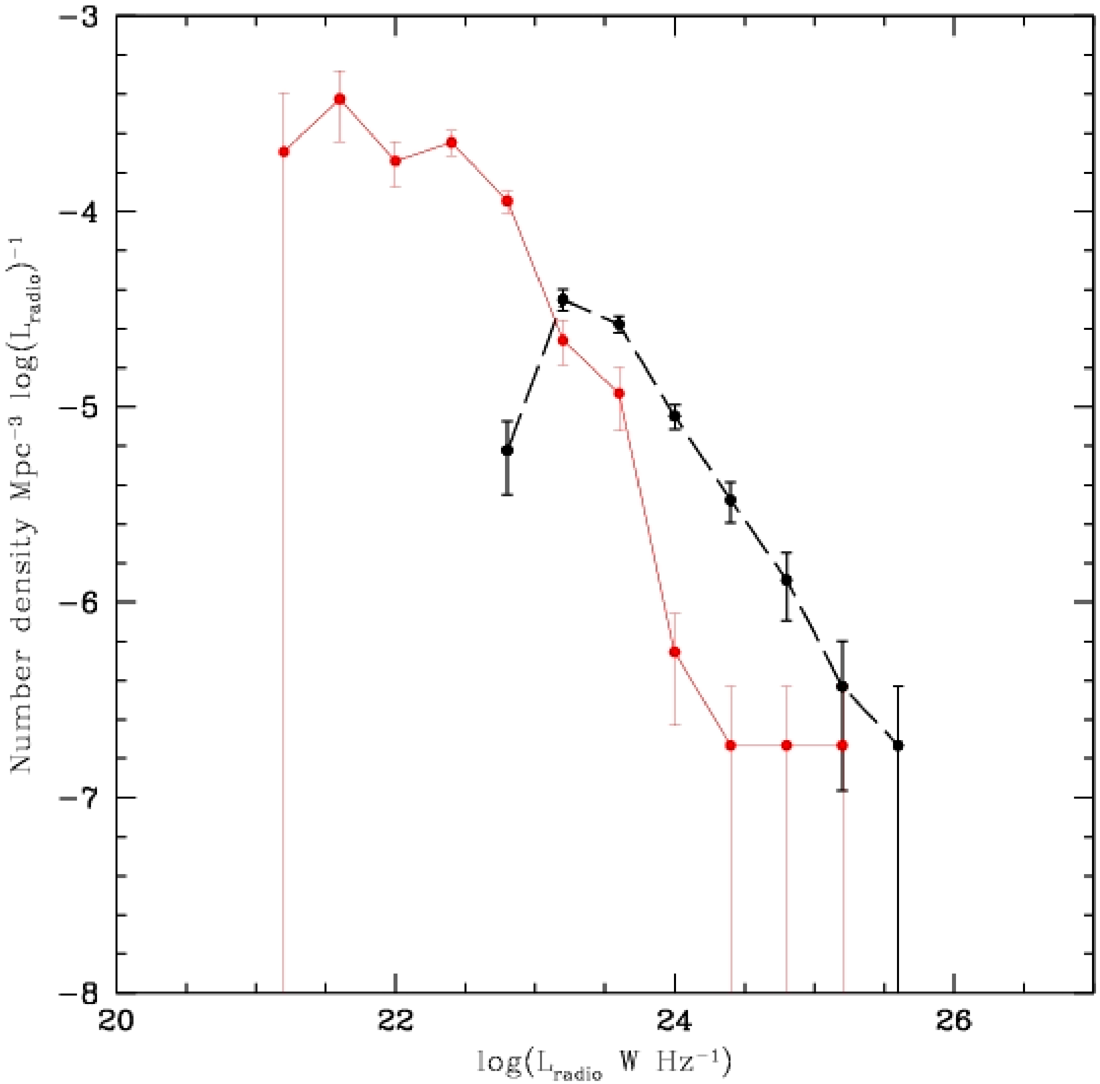

Red 0<z<0.5
Black 0.5<z<1.1

All types

LUMINOSITY FUNCTIONS

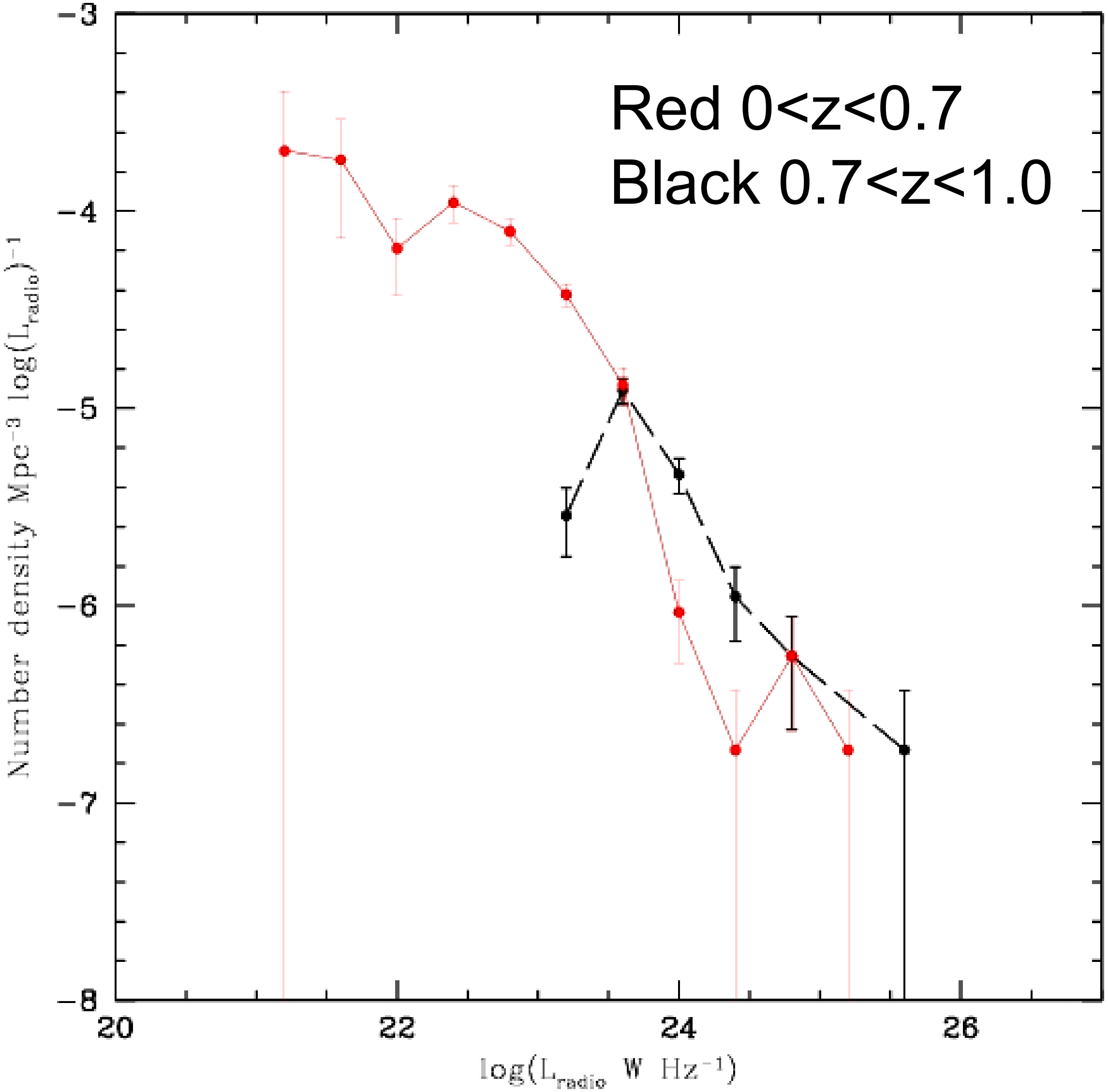

Type 1+2 (early)

$LF=\rho_0 (1+z)^k (L/L^*)^\alpha$

where

$L=L_0 (1+z)^\beta$

α= -1.78

β= 2.76

K= 0.04

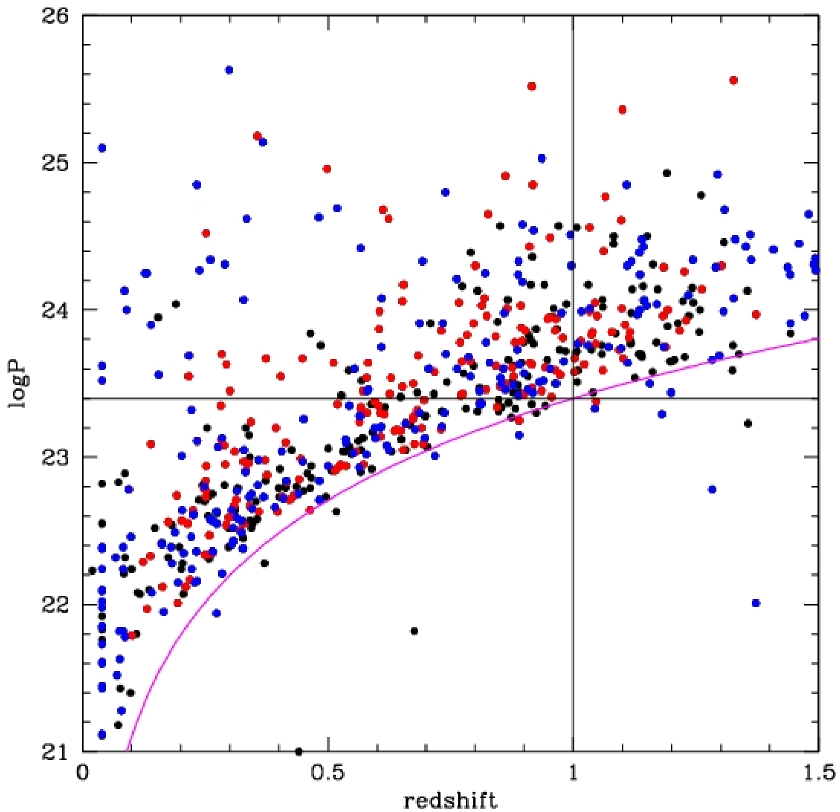
26
25
24
23
22
21
logP
0
0.5
1
1.5
redshift

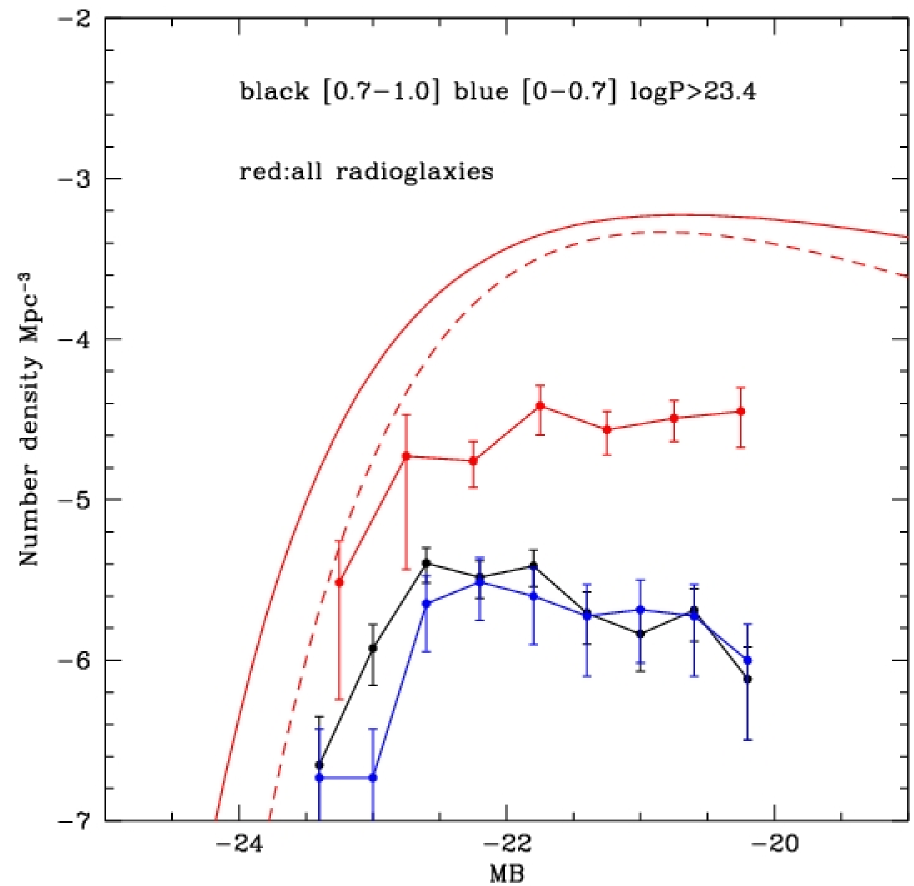
black [0.7−1.0] blue [0−0.7] logP>23.4
red:all radioglaxies
−2
−3
−4
−5
−6
−7
Number density Mpc⁻³
−24
−22
−20
MB

LUMINOSITY FUNCTIONS

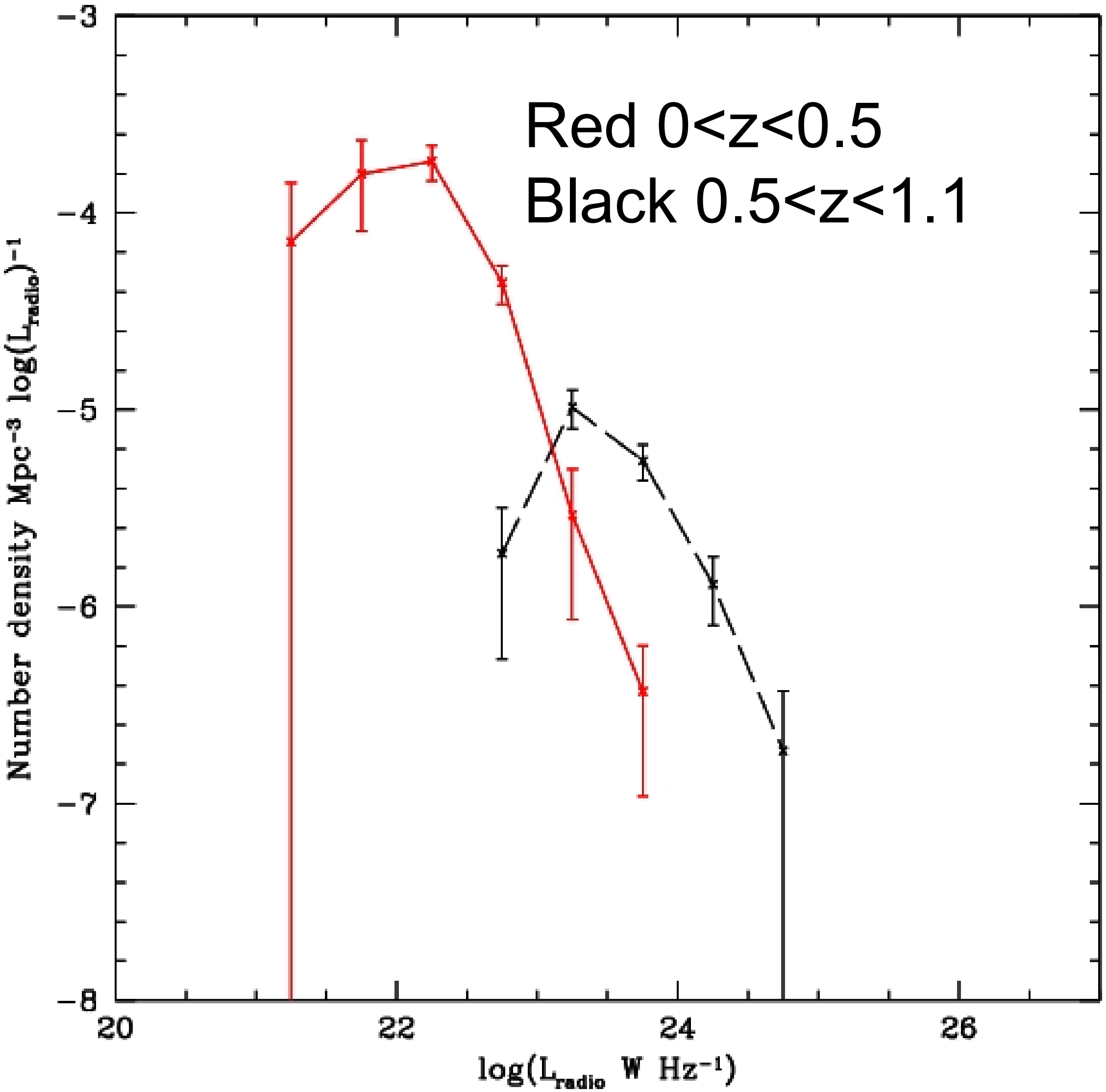

Type 3+4 (late)

$LF = \rho_0 (1+z)^k (L/L^*)^\alpha$

where

$L = L_0 (1+z)^\beta$

α= -1.84
β= 2.63
K= 0.43

LUMINOSITY FUNCTIONS

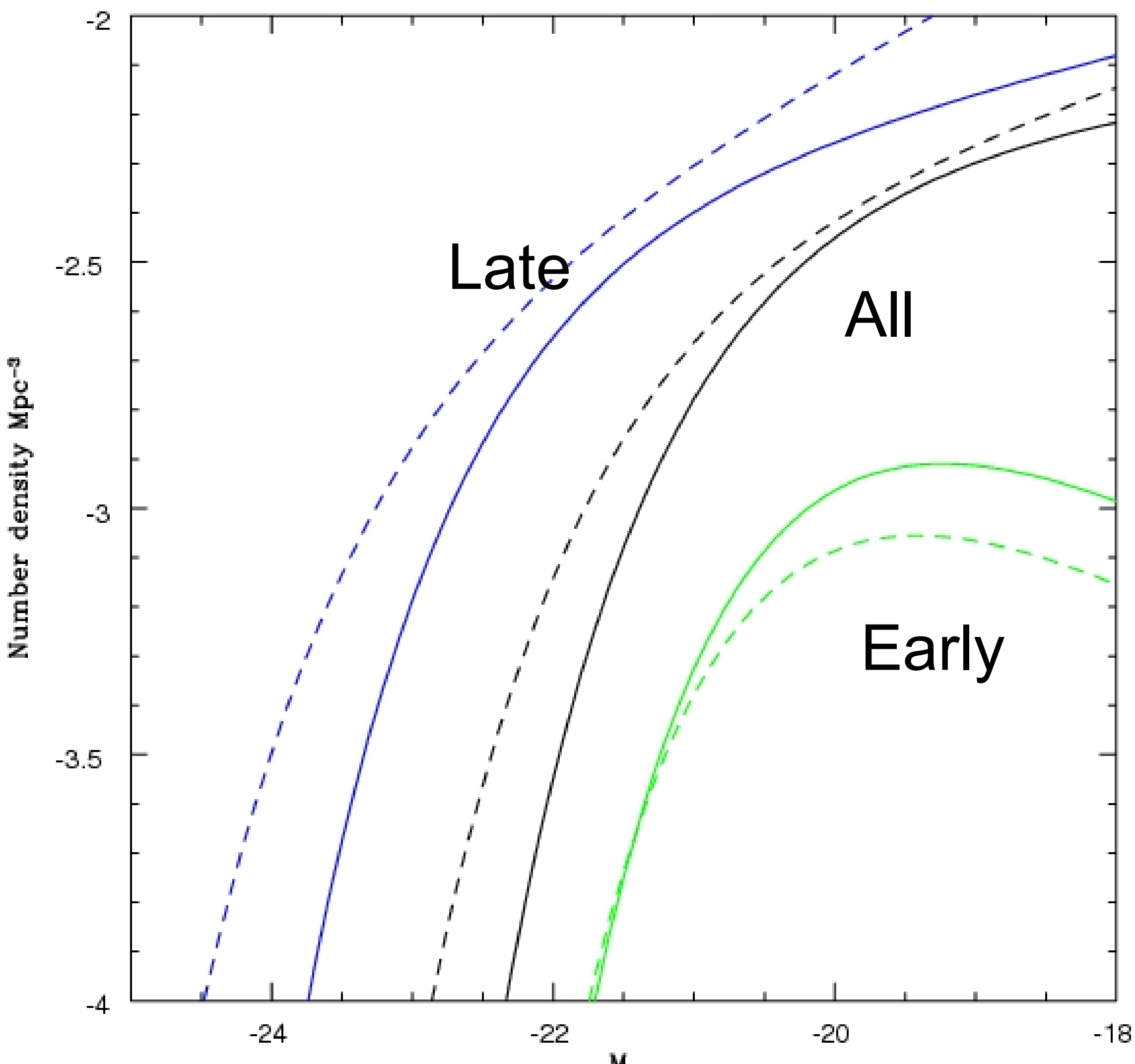

The optical
Luminosity Functions
Evolves
What about
Radio-optical ratios?

Radio - Optical ratio

Standard definition
(ratio between fluxes)
insufficient for deep surveys
Because of:

- redshift-band dependent
- flux limit dependent
- Volume-redshift dependence

▶Take ratio of rest-frame luminosities
and weight by V/V_{max}

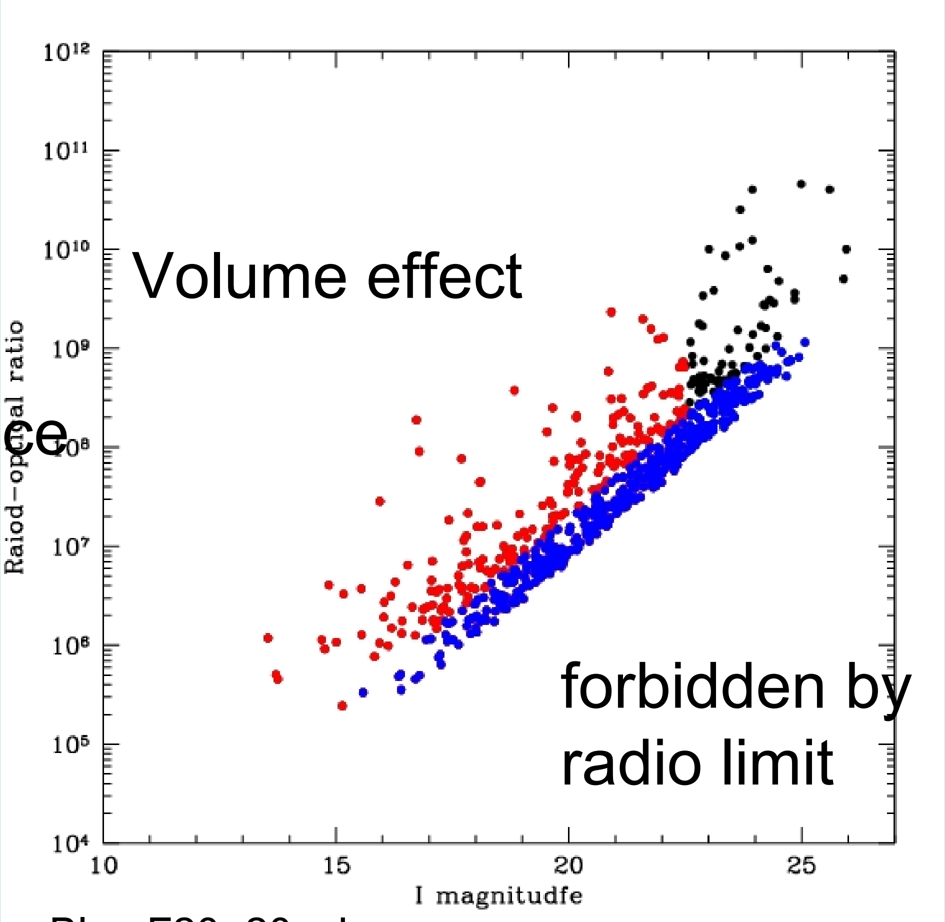

Blue F20<20 μJy

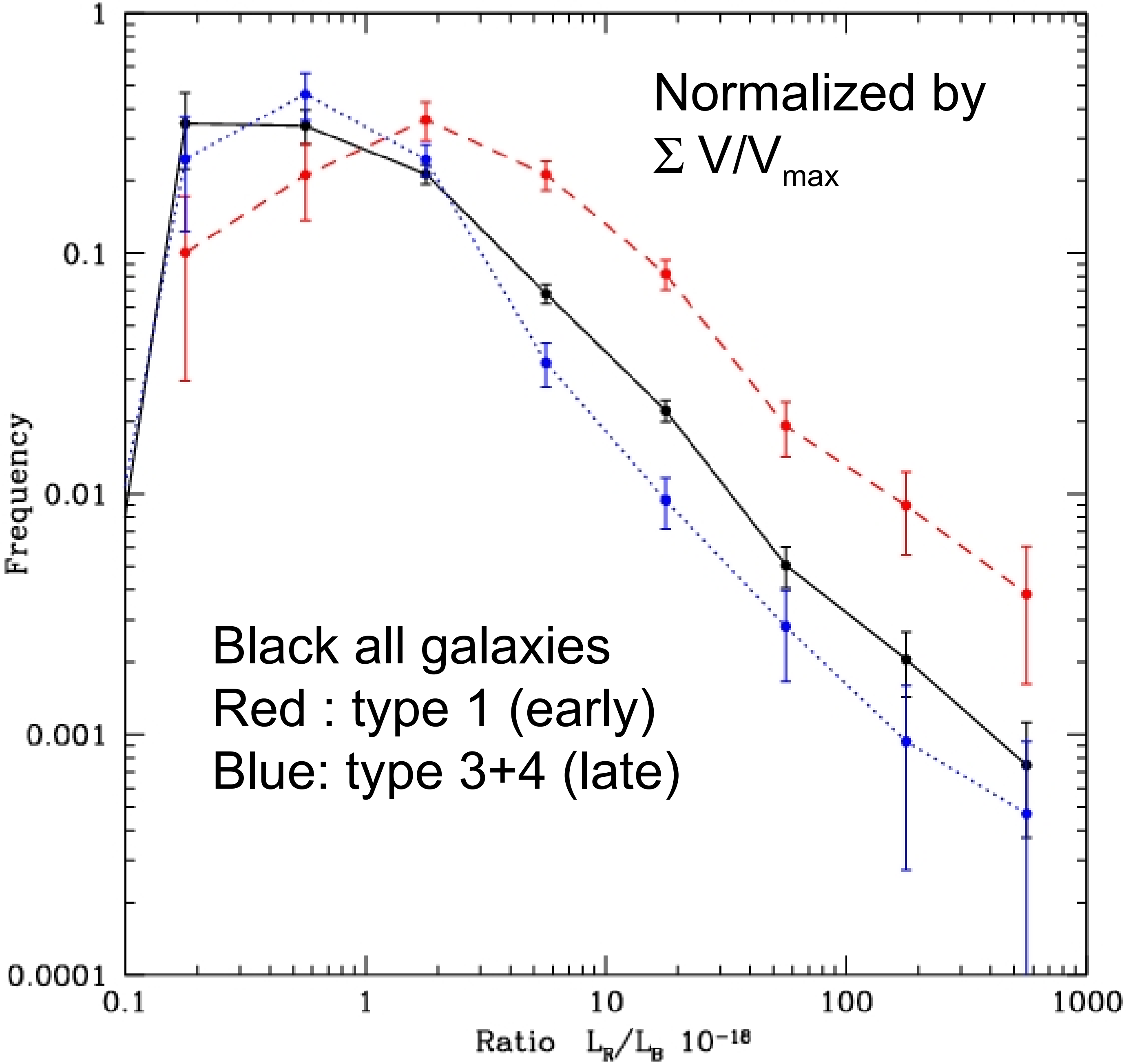

Normalized by
Σ V/V$_{max}$
Black all galaxies
Red : type 1 (early)
Blue: type 3+4 (late)
Frequency
Ratio L_R/L_B 10^{-18}
1
0.1
0.01
0.001
0.0001
0.1
1
10
100
1000

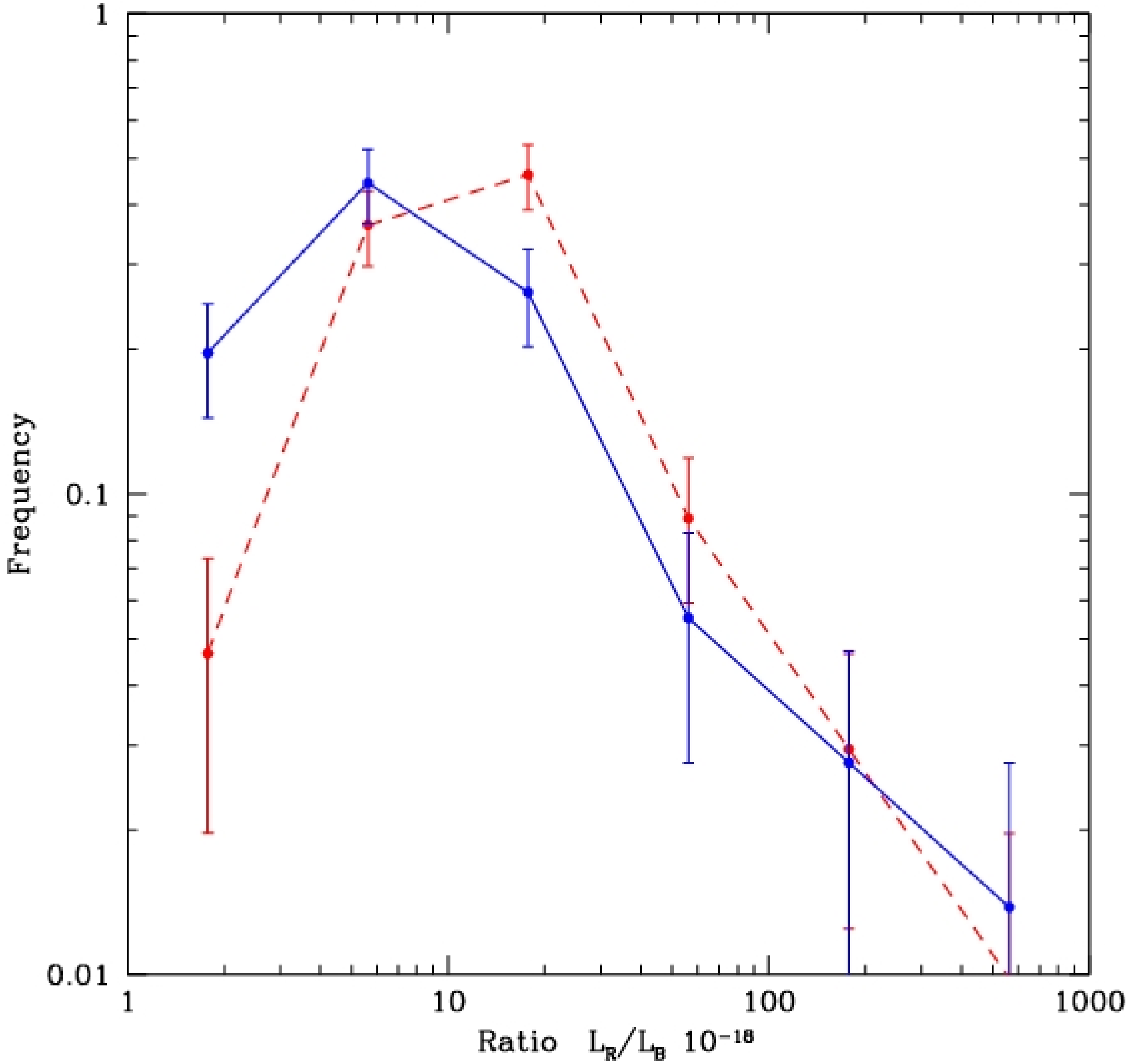

T1+2
z>0.7 red
z<0.7 blue

logP>23.1

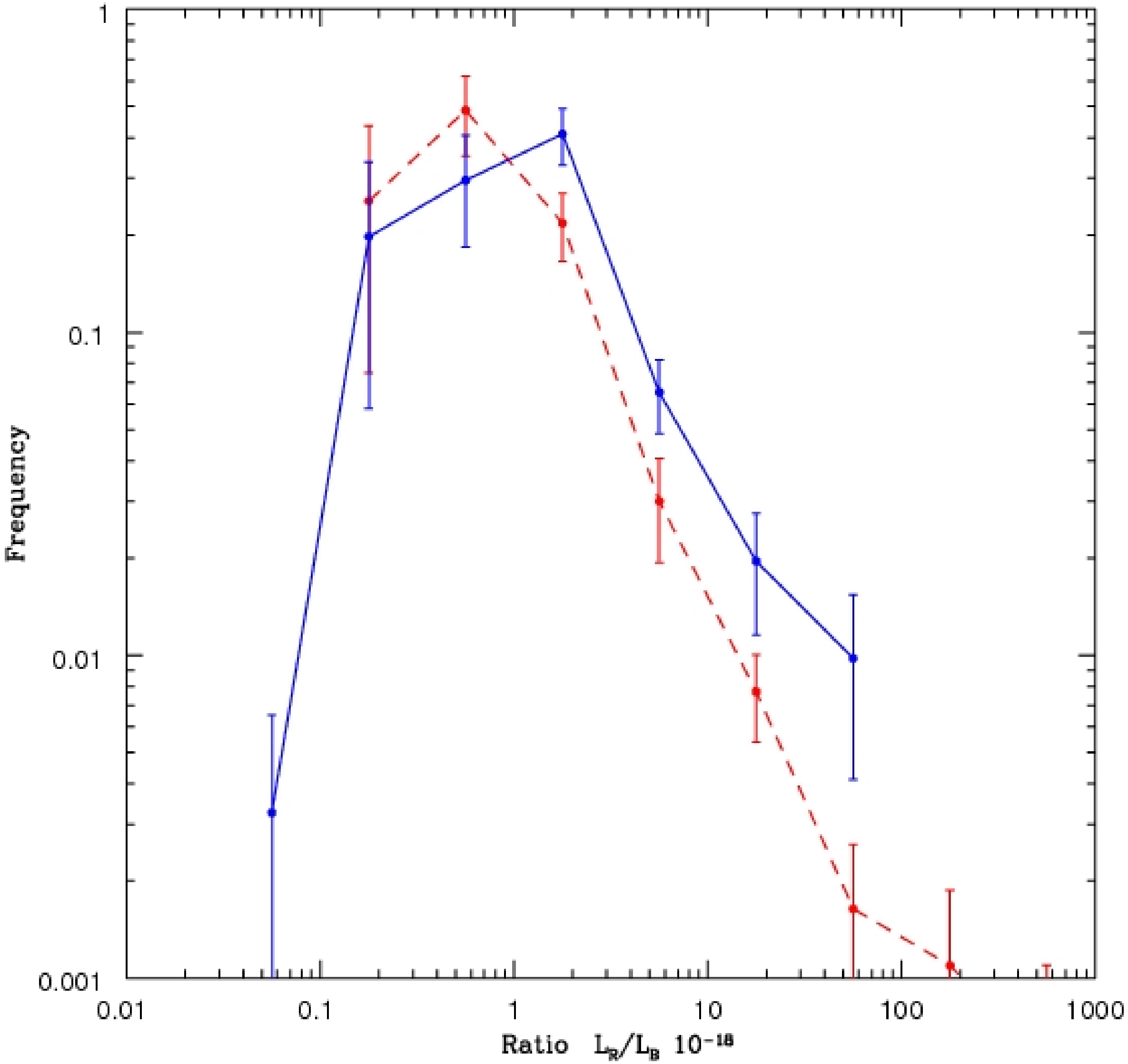

T3+4 (late)

MB<-21.5

Dependence on the optical luminosity

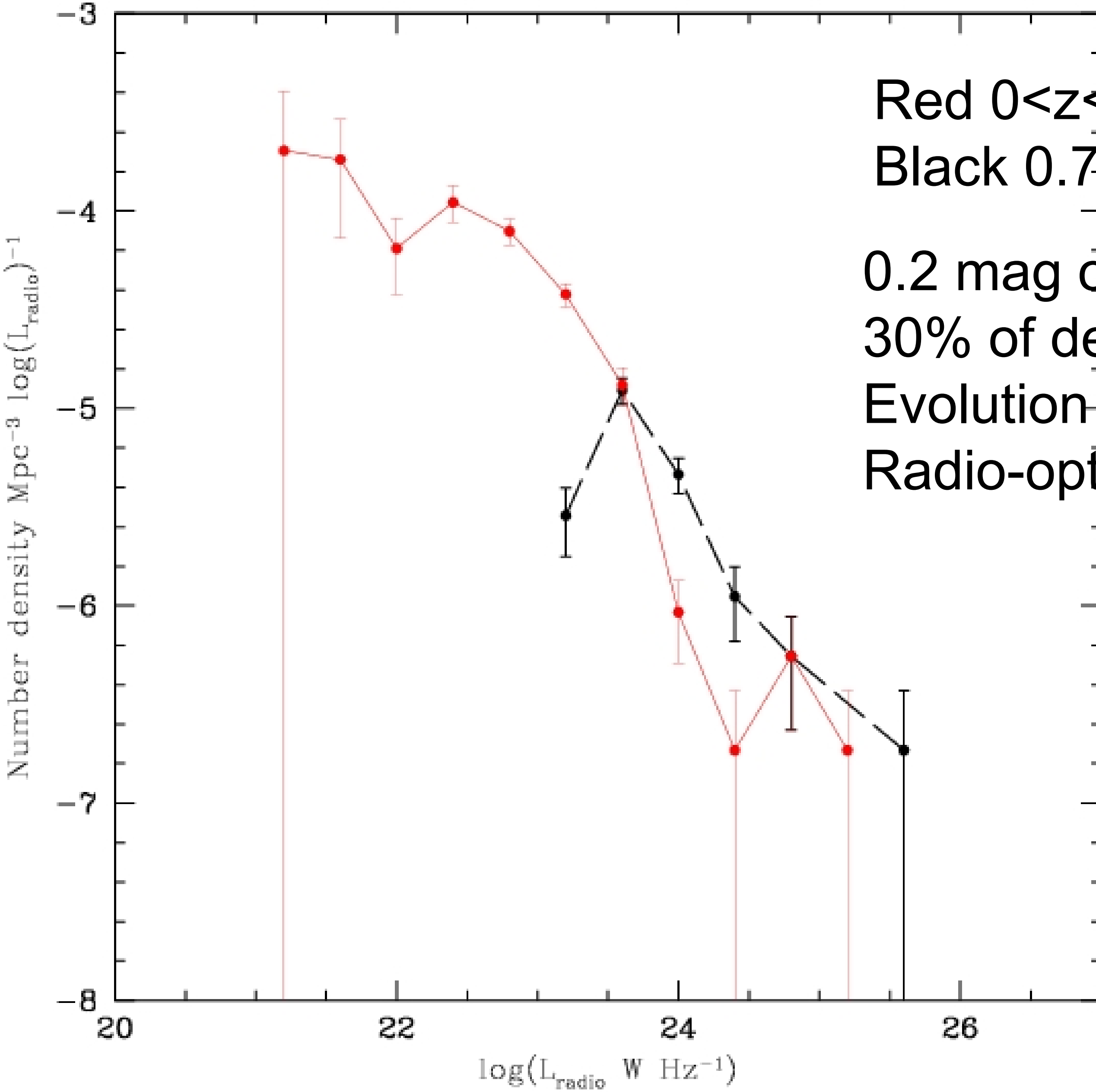

Red 0<z<0.7

Black 0.7<z<1.0

0.2 mag of brightening

30% of decrese in number

Evolution of 0.15 in log of the Radio-optical ratio

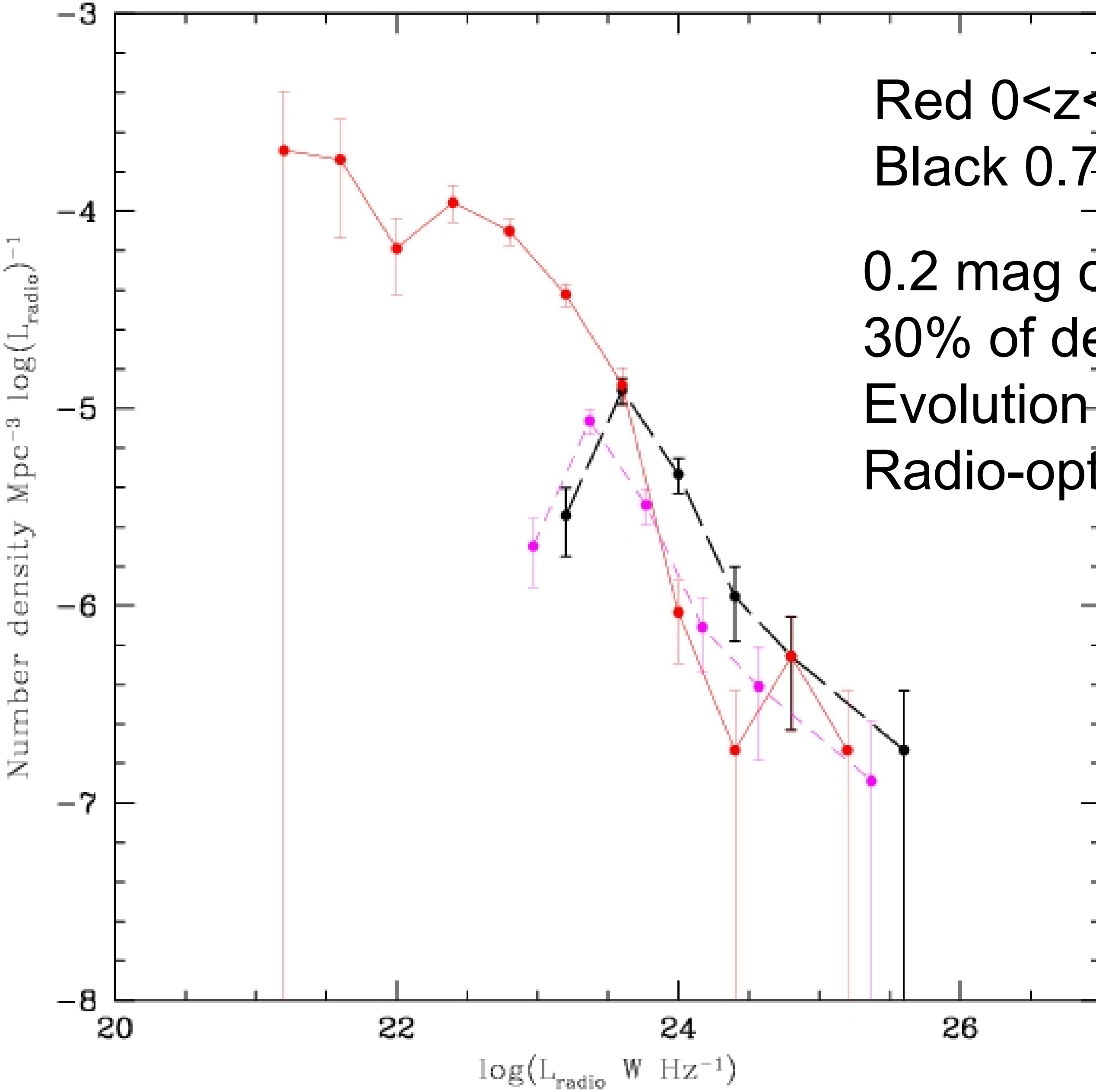

Red 0<z<0.7

Black 0.7<z<1.0

0.2 mag of brightening

30% of decreses in number

Evolution of 0.15 in log of the

Radio-optical ratio

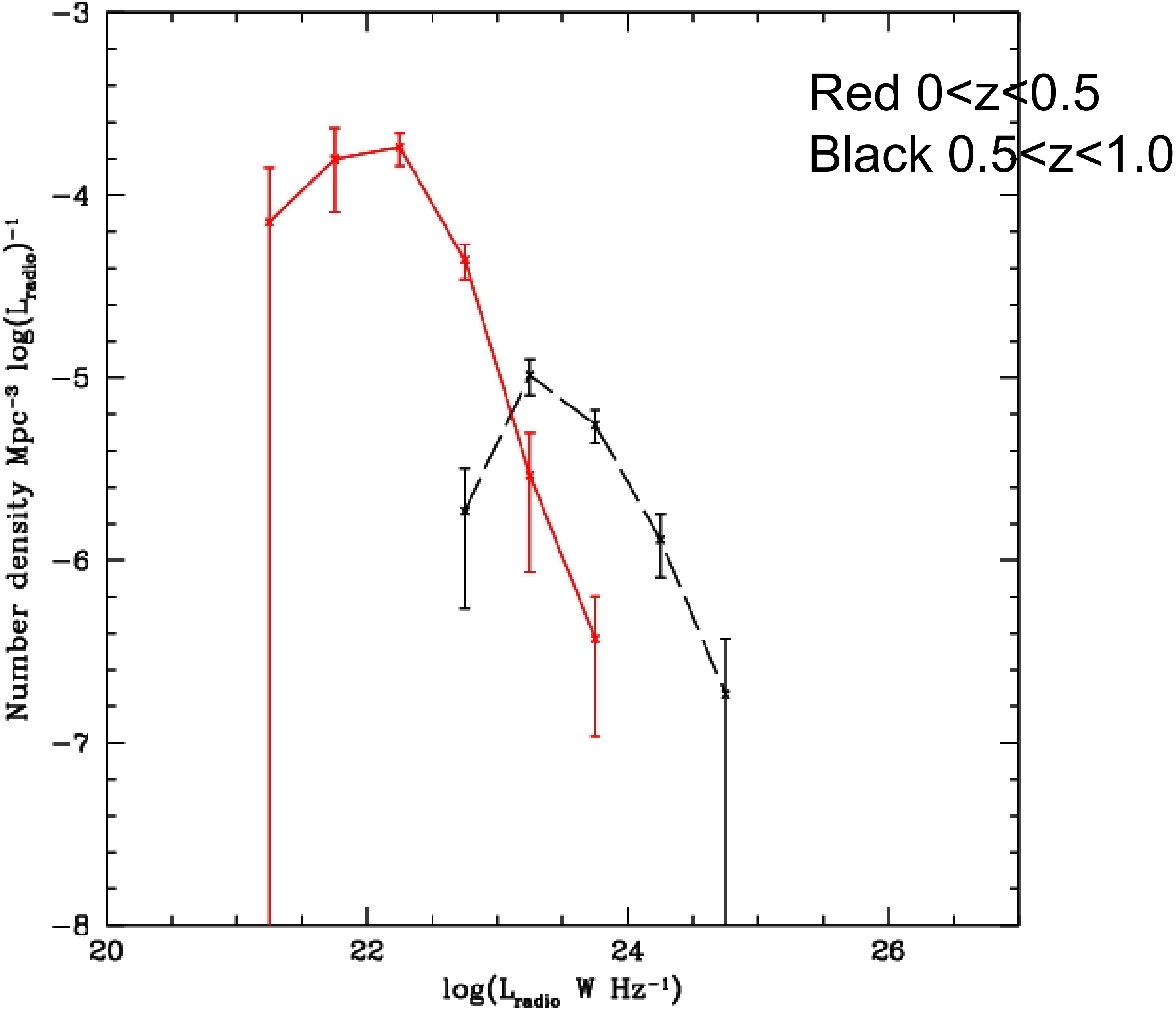

Red 0<z<0.5
Black 0.5<z<1.0
Number density Mpc⁻³ log(L_radio)⁻¹
log(L_radio W Hz⁻¹)
−3
−4
−5
−6
−7
−8
20
22
24
26

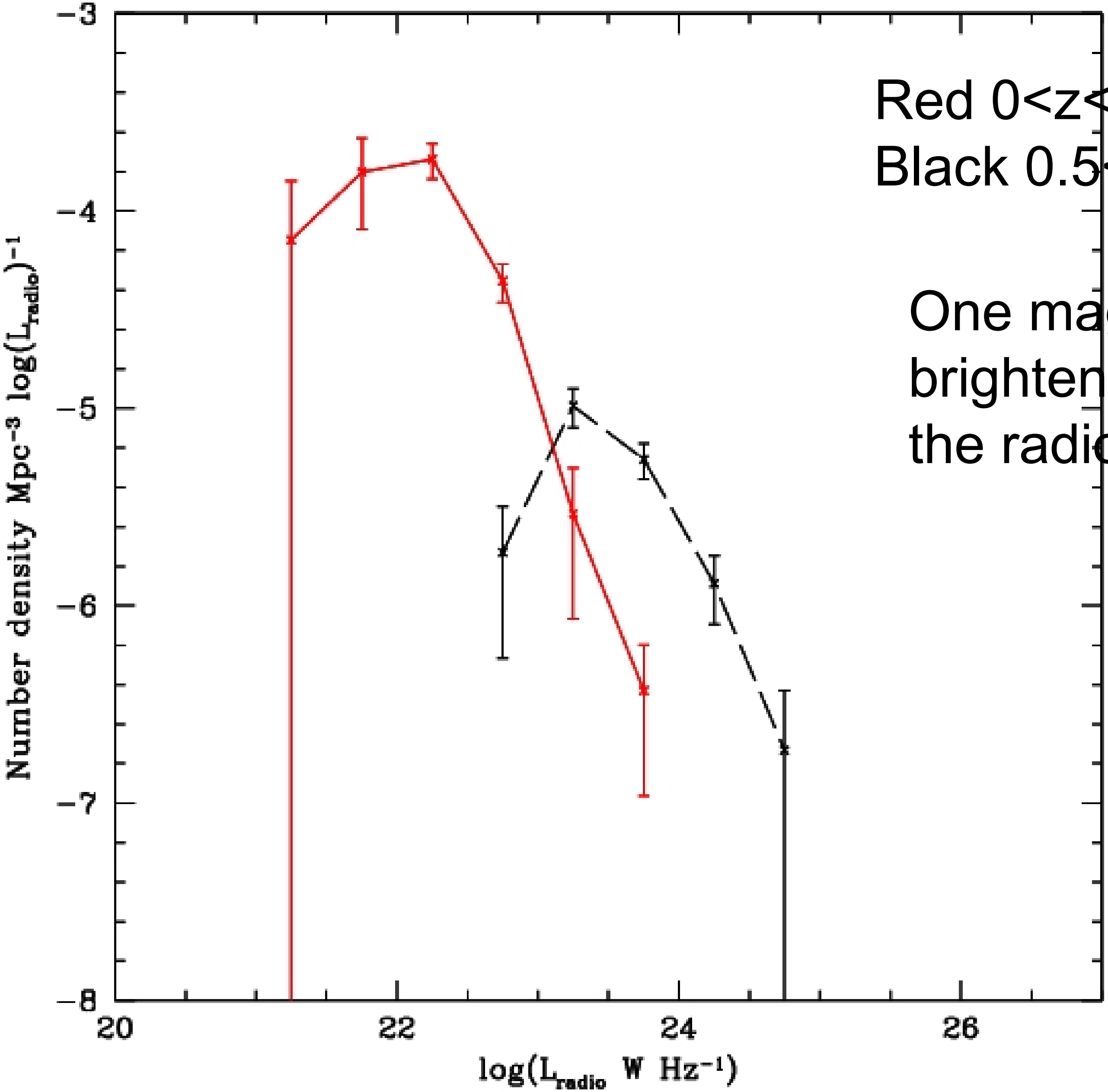

Red $0<z<0.5$
Black $0.5<z<1.0$

One magnitude of brightening no change in the radio-optical ratio

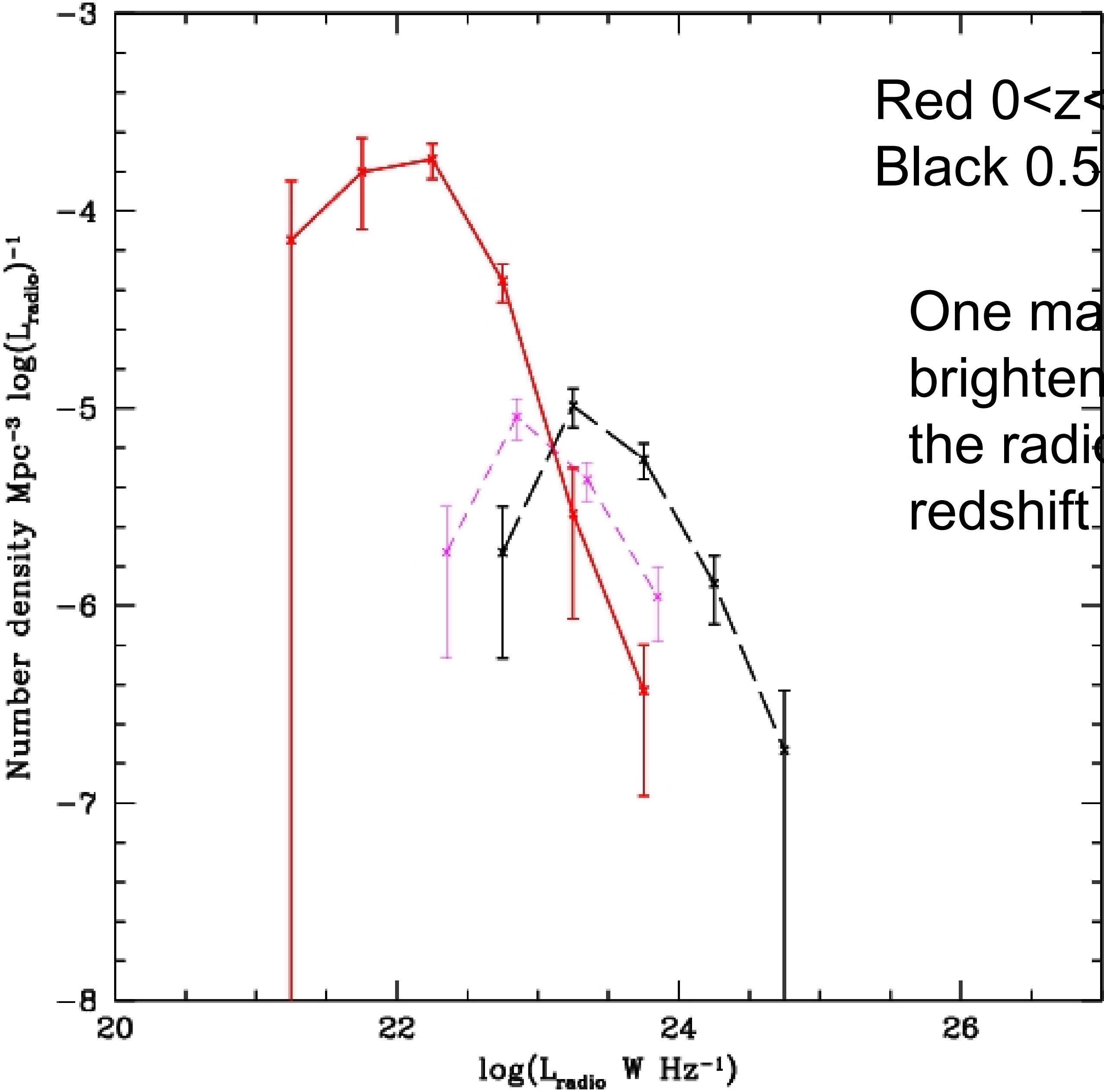

Red 0<z<0.5
Black 0.5<z<1.0

One magnitude of brightening no change in the radio-optical ratio with redshift

Stellar Masses and Star Formation Rates

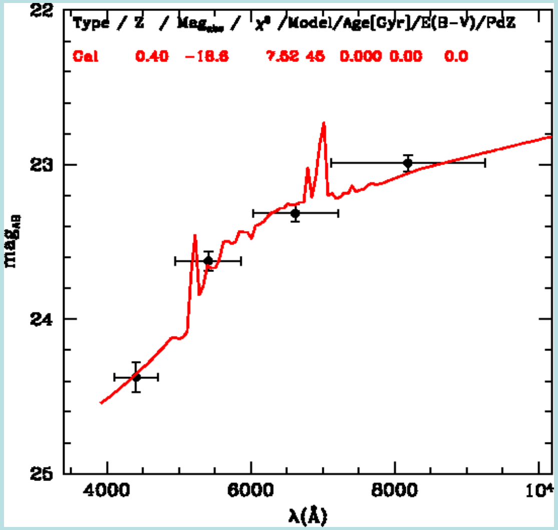

Optical:Match of photometric bands with a library of spectra including variable star formation rates and stellar masses

RADIO:

Star Formatio Rate = C * $L_{1.4\ GHz}$ $M_O\ yrs^{-1}$

C= 1.19 10^{-21} $L_{1.4\ GHz}$ Haarsma et al. (2000), Condon (1992)

C= 5.52 10^{-22} $L_{1.4\ GHz}$ Bell (2003)

SFR(radio) vs SFR(optical)

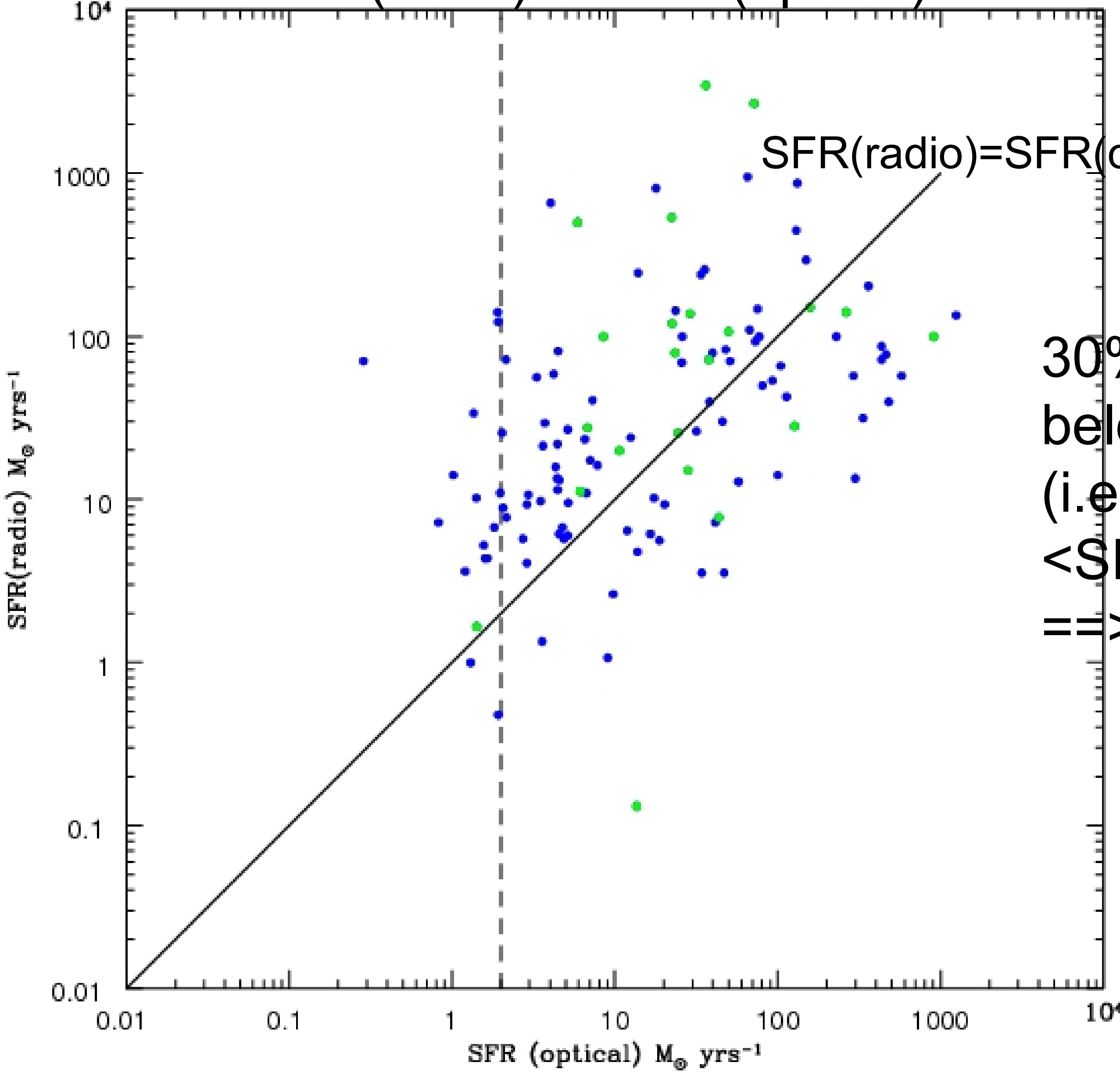

30% of objects below “equality line” (i.e. <SFR(radio)> > <SFR(optical)>)

==> effect of dust?

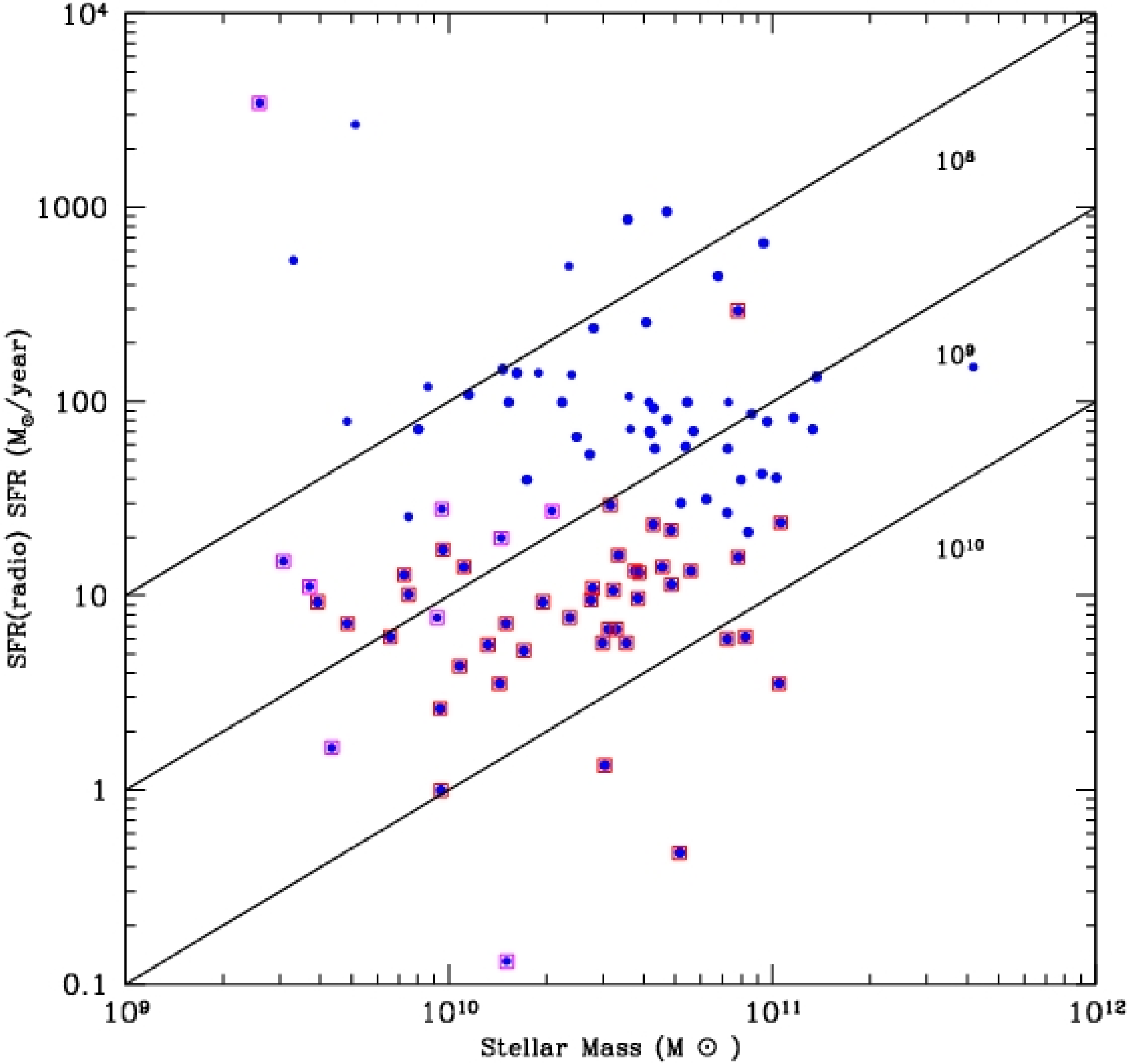

Type 3+4 (late)

blue z>0.5

magenta z<0.5

At higher z

Higher specific

Star Formation

Mass Functions

Red:Control Sample
Black: Complete Sample

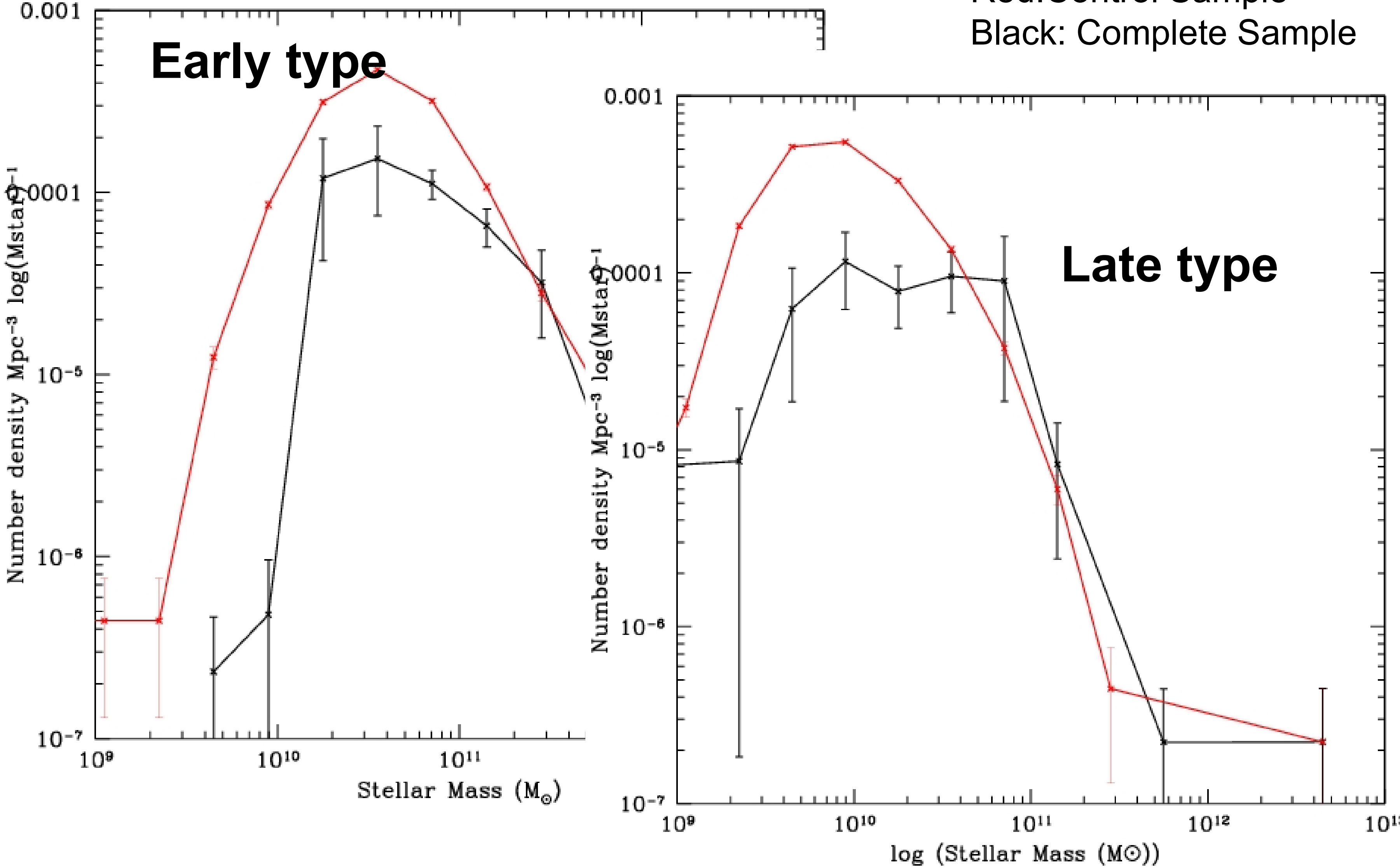

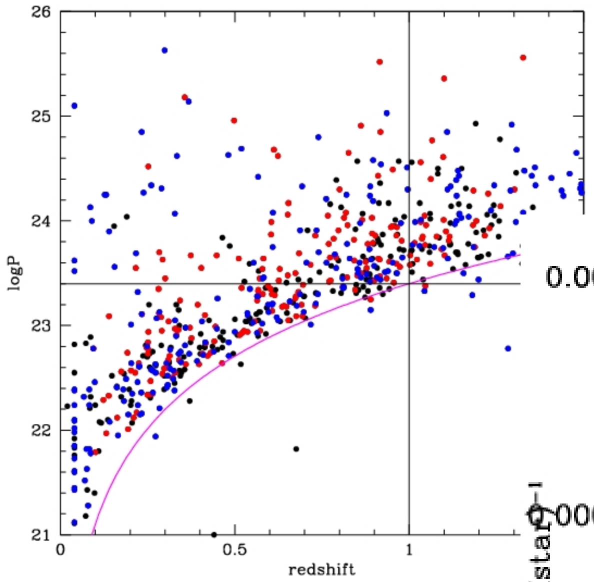

Little (if any)
Evolution in Stellar Mass

Red:Control Sample
Black: Complete Sample

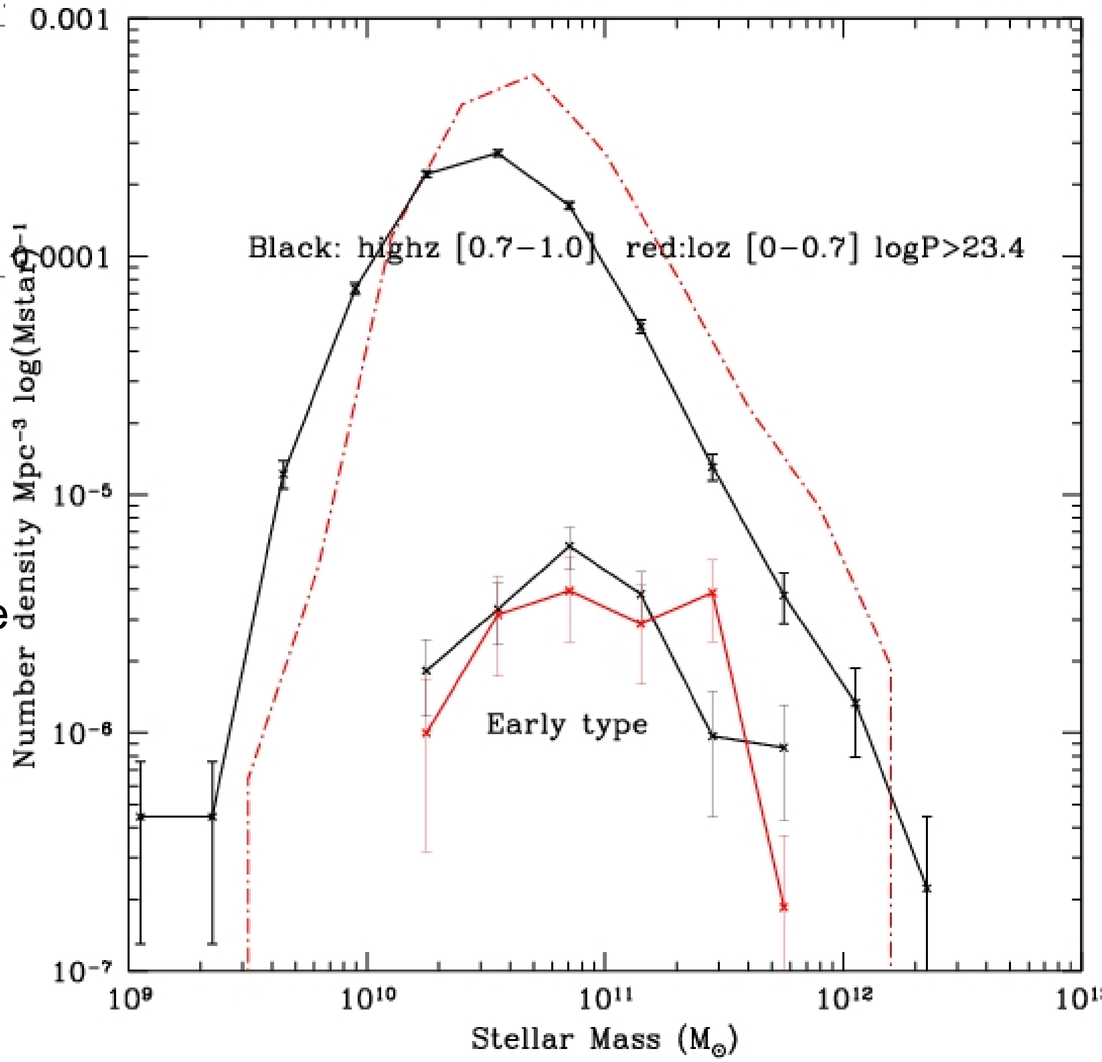

Star Formation History
from radio band

Two approaches:

2) Direct integration of radio-optical luminosity function in different redshift bins (low statistics)

2) Use optical galaxies as tracers for radio emission

SFR density= $C \int \Phi(L') (\int R\, D(R)\; L'\, dR)\, dL'$

$\Phi(L)$ Optical luminosity function

D(R) distribution of radio-optical ratios R

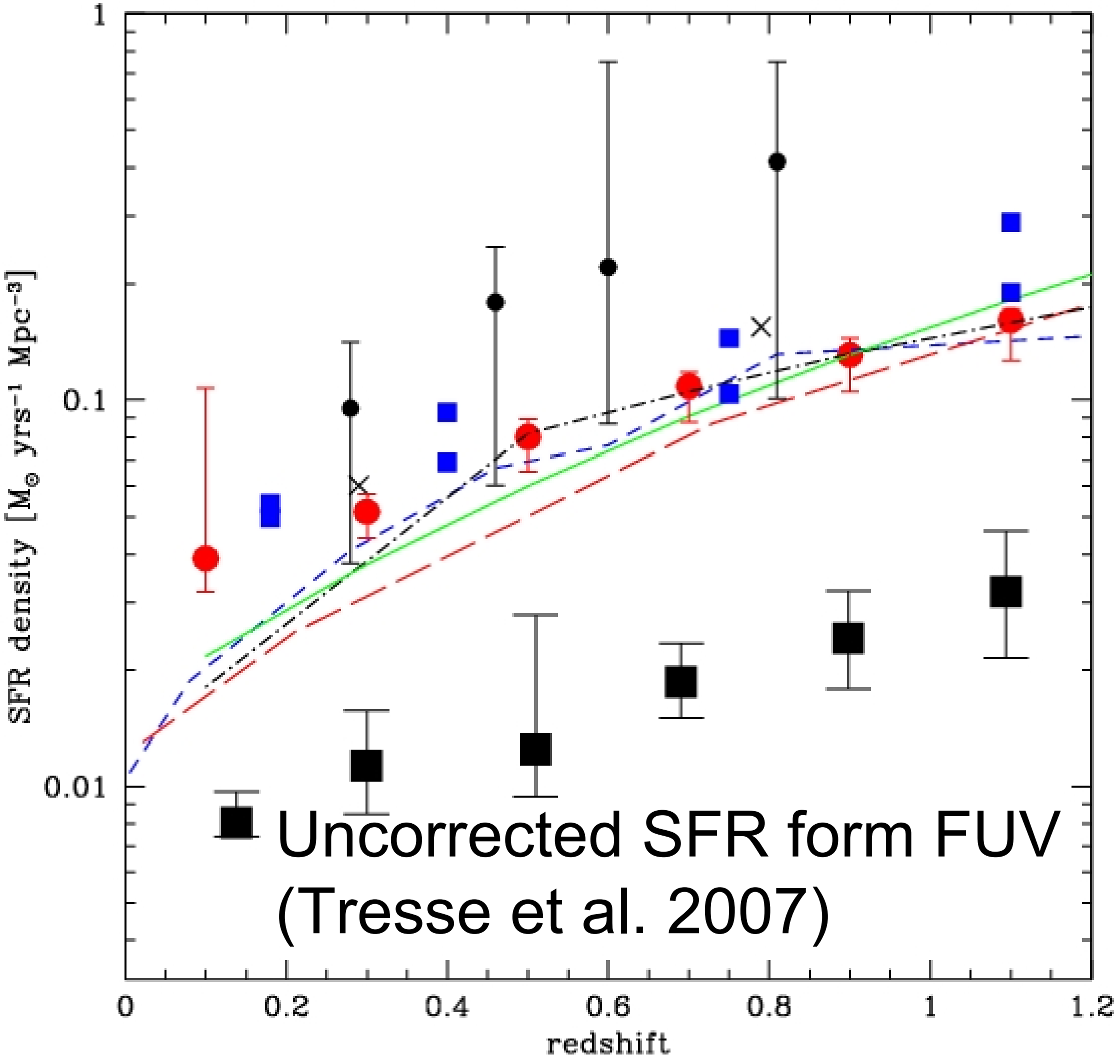

Log (sfrVVDS)-
Log (SFRradio)=

<0.73> +/- 0.02

Expected 0.74
From FUV (1500Å)
(Hopkins et al 2001)

SFR density $\propto(1+z)^{2.15}$

CONCLUSIONS

√Colors: radio faint early type radio galaxies redder than Control Sample
Late type radio loud galaxies significantly redder that Control Sample (dust)

√Radio Luminosity Functions evolution
Early: increase of radio-optical ratio compensated by decreas
of optical luminosity function
Late : one magnitude evolution of optical population, no
Evolution of radio-optical ratio

√<SFR(radio> > <SFR(optical)> (dust)

√Specific star formation rate higher in the past

CONCLUSIONS

√**Possible to use optical galaxies astracers for radio emission in particular for the estimation of the Star Formation History**

√**No significant redshift dependence of radio emission with Stellar Mass in case of AGN**

√**Specific star formation is decreasing with redshift**

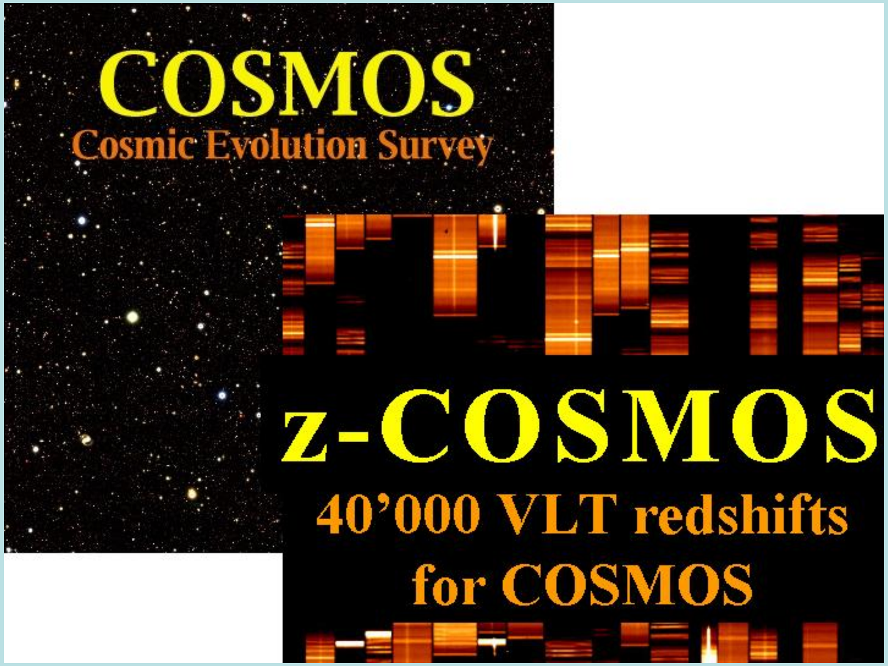

10 K sample Z-COSMOS

PI: S Lilly ETH-Zurich

~10000 redshift to I=22.5 over ~1.4 deg^2(forseen 20K over 2X2 deg^2)

Sampling rate 70%==> density estimate

Medium resolution spectra==>diagnostics R=600

zCOSMOS sample (bright)

-10509 redshifts
-8481 “statistical sample” (high quality, 99.8 % reliable)
-repeated 600 spectra yelds to <100 km/s errror

Cutting the sample
z<0.9 MB<-20.75
2567 objects

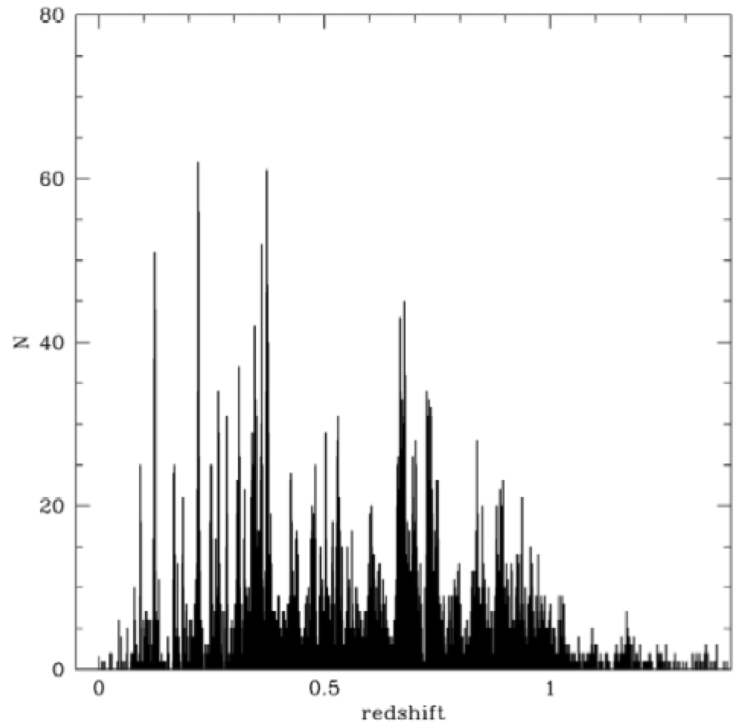

Fig 3: Redshift distribution of extragalactic objects in the zCOSMOS-bright 10k sample with secure redshifts, binned in intervals Δz = 0.001, which is larger than the redshift uncertainty by a factor of three at z = 0 and of two at z ~ 1. Despite the large transverse dimension of the survey, the redshift distribution shows structure on all scales from the velocity resolution up to Δz ~ 0.05.

DENSITY ESTIMATE

Kovac et al. (2008)

Battery of density estimator

Mass-weighted 5 nearest neighbour

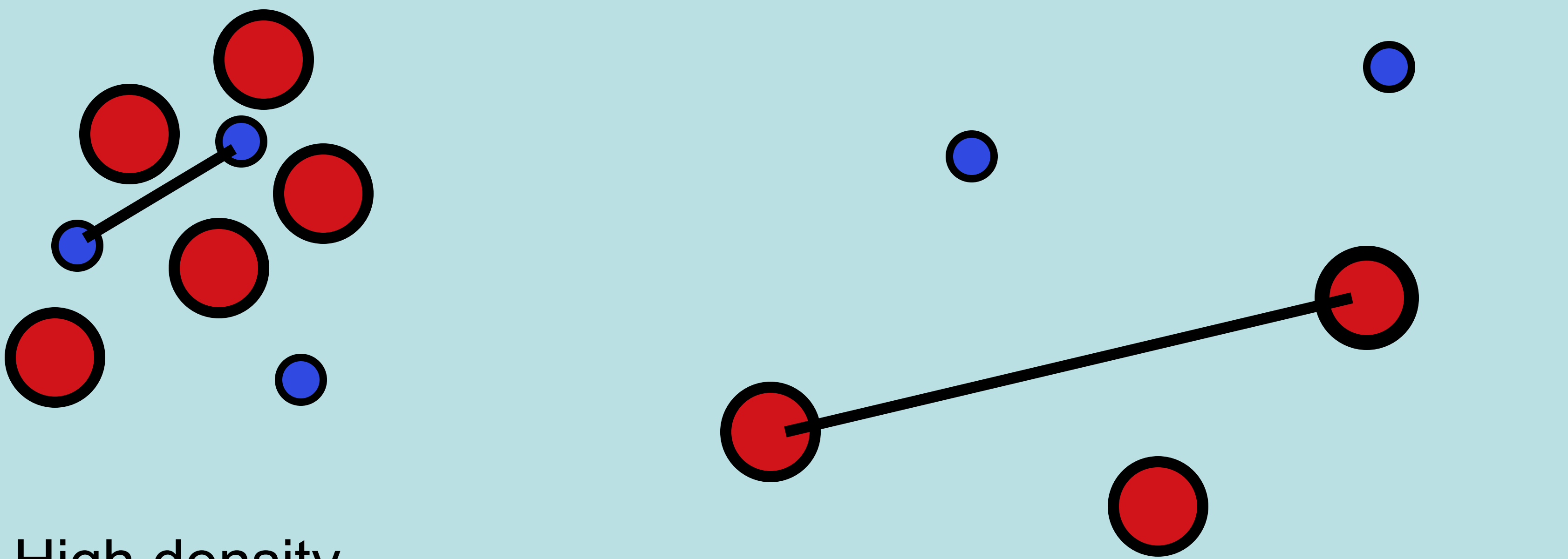

High density environment

low density environment

VLA-COSMOS

Bondi et al. (2008)

1.4 GHz over 2x2 deg^2 ~2501 sources
1.5 arcsec resolution to 11μ Jy

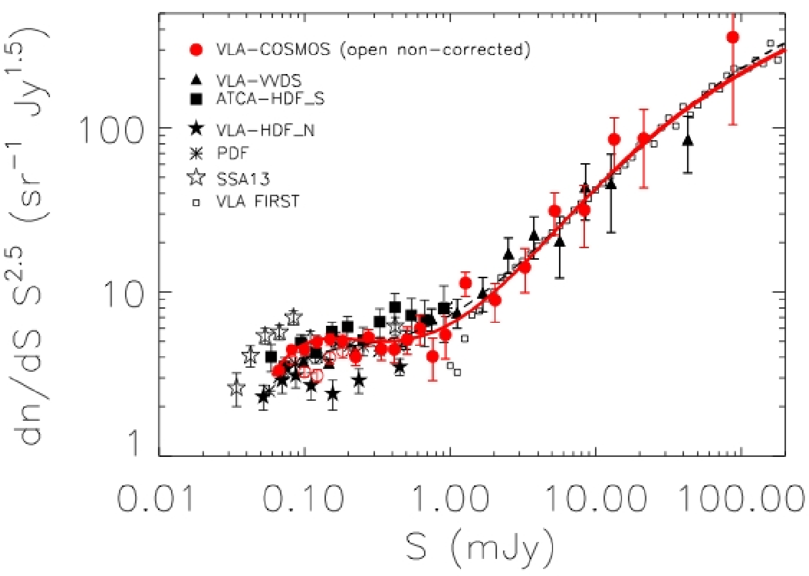

Fig. 5.— Radio source counts at 1.4 GHz from the VLA-COSMOS survey (dots) and fi
other surveys. Empty circles show the radio counts not corrected for incompleteness, fi
circles the corrected ones using $m = 0.5$. The VLA-COSMOS source counts are shown al
with those obtained by other deep surveys (see text). The solid line is least-squares si
order polynomial fit obtained using the VLA-COSMOS and the FIRST source counts. '
dashed line is the fit obtained by Hopkins et al. (2003).

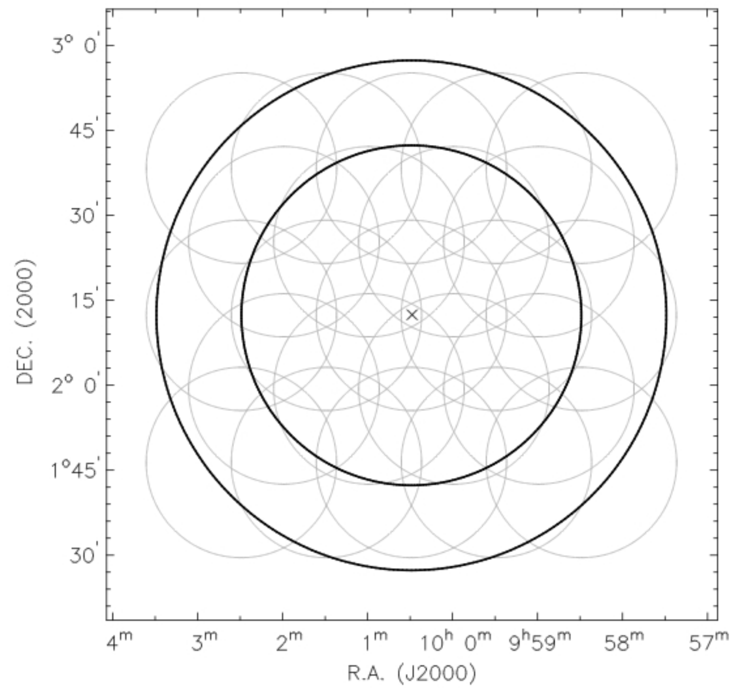

Fig. 2.— Layout of the 23 pointings for the VLA-COSMOS observations. The two circles have a radius of 30′ and 45′.

Previous Results on AGN environment

-X-ray AGN have correlation function at $z \approx 1$ similar to Massive ($3 \times 10^{10}\ M_o$ galaxies at same redshift)
(Gilli et al. (2008, in press)

-24 μm galaxies (I<22.5): LIRGs have more ellipticals neighbour than other galaxies, ULIRGs are in “active SFR regions” . LIRG in overdens, ULIRG in underdens regions.
(Kaputi et al. (2008)

-Effect with environment in 2dFGRS radio-loud AGN and star forming radio objects (Best 2004)

Previous Results on AGN environment

-radio loud Luminous Red Galaxies have correlation Length of 12.3+/- 1.2 (control sample 9.02+/-0.52) (Wake et al. 2008)

-X-Ray AGN in the A901/A902 supercluster avoid extreme (high and low) environments (Gilmour et al. 2007)

-X-ray AGN from COSMOS: low stellar mass AGN ($<10^{11} M_0$) same environment as non AGN massive AGN are in higher environment (Silverman et al. (2008)

CAUTIONS (..again..)

1) AGN vs SFR division
2) CONTROL SAMPLE

f.i. be careful that this is nothing else that the optical morphology-density relation Best (2004)

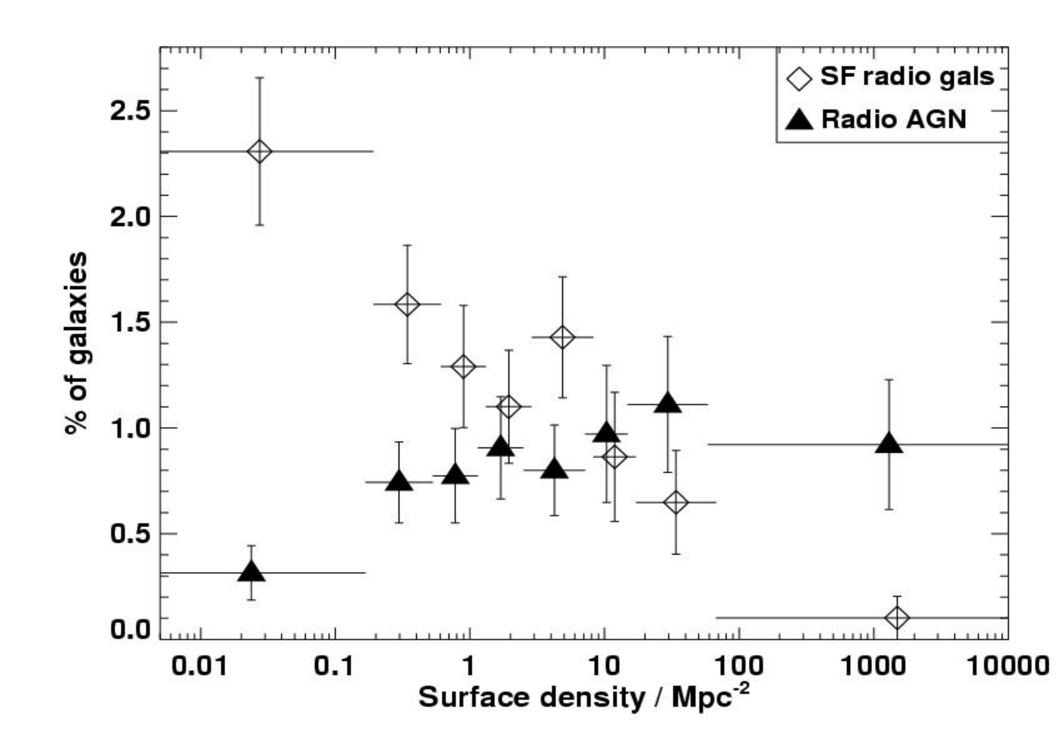

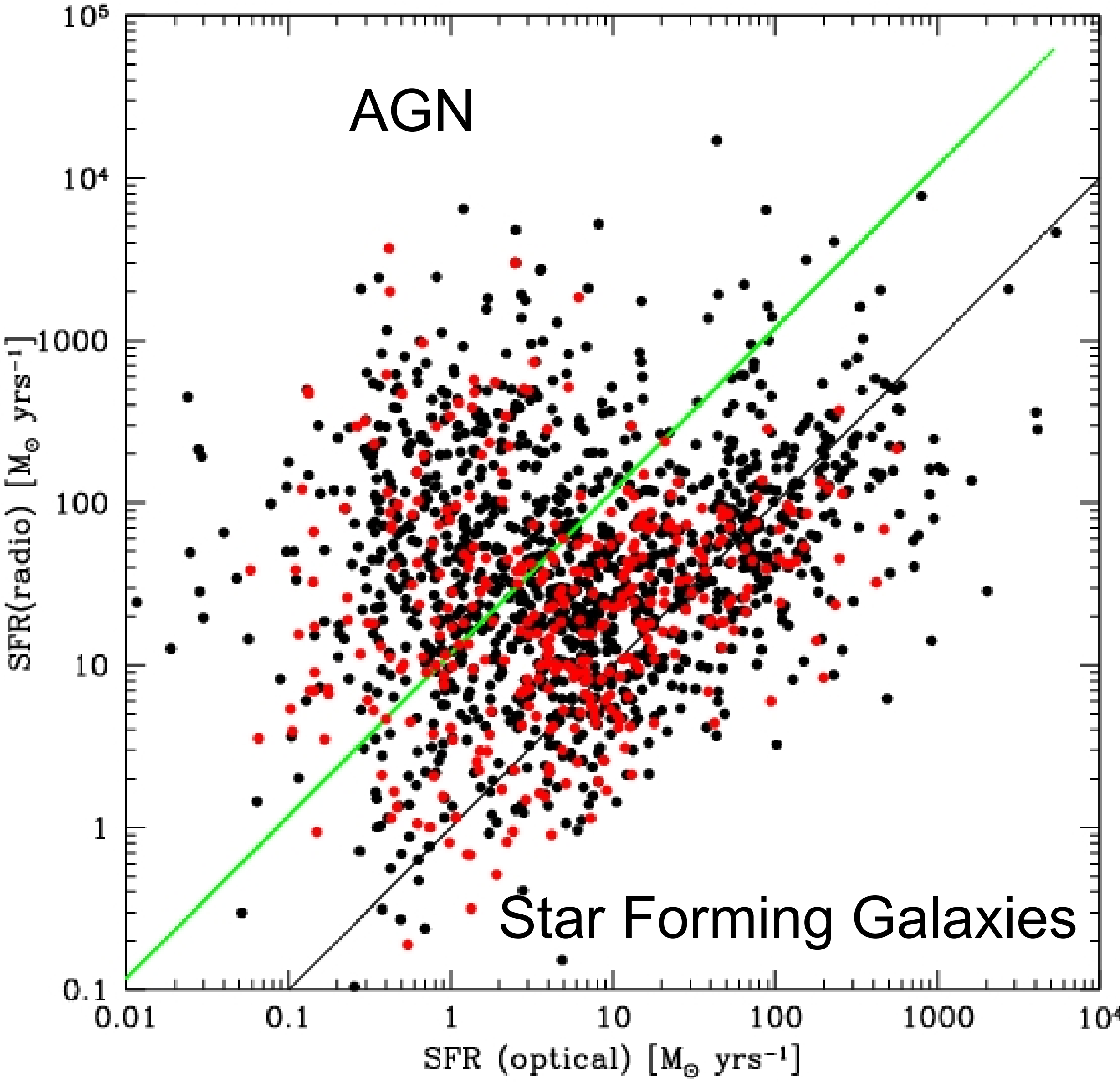

2060 optical Identifications Ciliegi et al.(2008)

1232 with I<22.5 (Black)

373 sources in the “statistical” zCOSMOS 10K sample (8481 objects) (Red)

How reliable is the method?

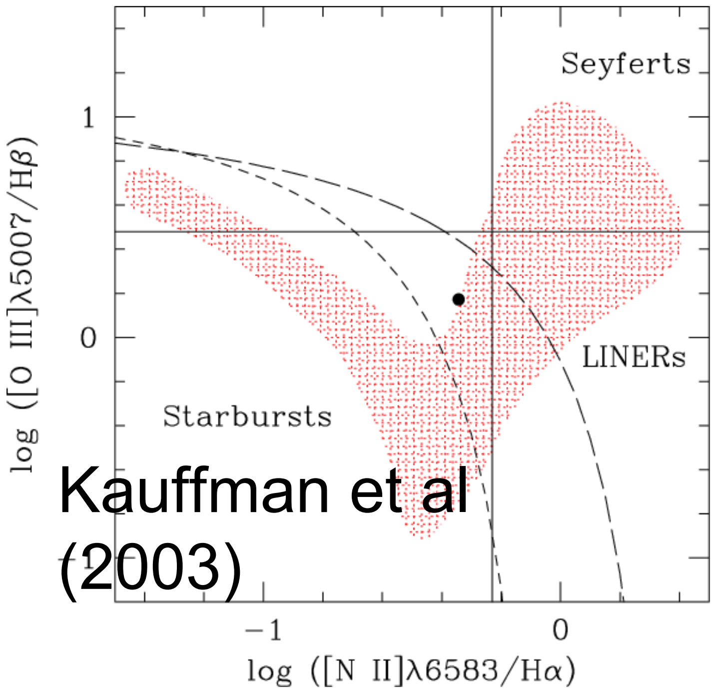

Kauffman et al (2003)

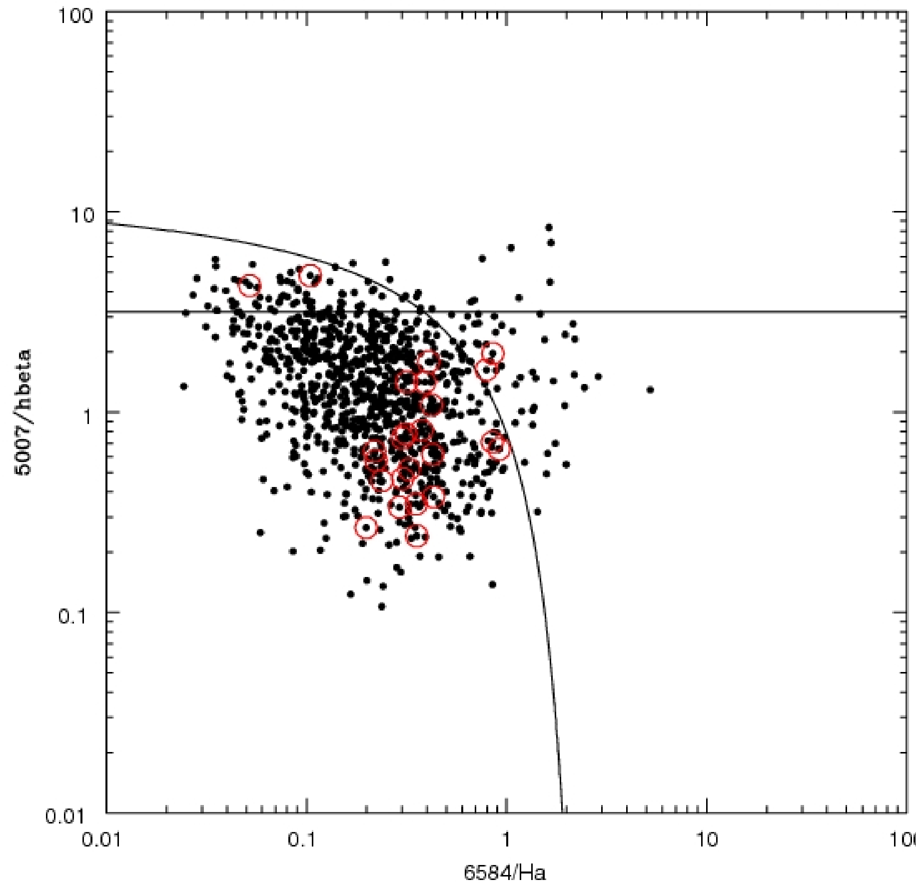

0.15<z<0.45
[OIII]/Hβ vs [SII]/Hα
[OIII]/Hβ vs [NII]/Hα

0.5<z<0.93
[OIII]/Hβ vs [OII]/Hβ

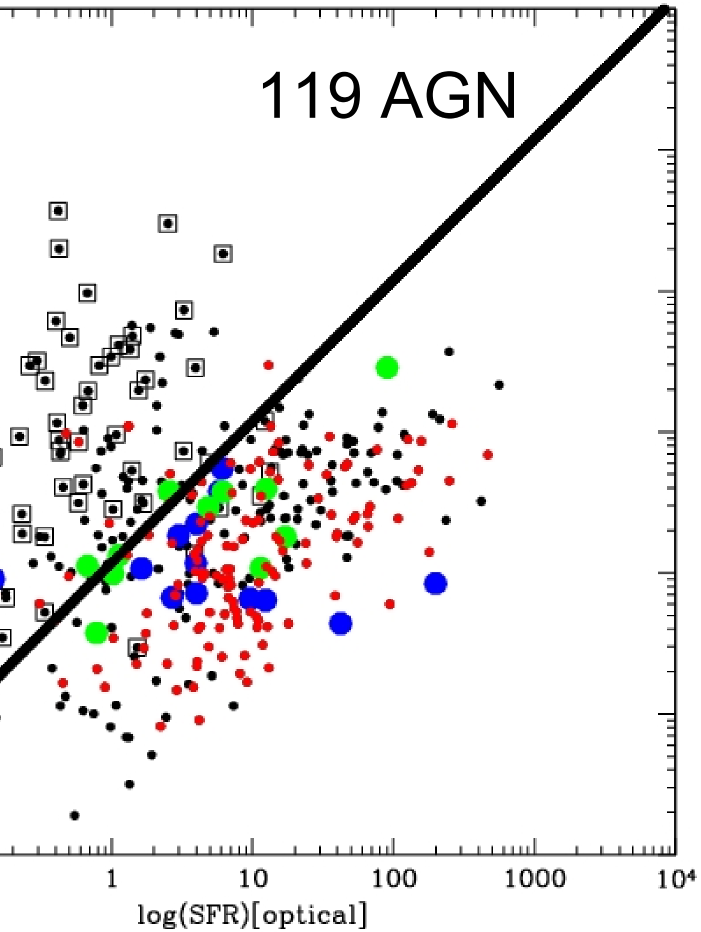

Only 15% of Sy and LINER in the “excess” area.

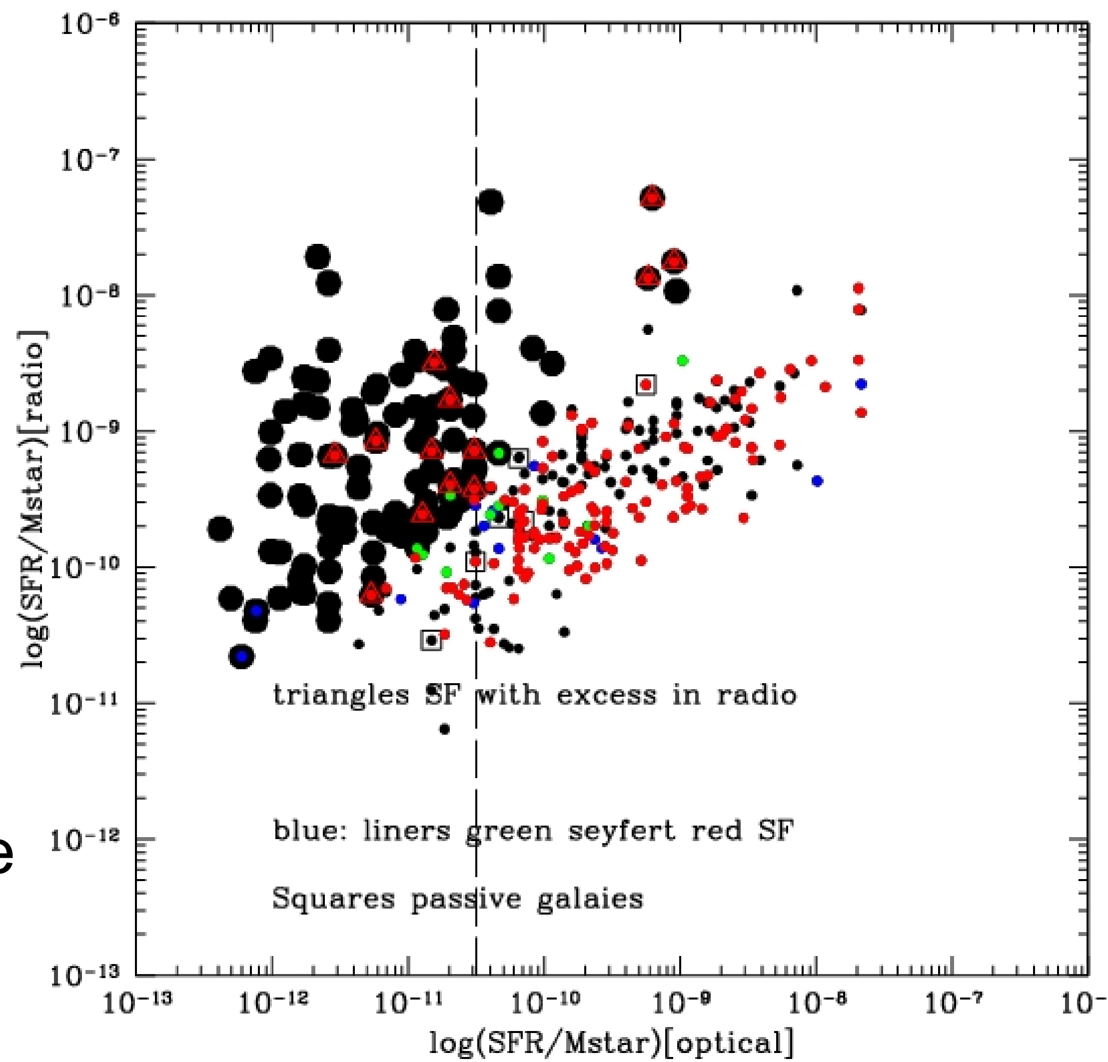

Among 133 SFR (from diagnostics) 13 are in the AGN area.

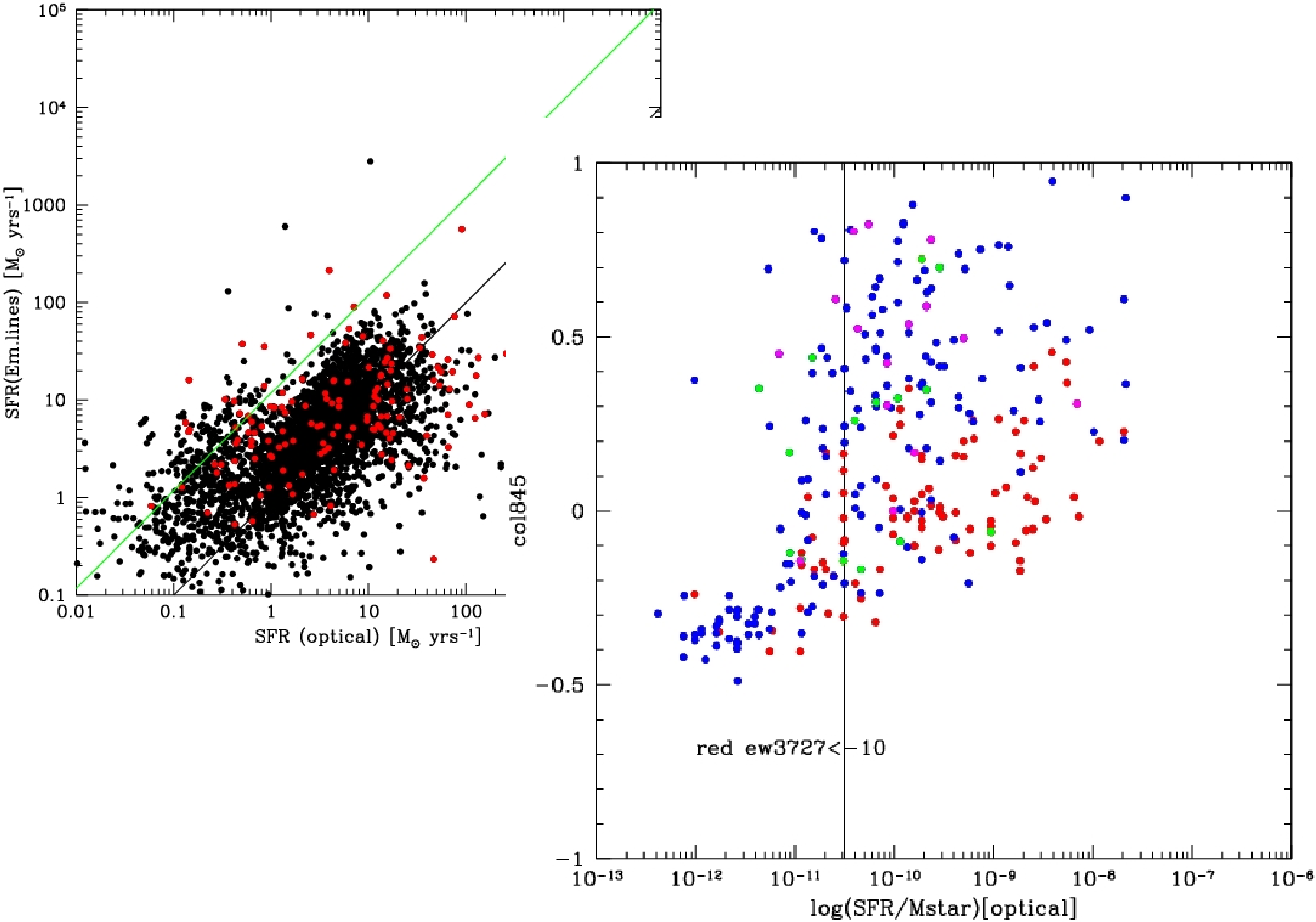

SFR(Em.lines) [M$_\odot$ yrs^{-1}]
SFR (optical) [M$_\odot$ yrs^{-1}]
col845
log(SFR/Mstar)[optical]
red ew3727<-10

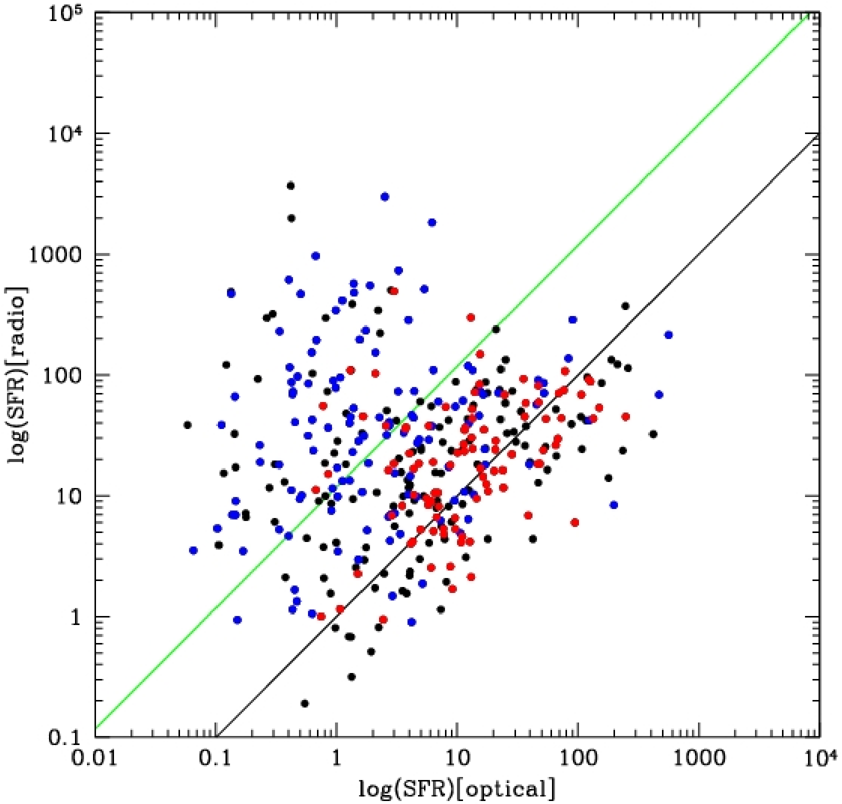

Smolcic et al (2008) Classification

Blue: AGN
Red :SFR

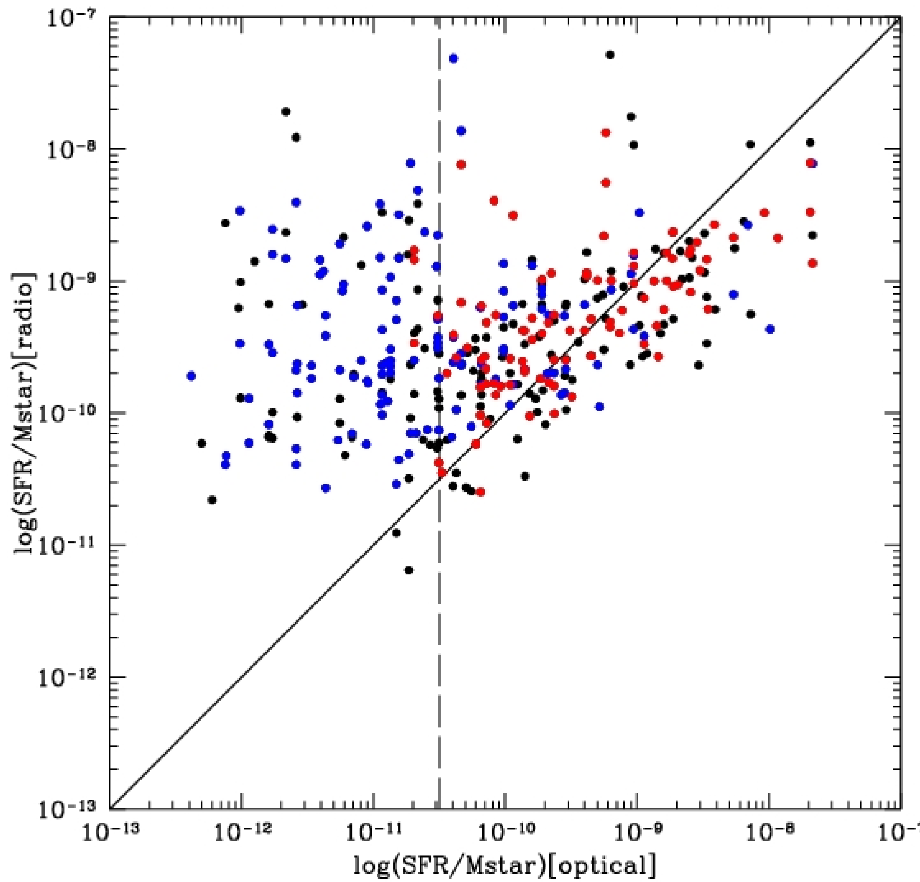

From 129 Smolcic's AGN 66 are in our AGN region

IR colors

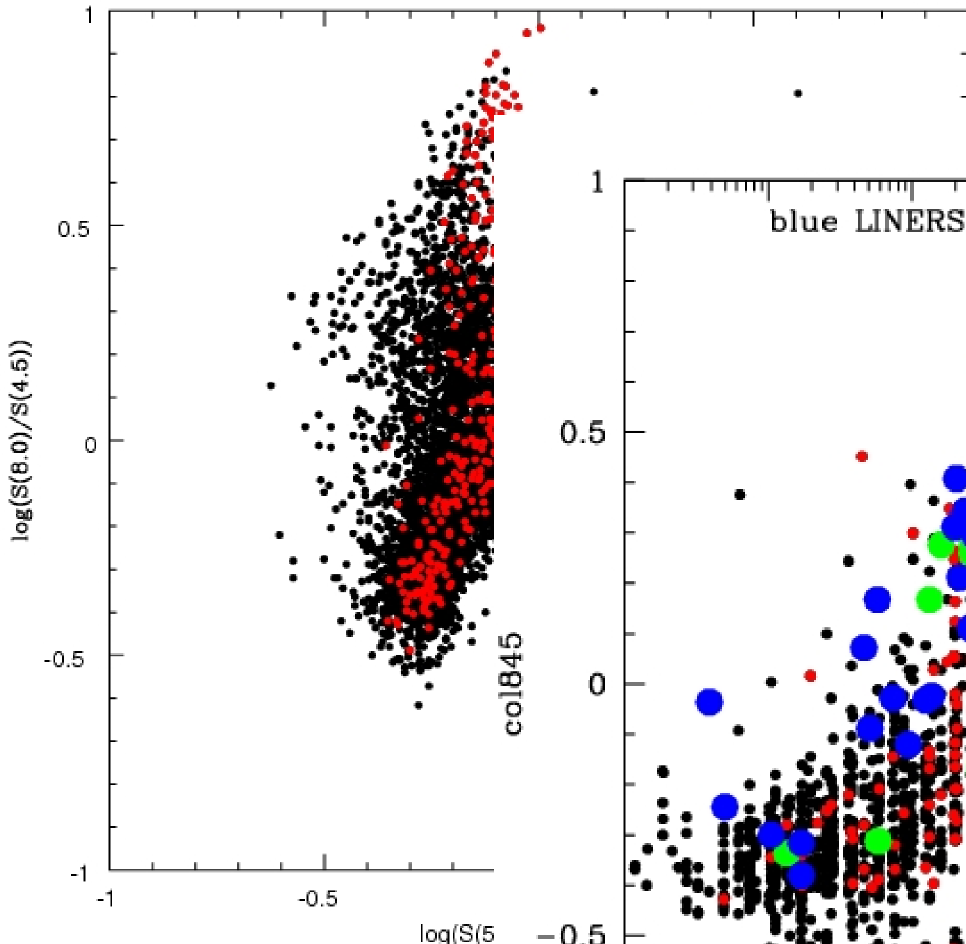

1
0.5
0
-0.5
-1
log(S(8.0)/S(4.5))
-1
-0.5
log(S(5

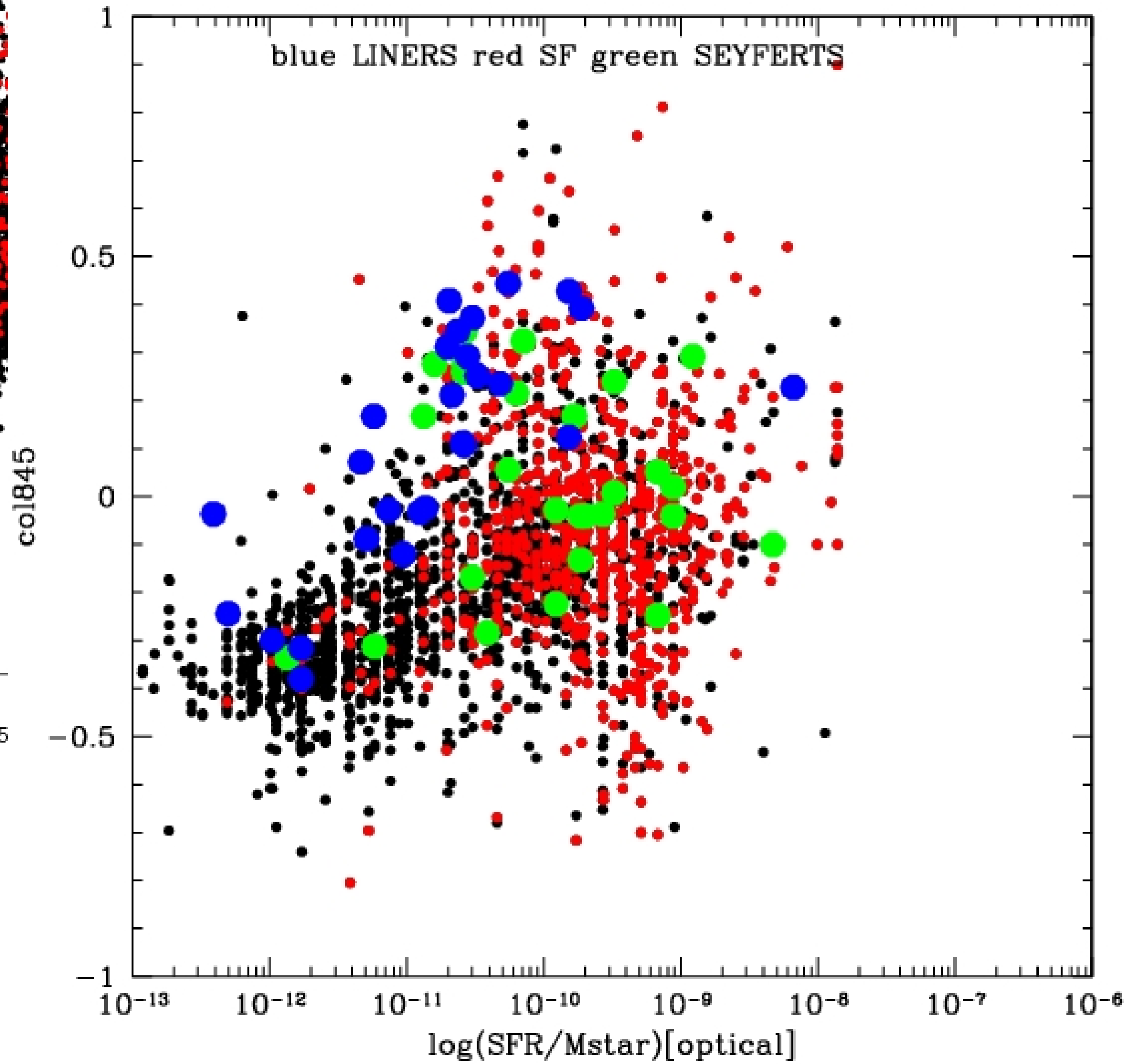

blue LINERS red SF green SEYFERTS
1
0.5
0
−0.5
−1
col845
10^{-13} 10^{-12} 10^{-11} 10^{-10} 10^{-9} 10^{-8} 10^{-7} 10^{-6}
log(SFR/Mstar)[optical]

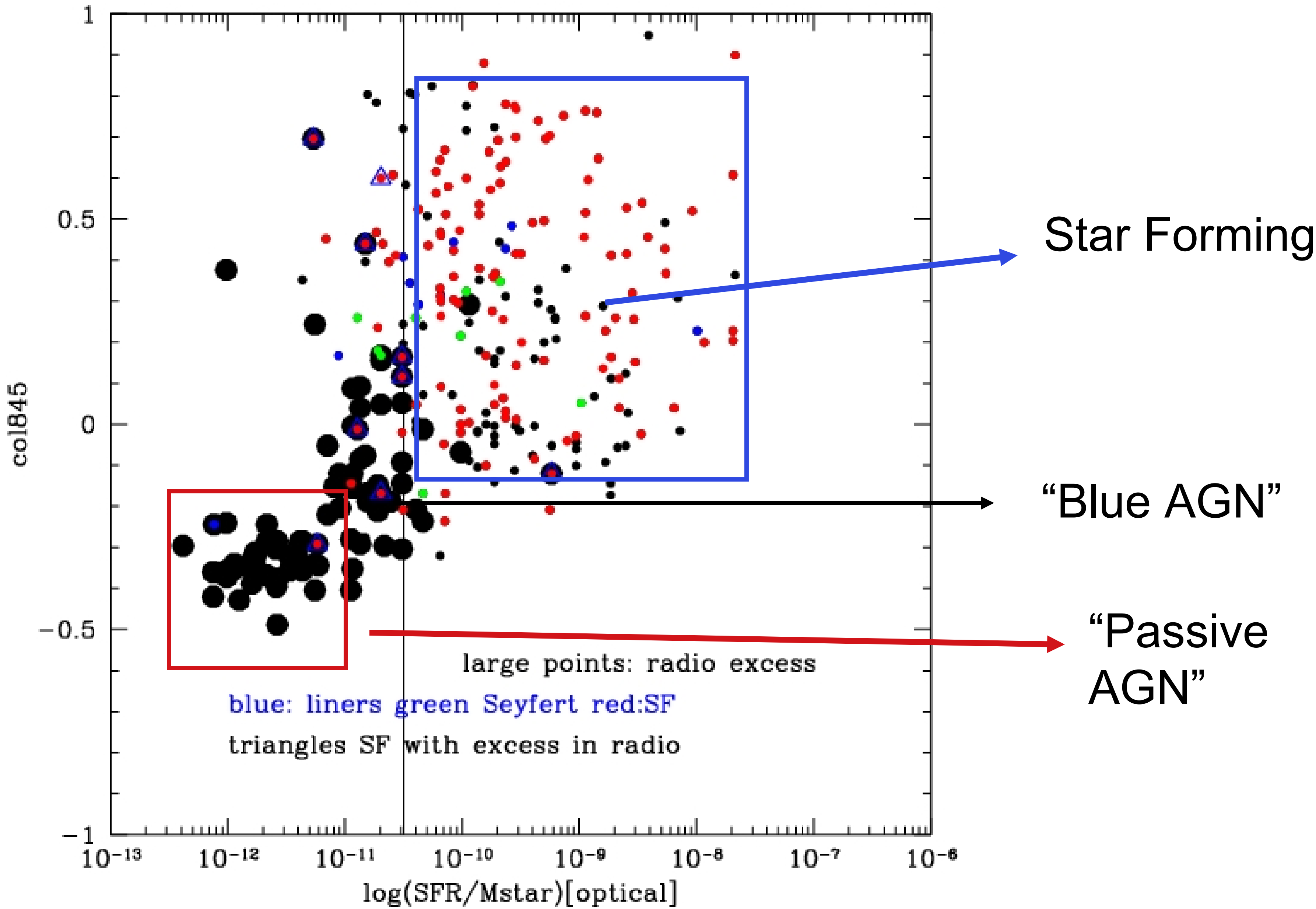

col845
log(SFR/Mstar)[optical]
large points: radio excess
blue: liners green Seyfert red:SF
triangles SF with excess in radio
Star Forming
"Blue AGN"
"Passive AGN"

“Passive AGN”

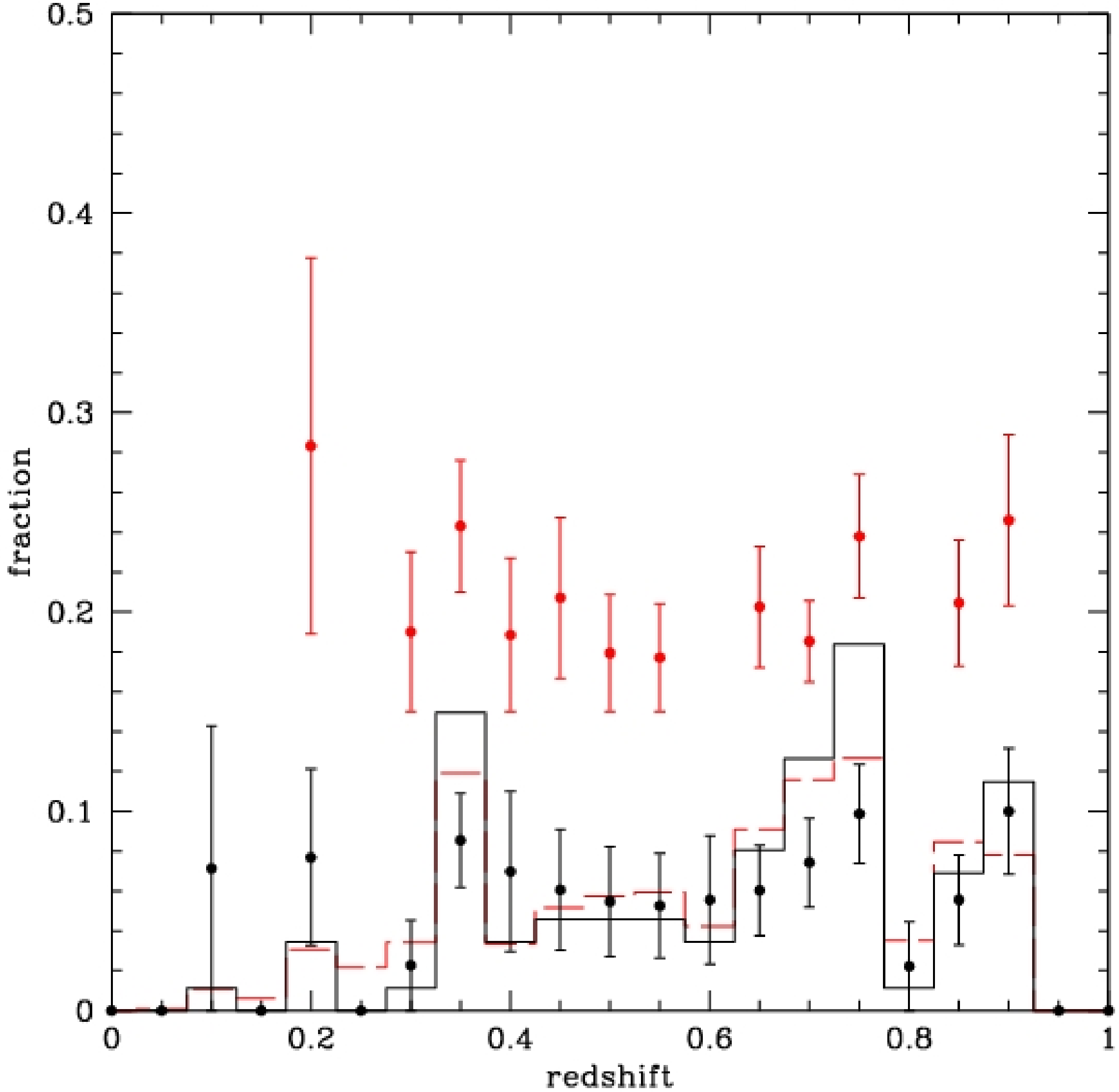

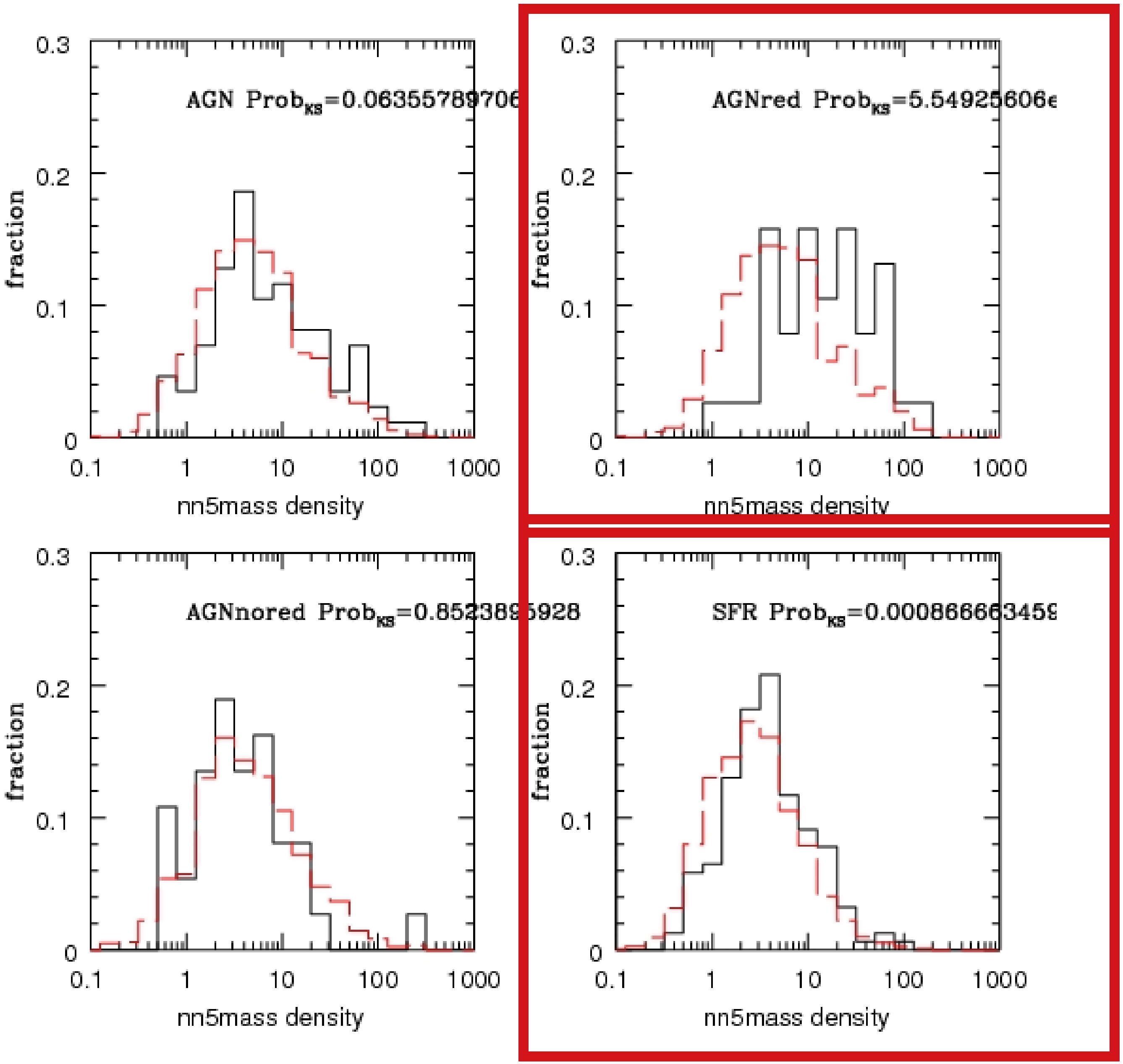
AGN $Prob_{KS}$=0.06355789706
AGNred $Prob_{KS}$=5.54925606e
AGNnored $Prob_{KS}$=0.8523895928
SFR $Prob_{KS}$=0.00086666345
fraction
nn5mass density
0.1
1
10
100
1000
0
0.1
0.2
0.3

SFR

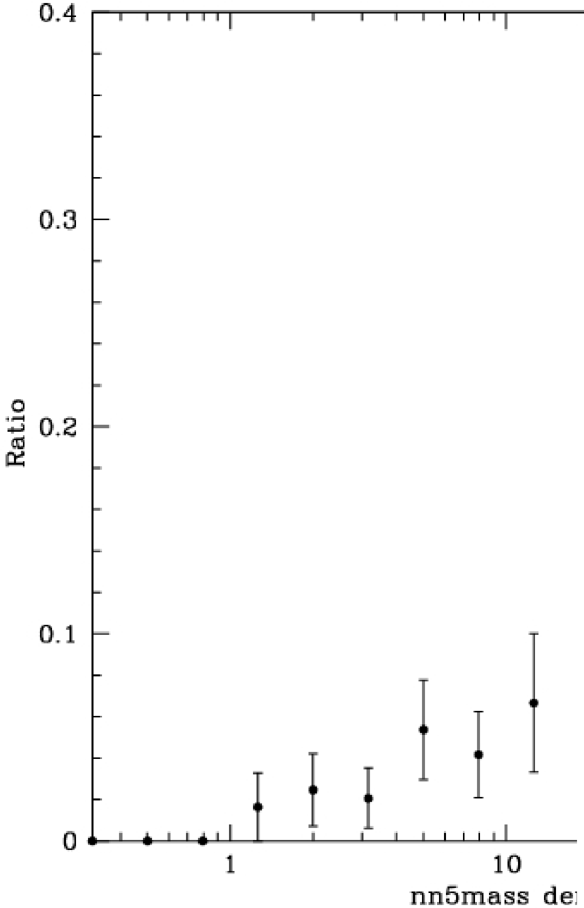

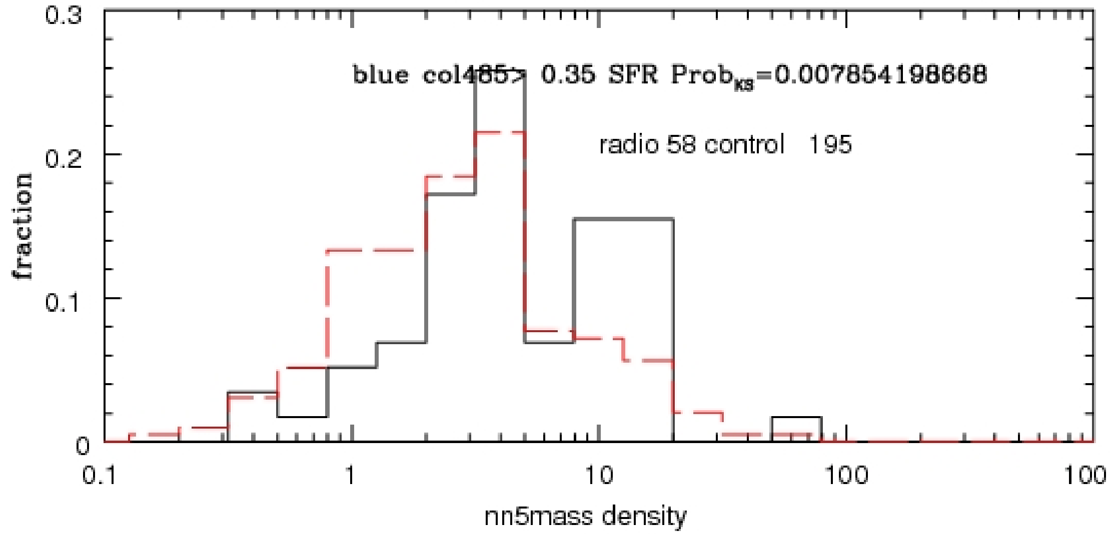

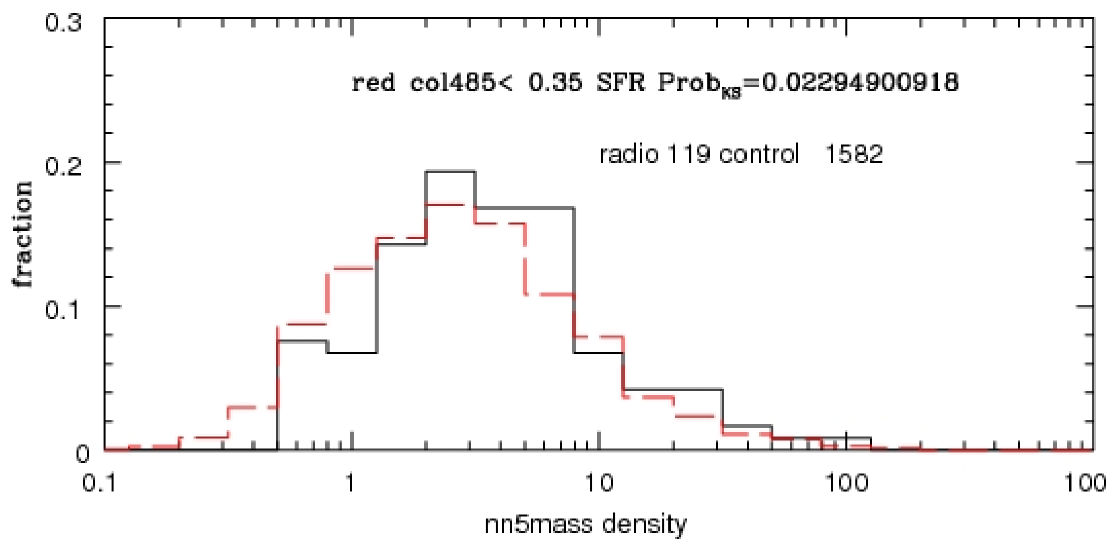

“Passive AGN”

Groups Multeplicity (Knobel et al. 2008)

Red Control sample
Black : Passive AGN

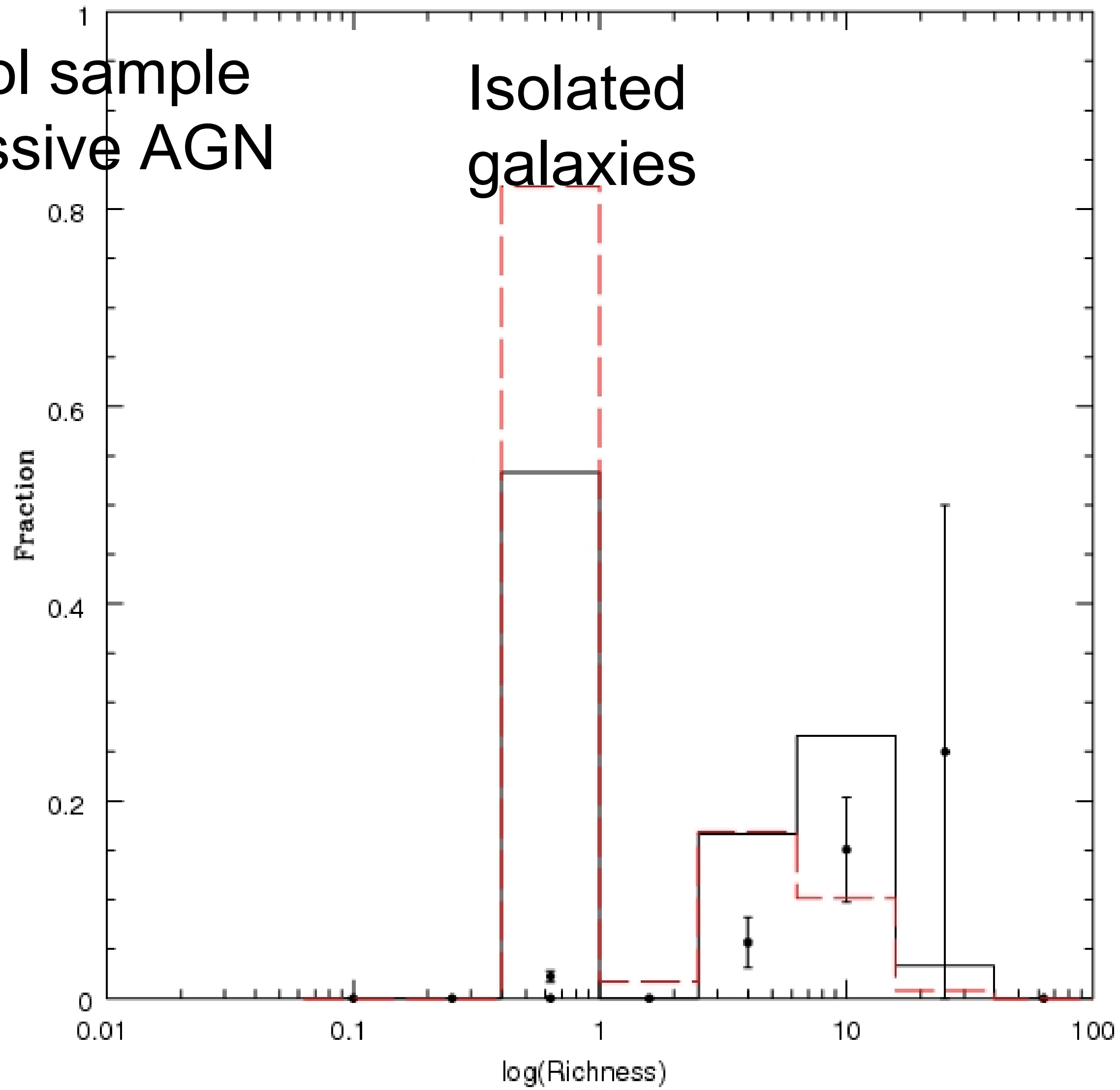

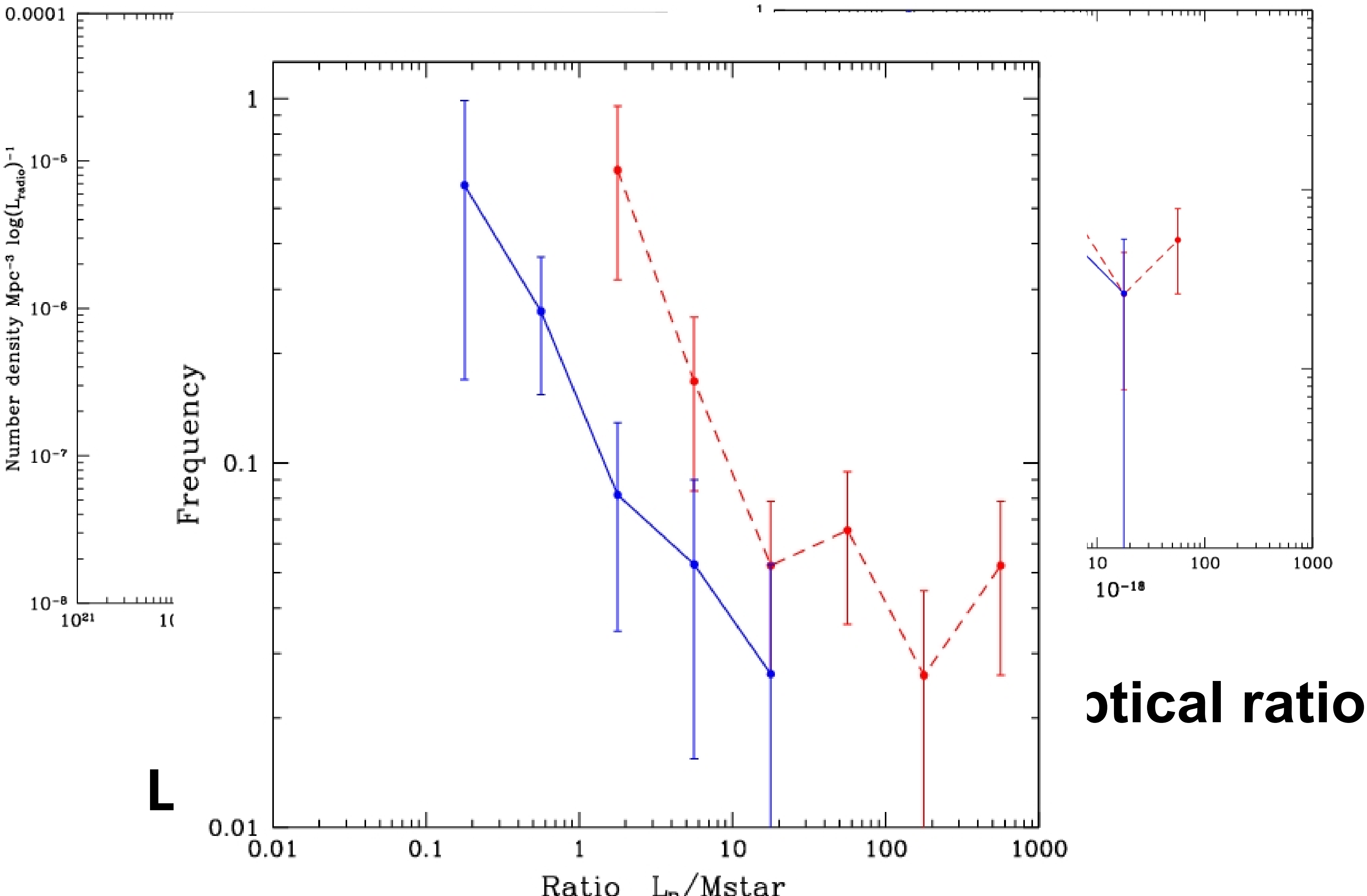

Radio-mass ratio

-Only the red “passive” AGN show a density dependency

-In higher environments the ratio between stellar mass and emissivity is higher (higher efficiency or more cooling?)

-Effect also for Star Forming galaxies

END

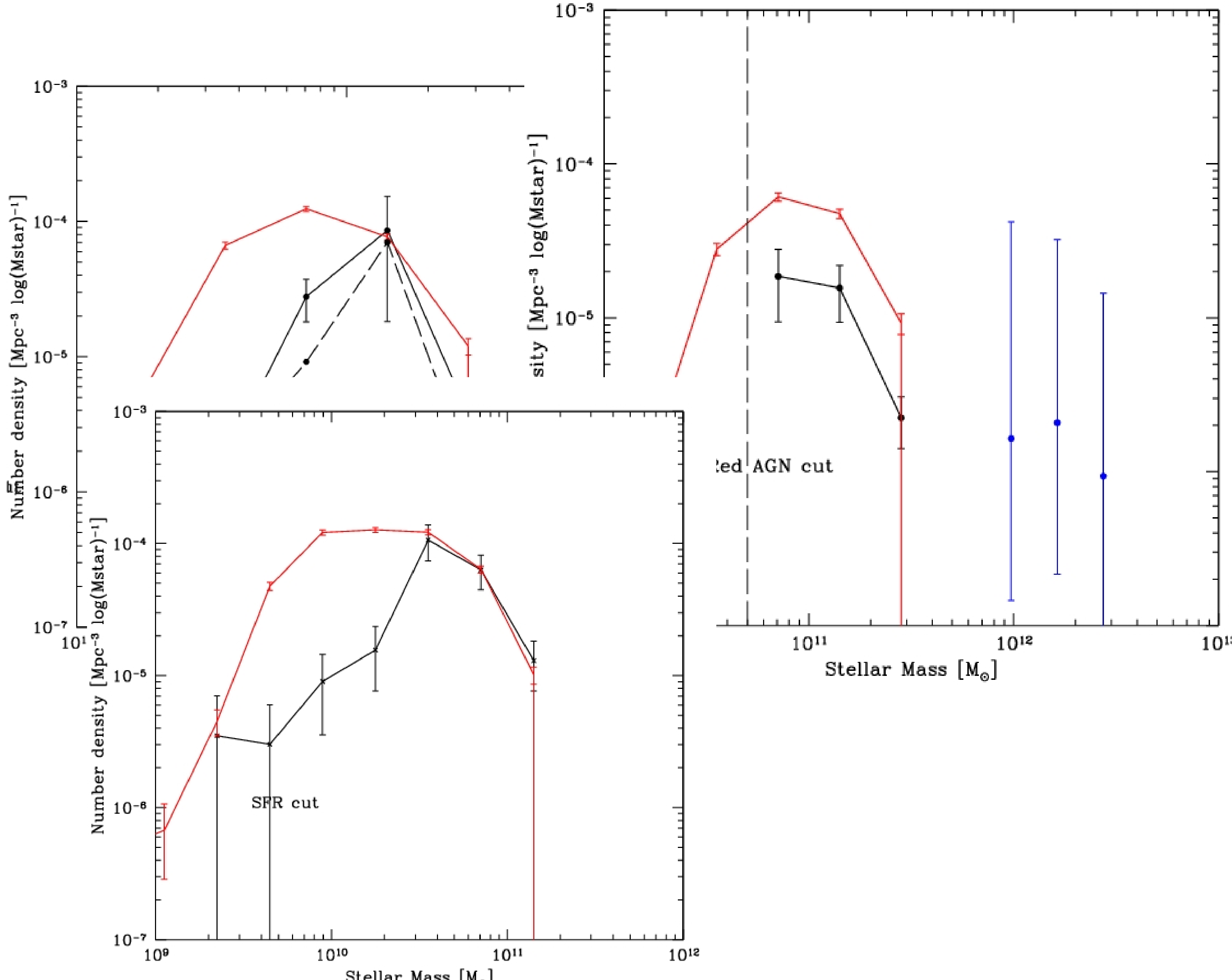

Number density [Mpc⁻³ log(Mstar)⁻¹]
Stellar Mass [M⊙]
ed AGN cut
SFR cut

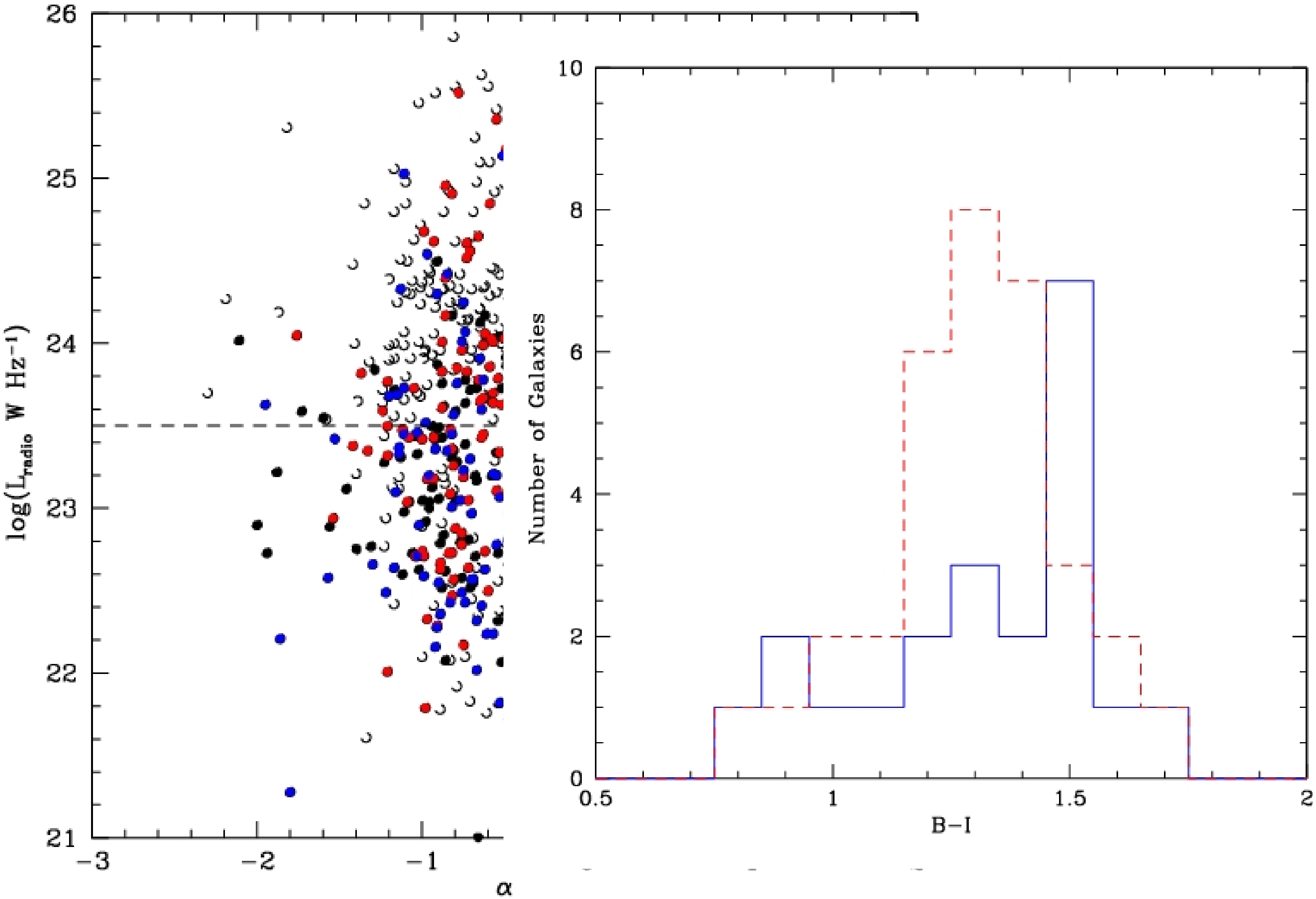

26
25
24
23
22
21
$\log(L_{radio}\ W\ Hz^{-1})$
−3
−2
−1
α
10
8
6
4
2
0
Number of Galaxies
0.5
1
1.5
2
B−I

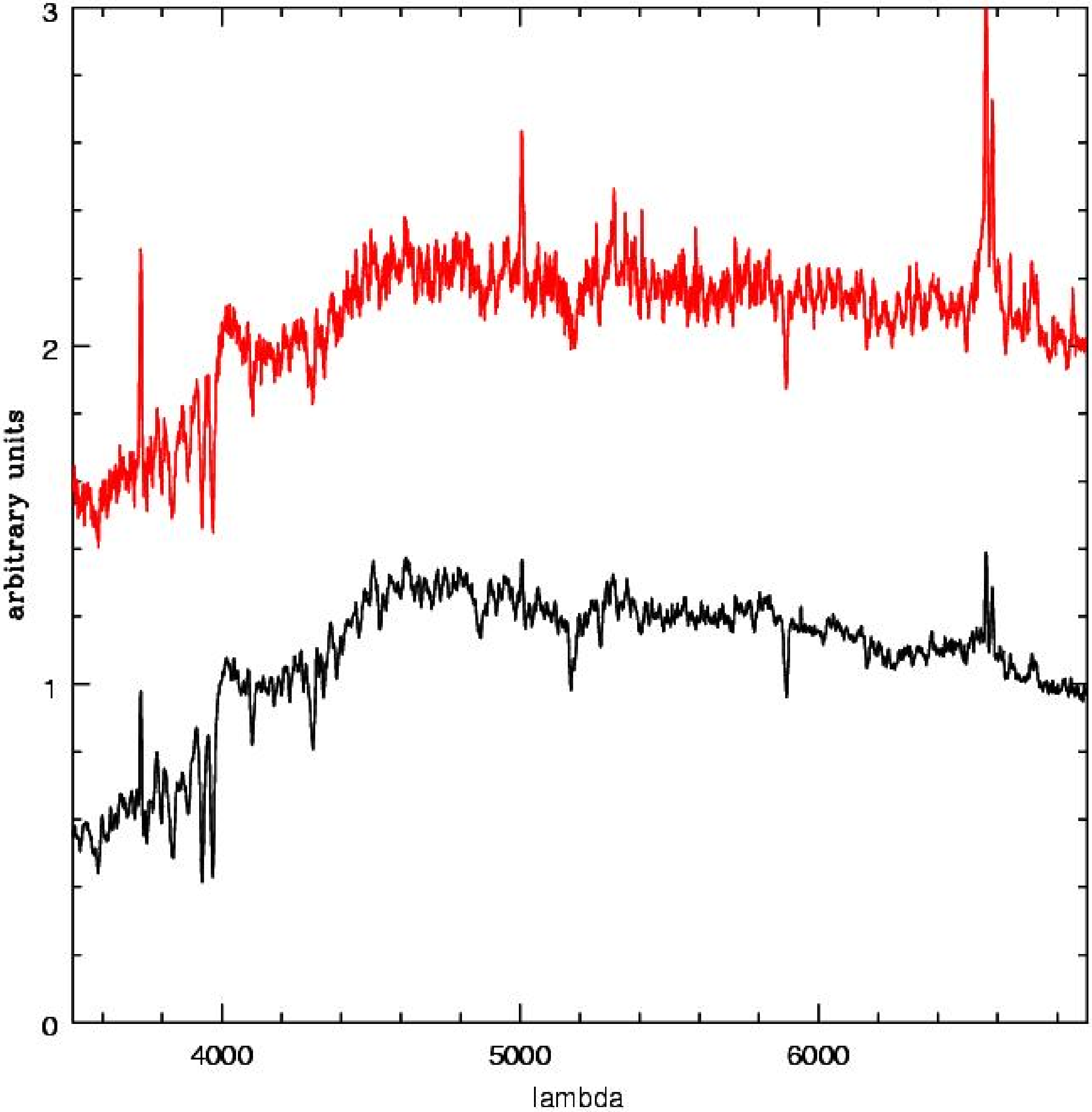

SPECTRA

Early type

Red: radio emission

Black: Control Sample

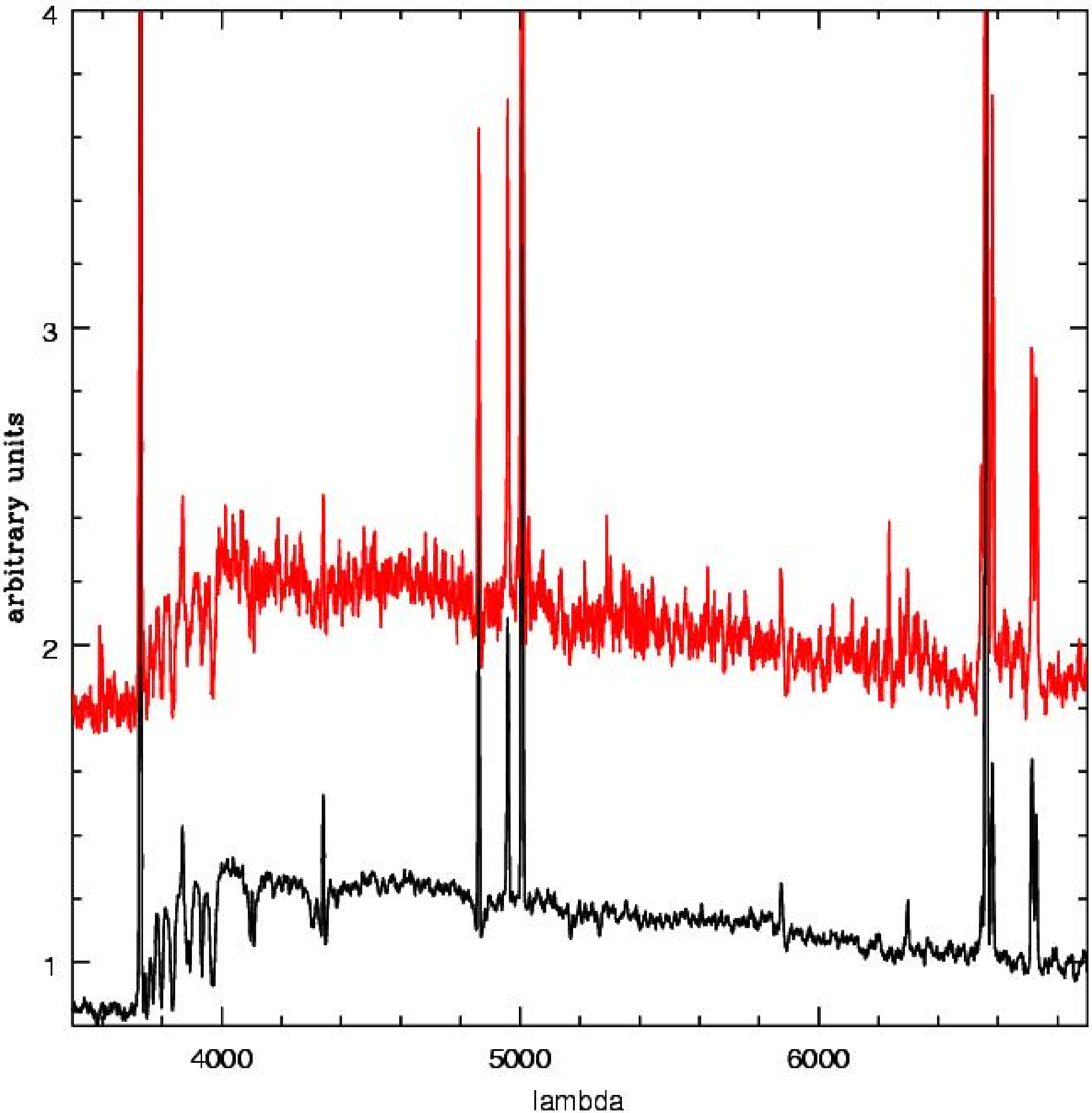

Late type

Red: radio emission

Black: Control Sample

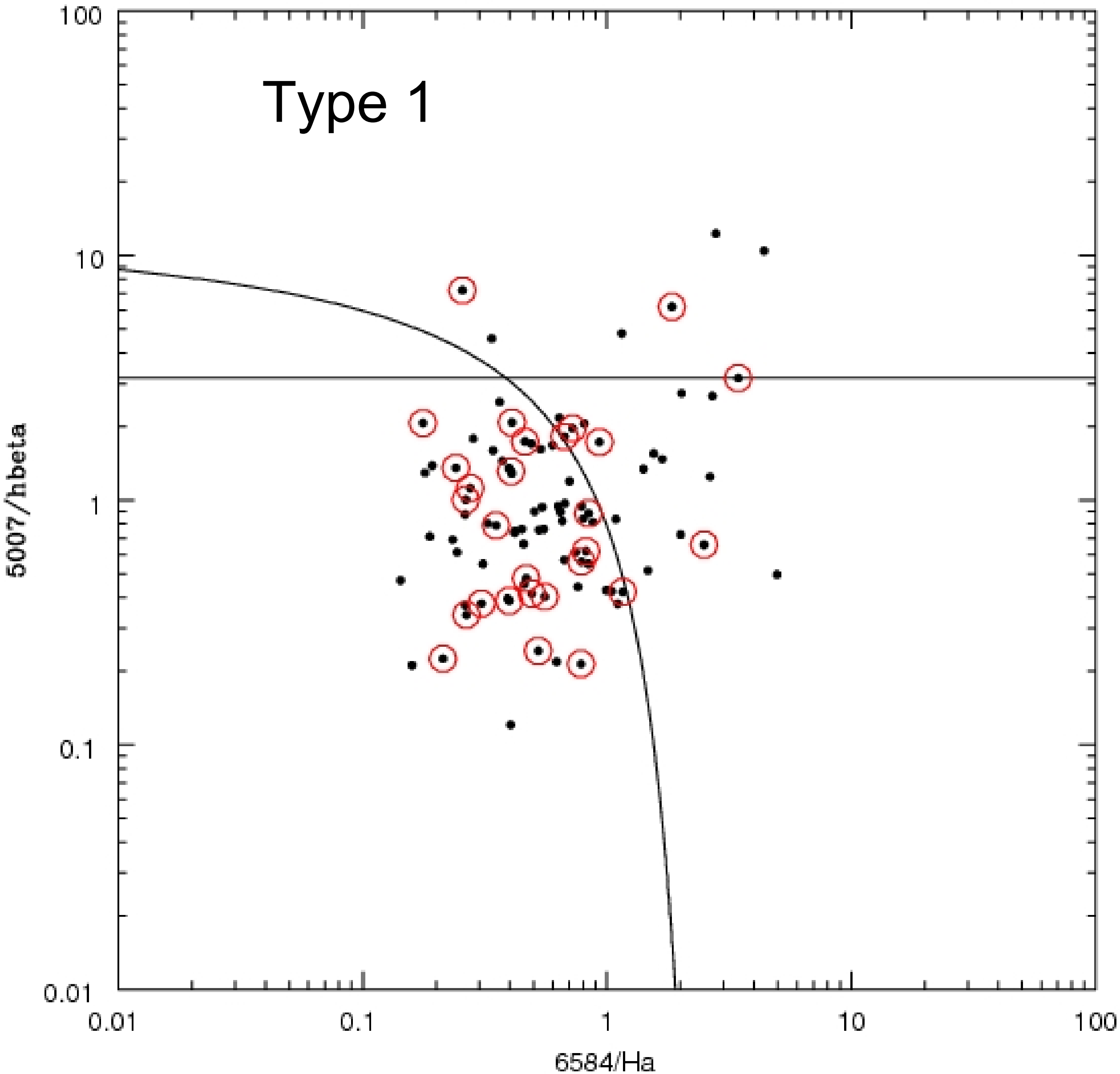

91 detected
1882 all
(5%)
Sy (8%-0.4 %)
Liners (17%-0.8%)
Star forming
3.6%
Radio:
28 detected
146 all
(20%)

Sy (7%-1.4 %)
Liners (14%-3%)
Star forming
13%

TYPE 1

	RADIO SAMPLE	CONTROL SAMPLE
	73	879
SF	18% ± 4	6% ± 0.4
Sey2	5% ± 2	1% ± 0.3
LINER	5 % ± 2	2% ± 0.4

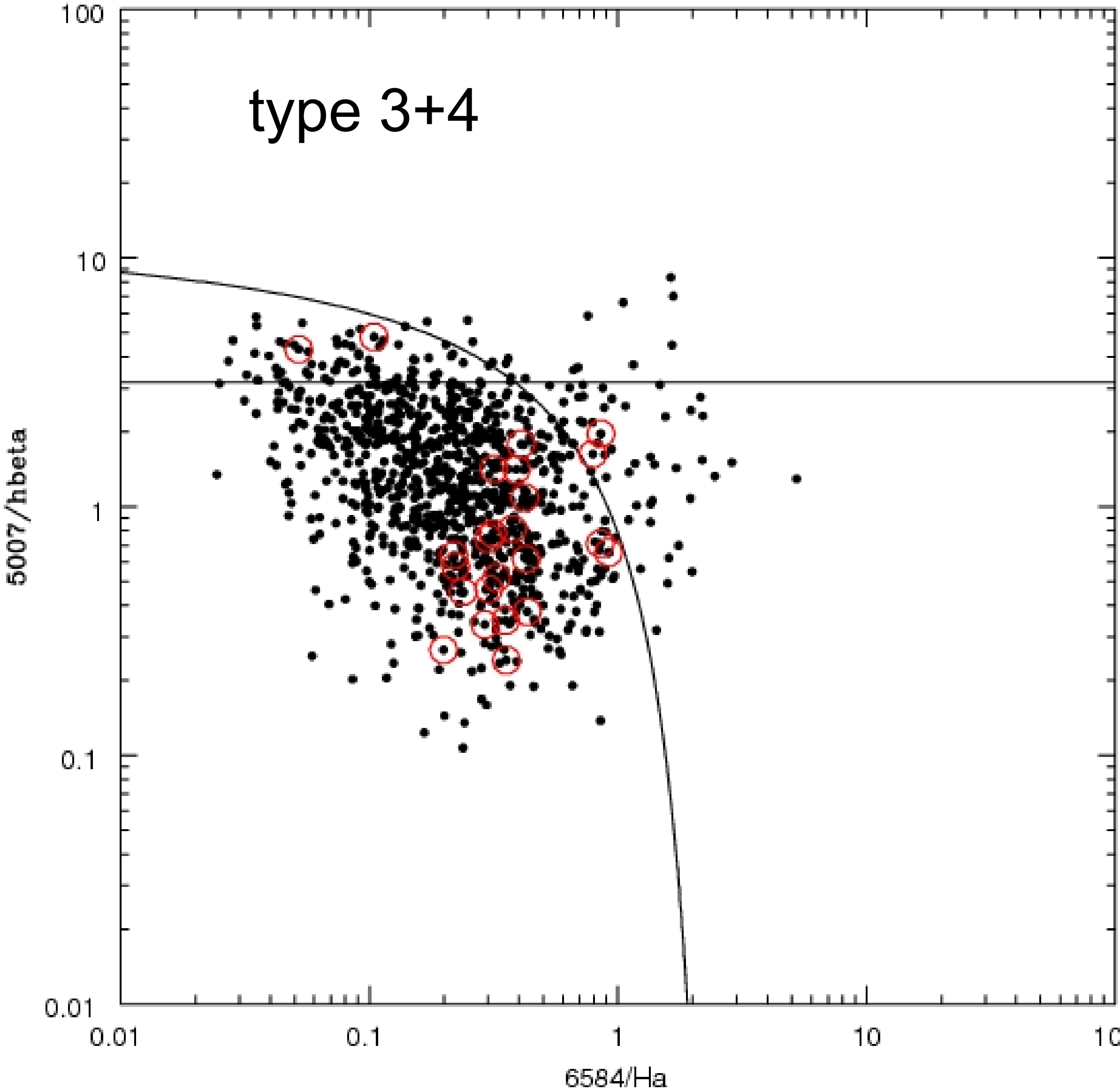

988 detected
4417 all
(22 %)
Sy (1.7 %-0.4 %)
Liners (4.5 %-0.4 %)
SF
(94 %)

Radio
25 detected
73 all
(34 %)
Sy none
Liners (8 %-2.7 %)
SF
(92 %)

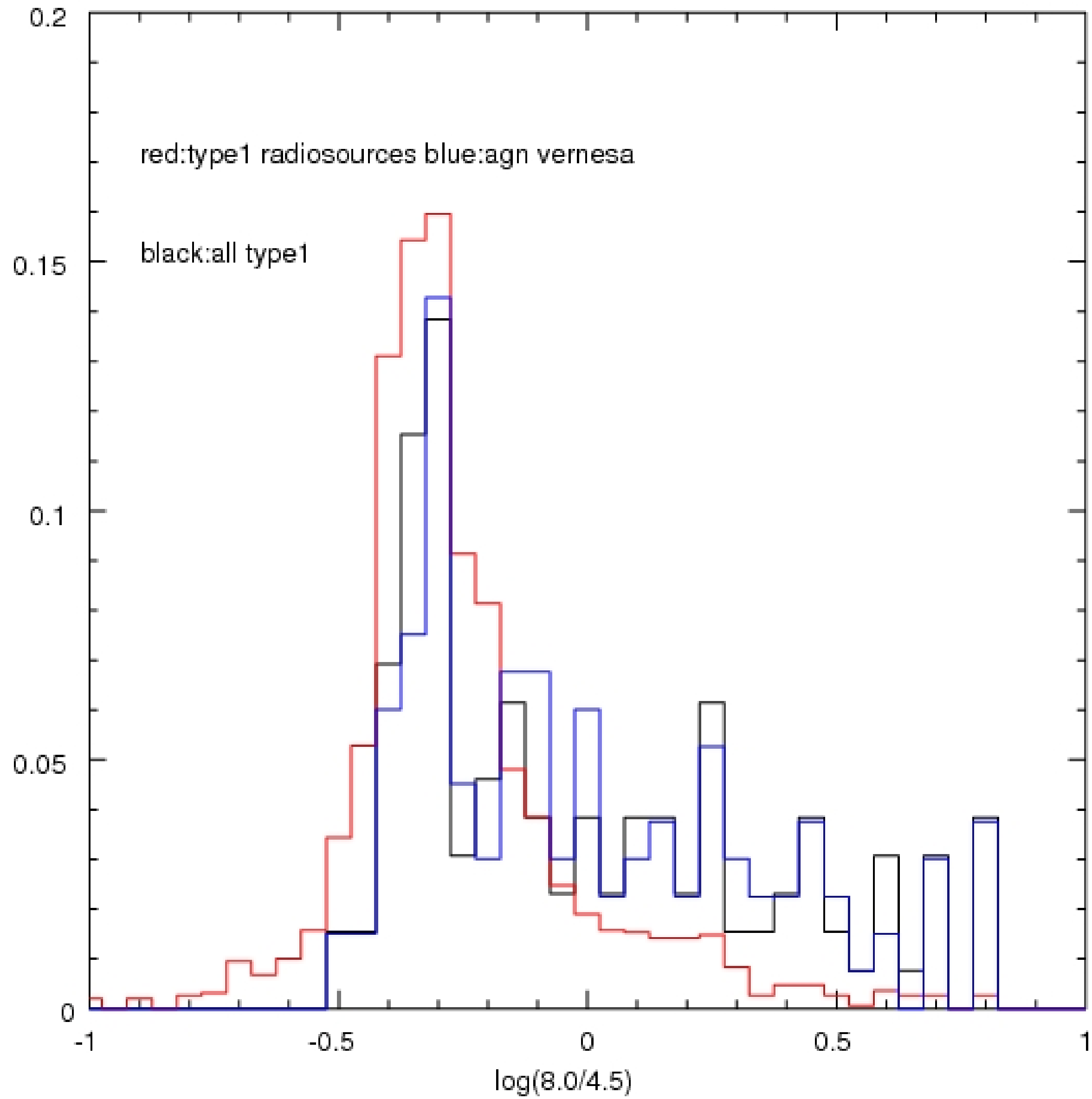

red:type1 radiosources blue:agn vernesa
black:all type1
0.2
0.15
0.1
0.05
0
-1
-0.5
0
0.5
1
log(8.0/4.5)

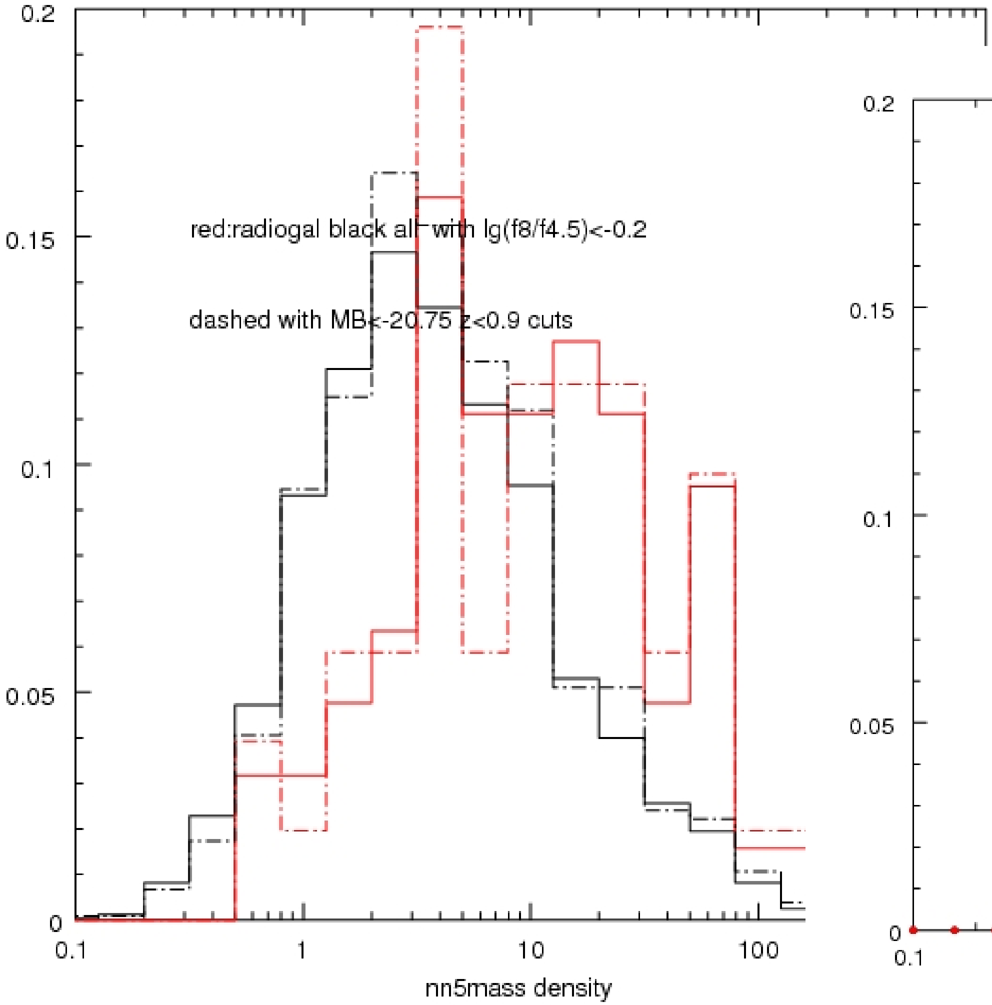
red:radiogal black all with lg(f8/f4.5)<-0.2
dashed with MB<-20.75 z<0.9 cuts
0.2
0.15
0.1
0.05
0
0.1
1
10
100
nn5mass density

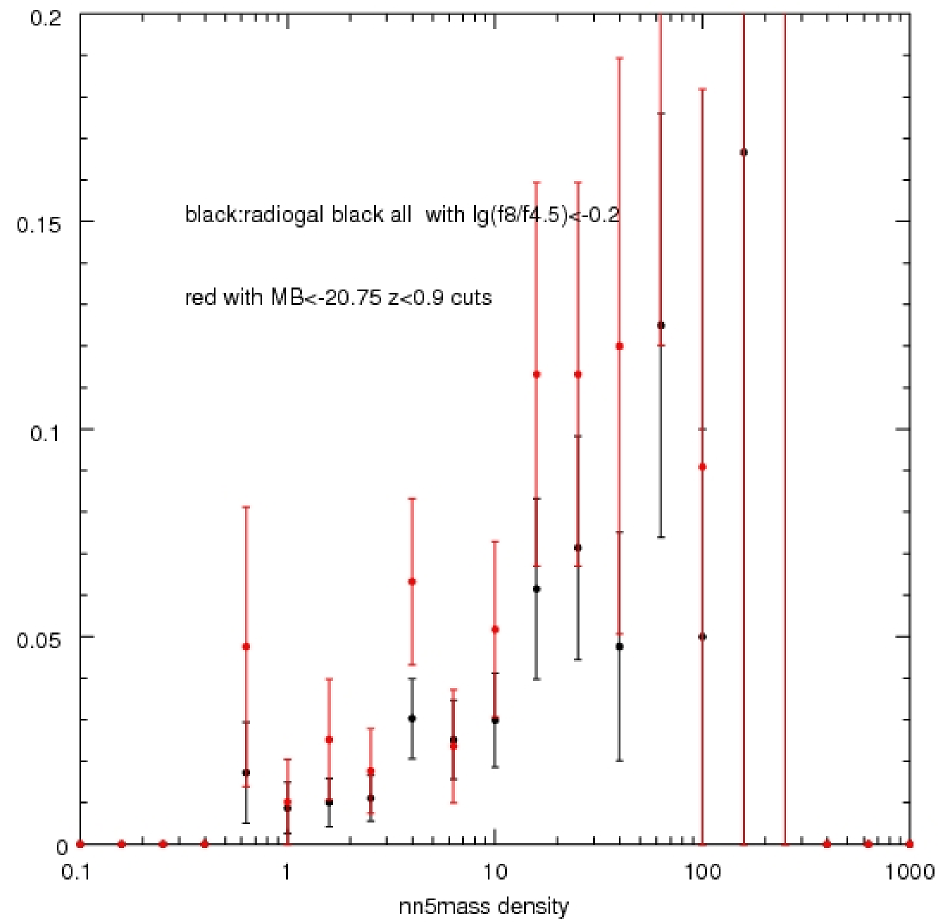
black:radiogal black all with lg(f8/f4.5)<-0.2
red with MB<-20.75 z<0.9 cuts
0.2
0.15
0.1
0.05
0
0.1
1
10
100
1000
nn5mass density

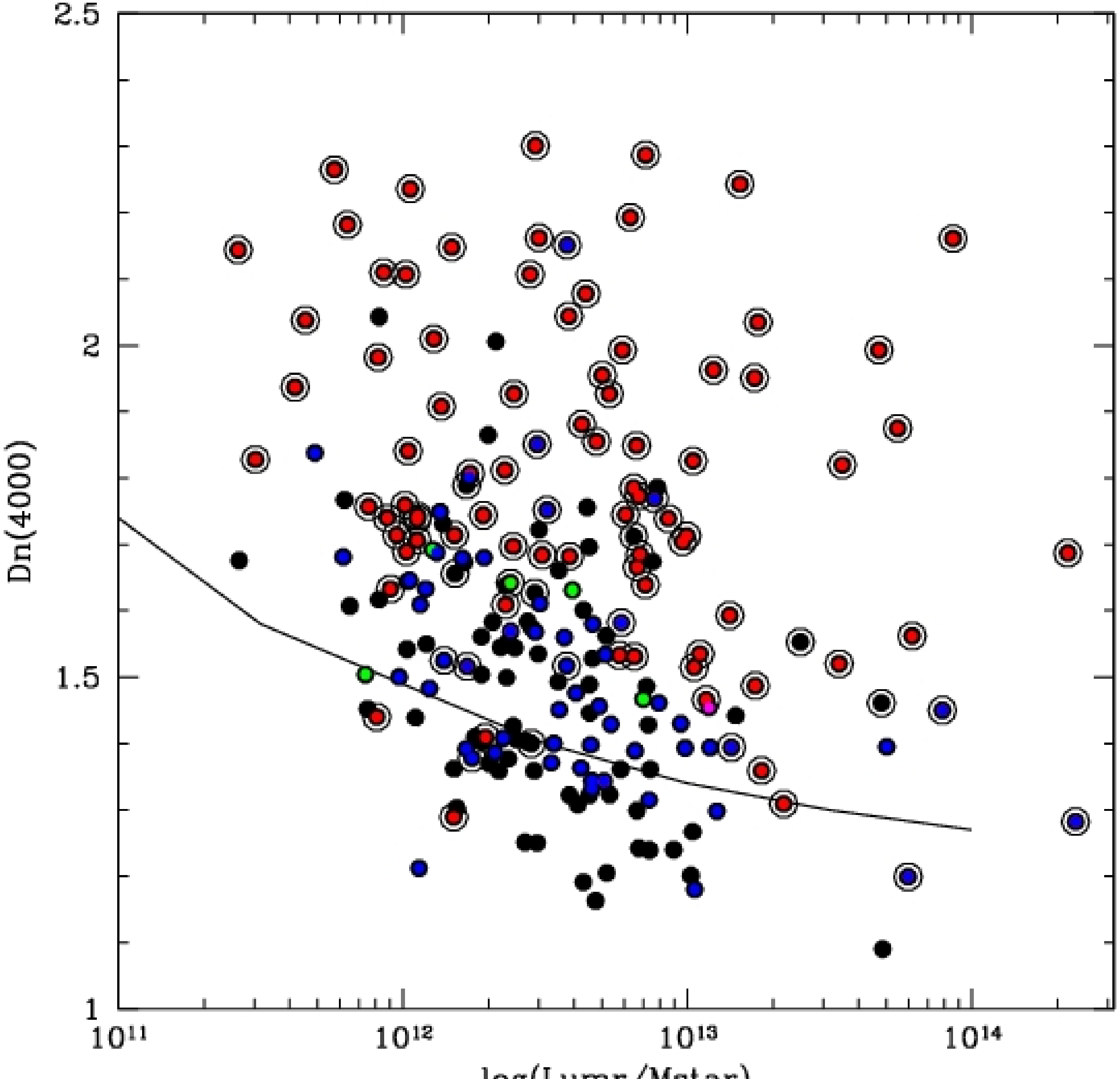

2.5
2
1.5
1
Dn(4000)
10^{11}
10^{12}
10^{13}
10^{14}
log(Lumr/Mstar)

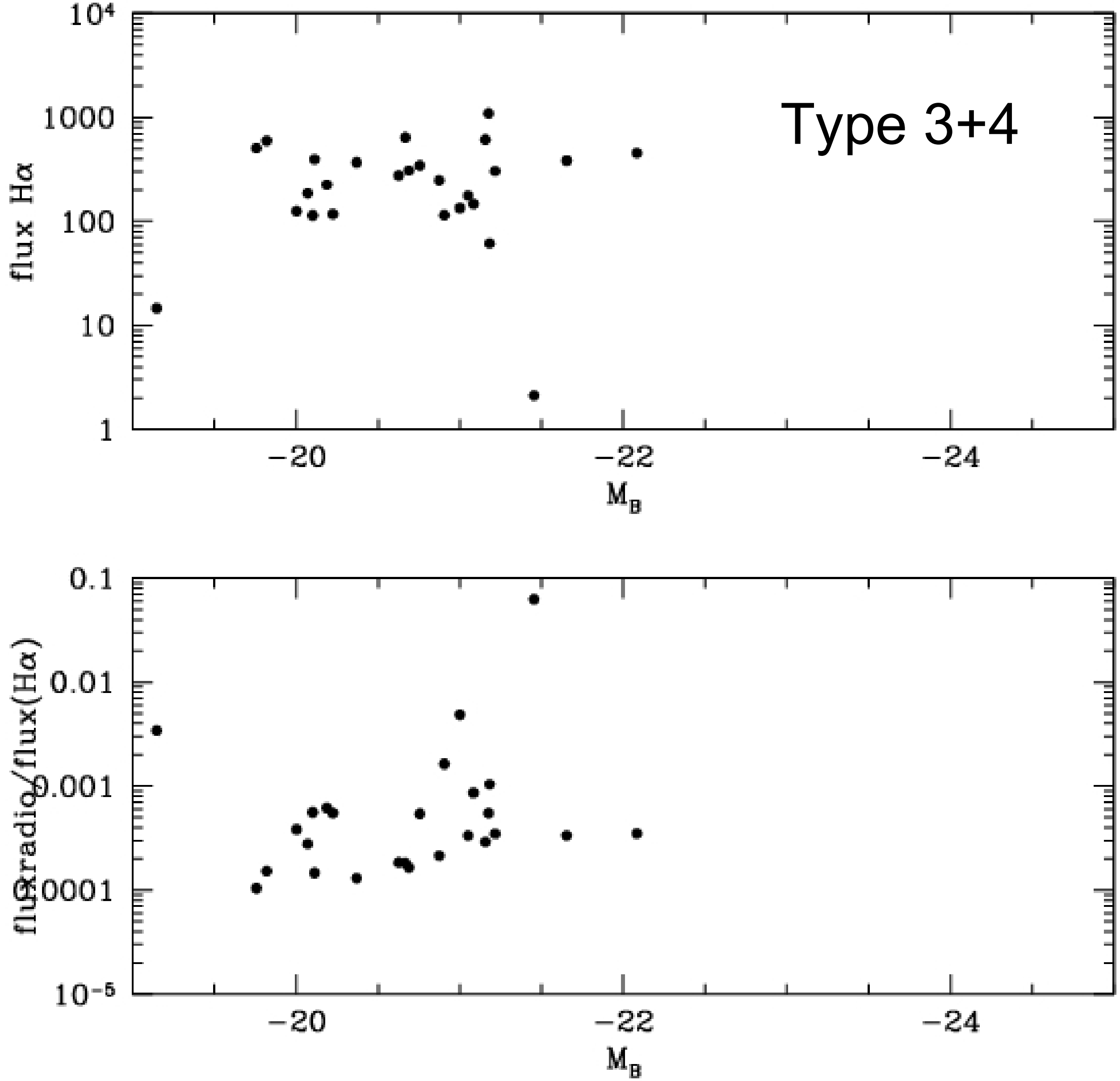
Type 3+4
flux Hα
MB
flux radio/flux(Hα)
MB

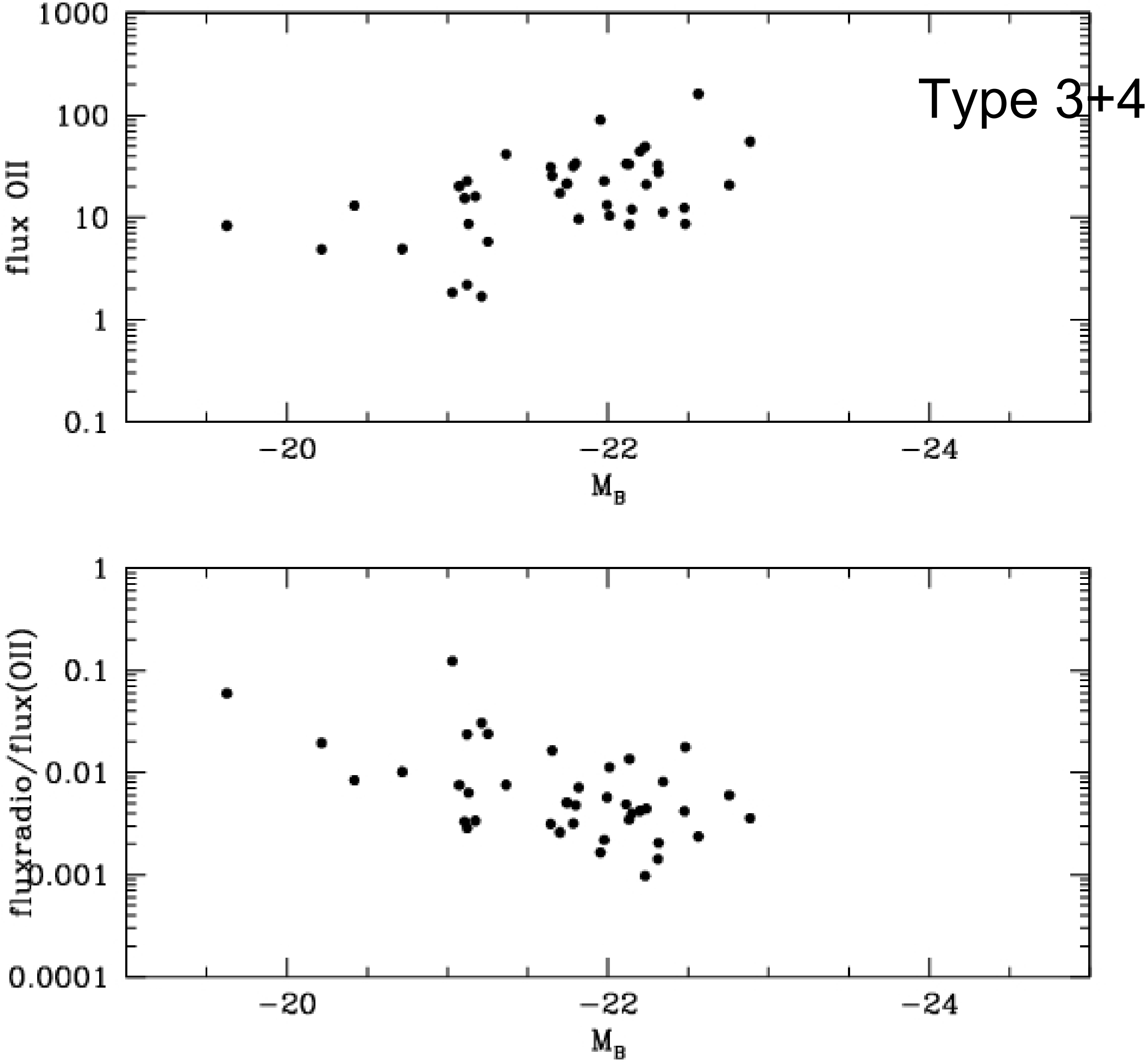
Type 3+4
flux OII
1000
100
10
1
0.1
−20
−22
−24
M_B
fluxradio/flux(OII)
1
0.1
0.01
0.001
0.0001
−20
−22
−24
M_B

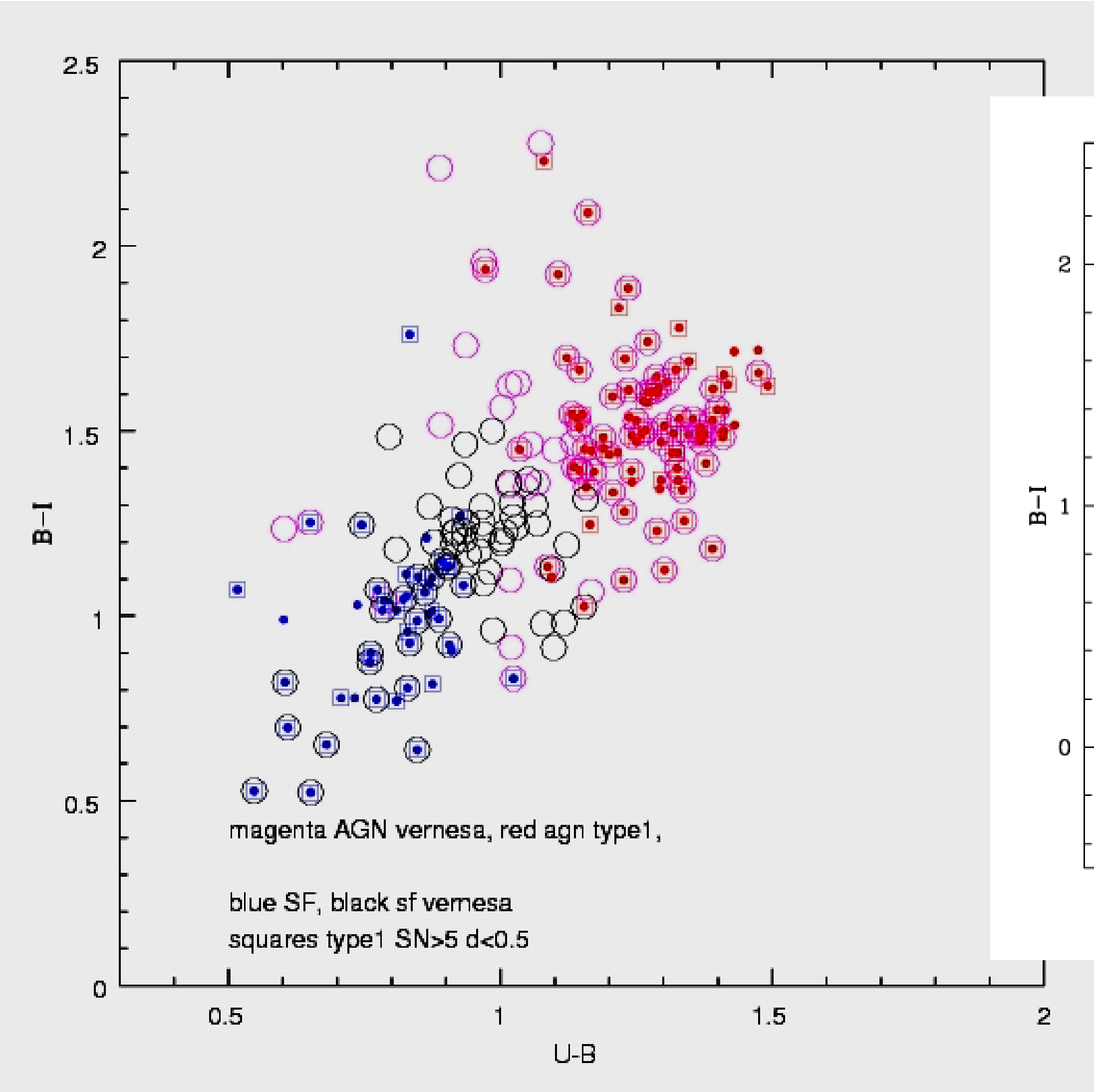
2.5
2
1.5
1
0.5
0
B-I
0.5
1
1.5
2
U-B
magenta AGN vernesa, red agn type1,
blue SF, black sf vernesa
squares type1 SN>5 d<0.5

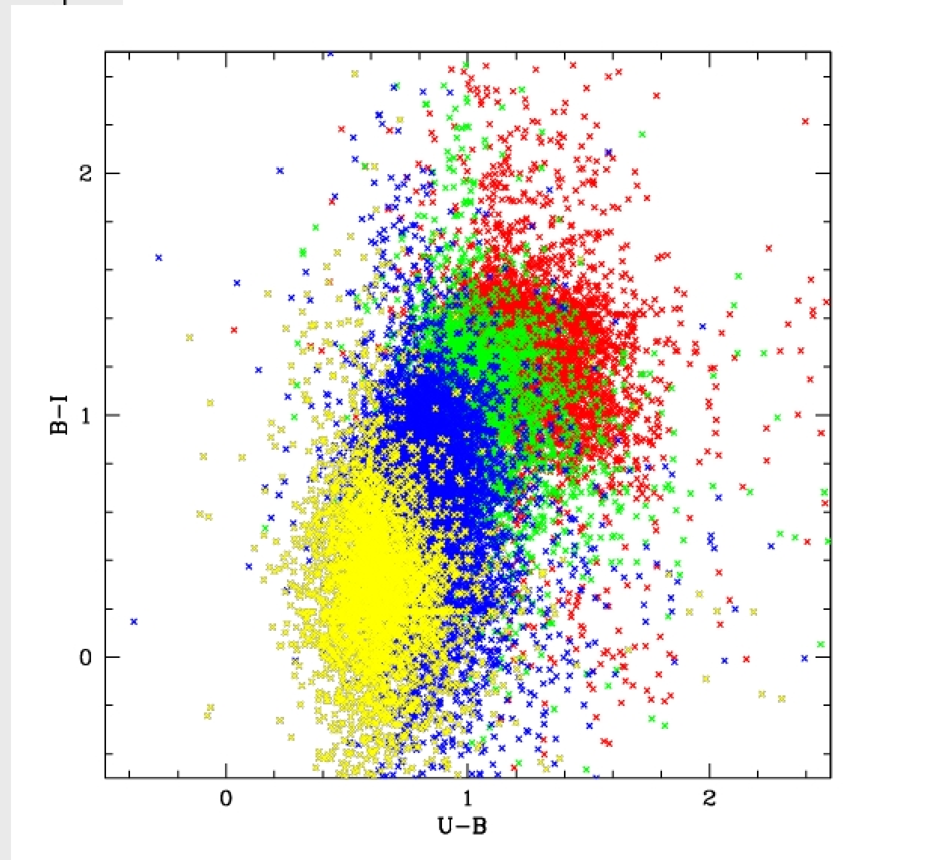
2
1
0
B−I
0
1
2
U−B

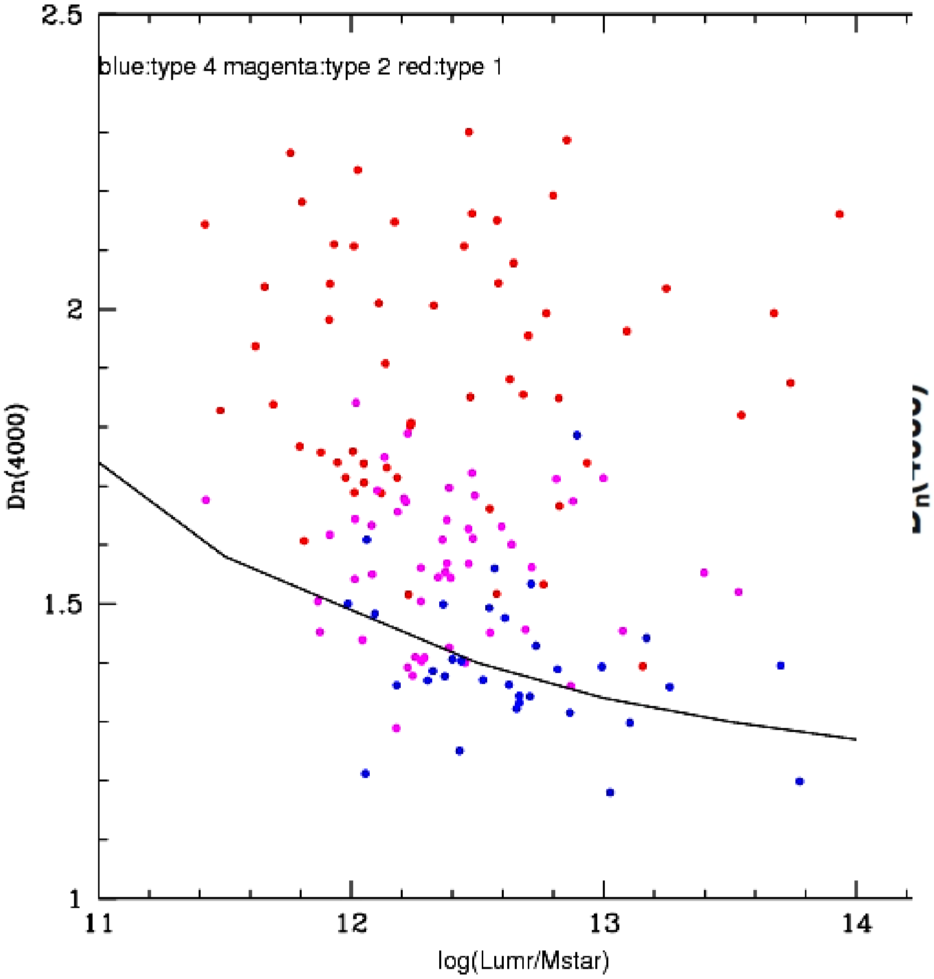

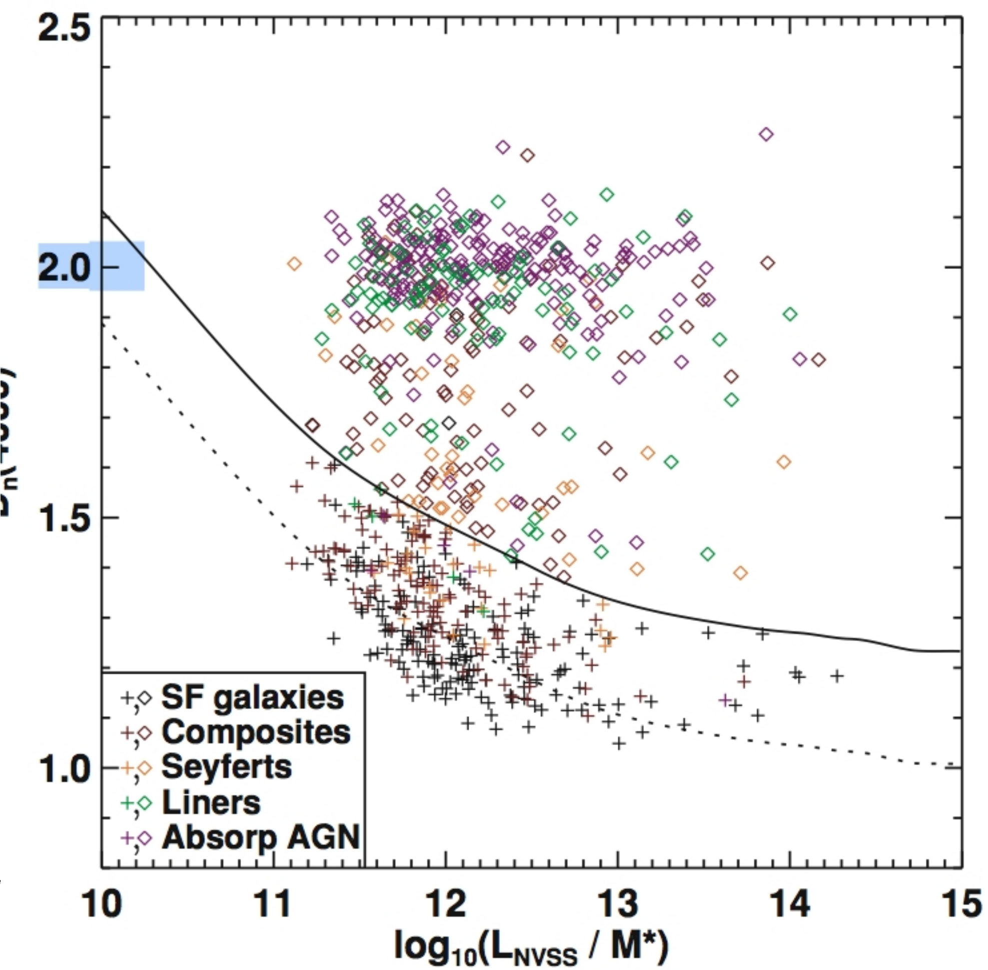

Best et al
(2005)

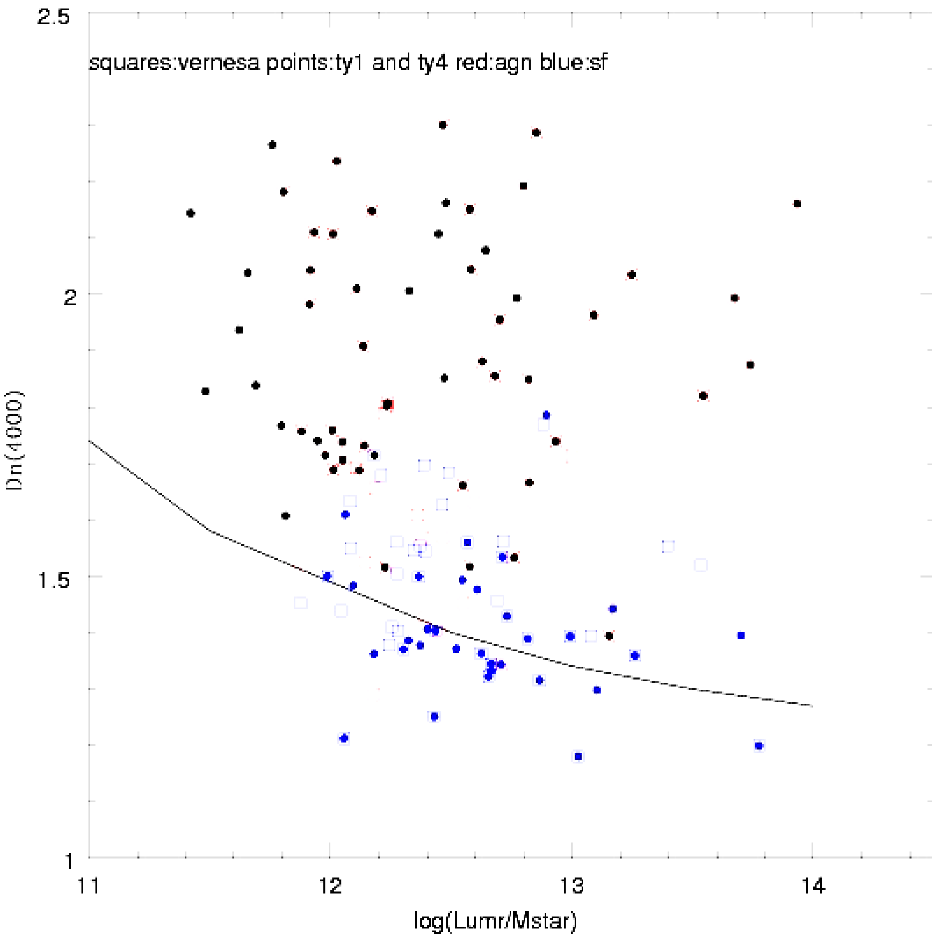

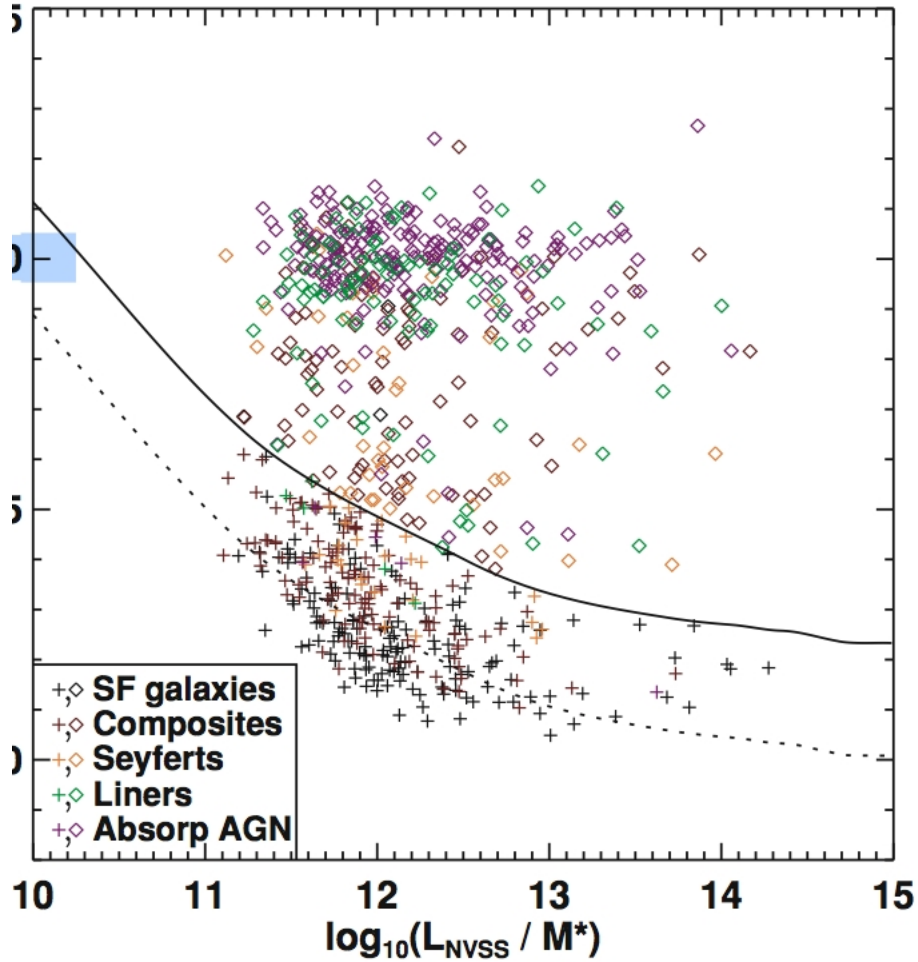

Best et al
(2005)

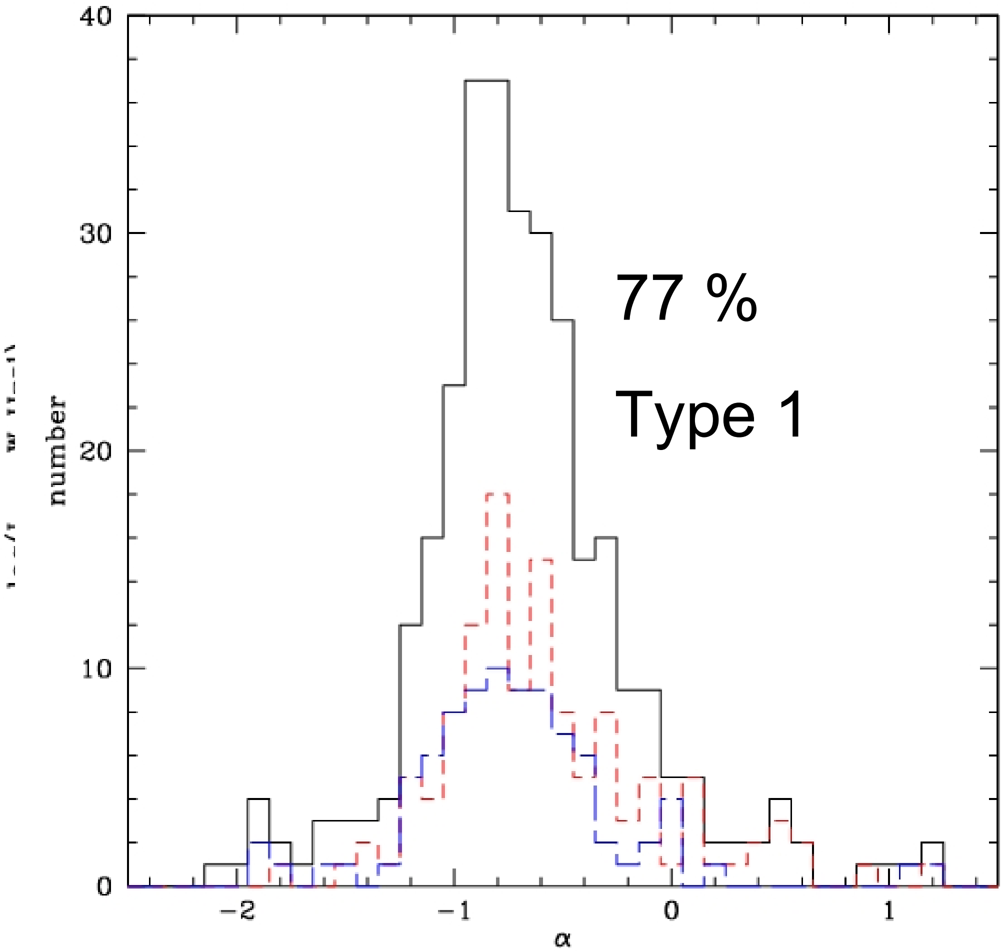

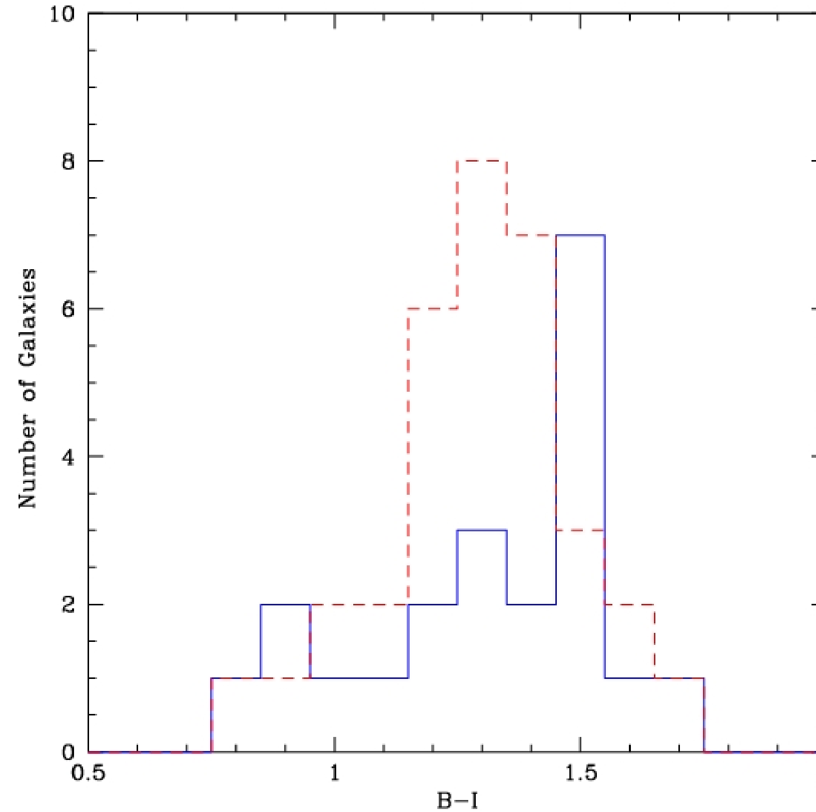

610 MHz at GMRT 514 sources flux>200 μJy

448 in common wih VLA

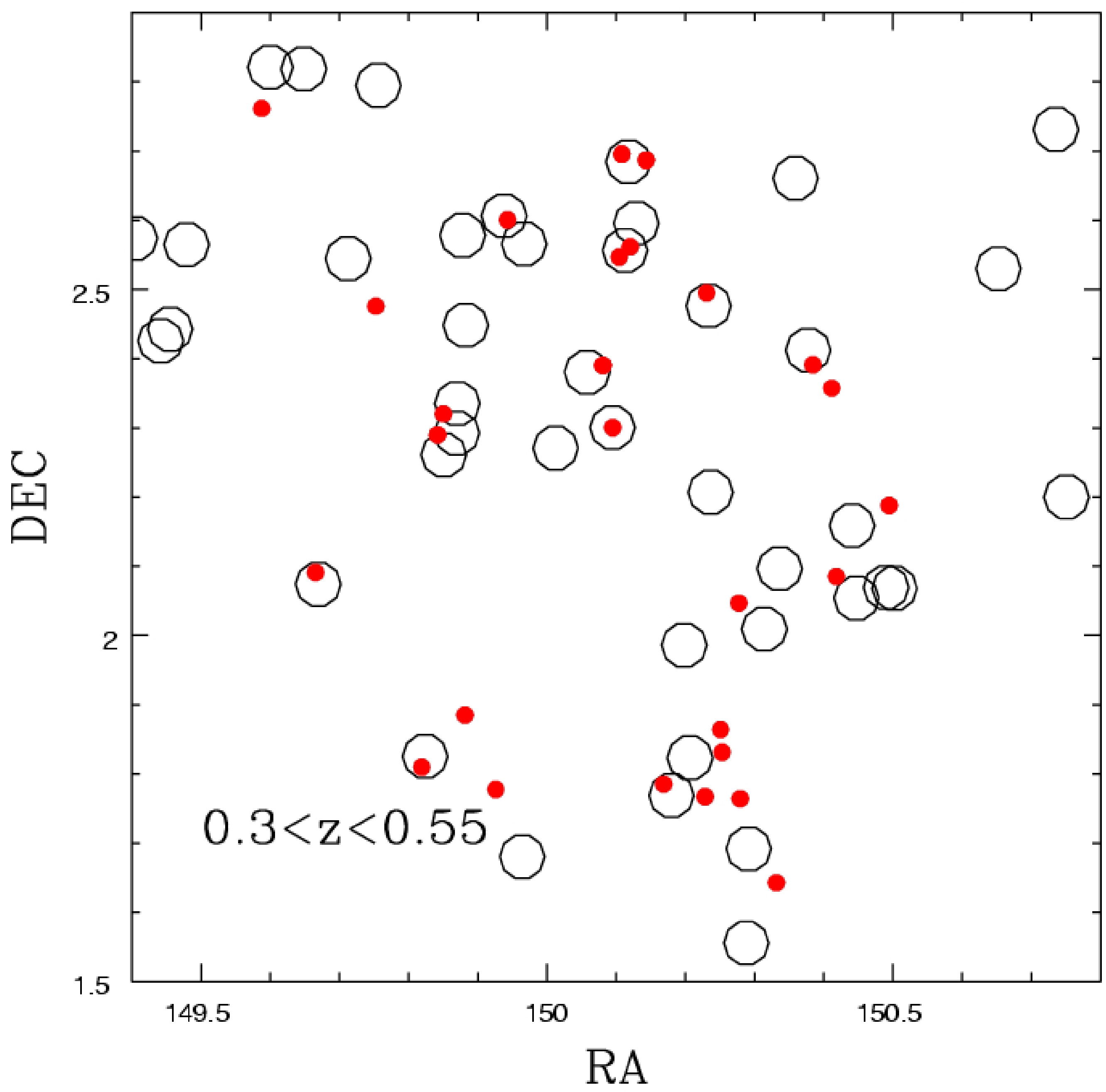
0.3<z<0.55
DEC
RA
2.5
2
1.5
149.5
150
150.5

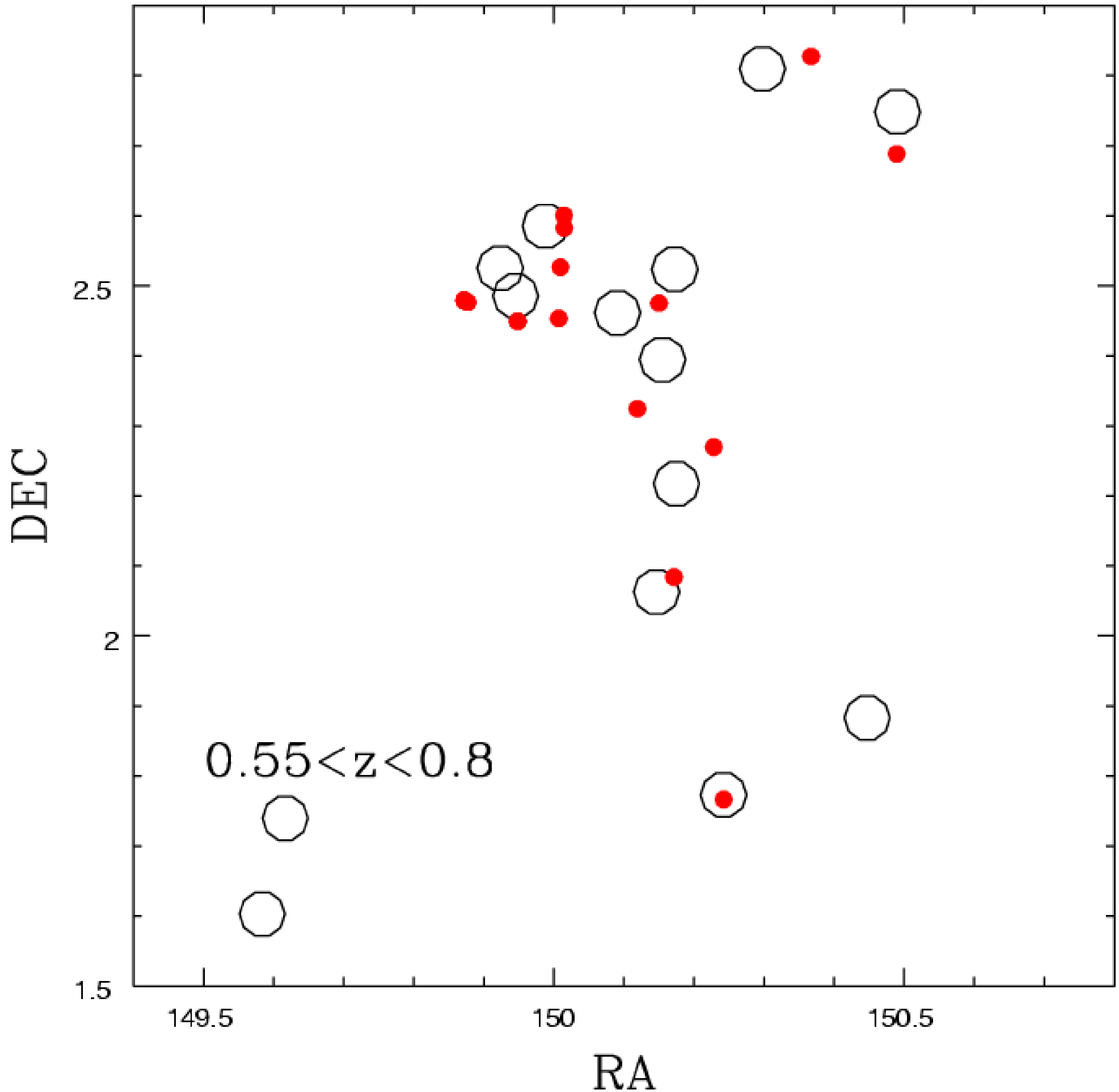

DEC
RA
2.5
2
1.5
149.5
150
150.5
0.55<z<0.8

Redshift Distribution

Red: Control Sample

Black: radio galaxies

All types

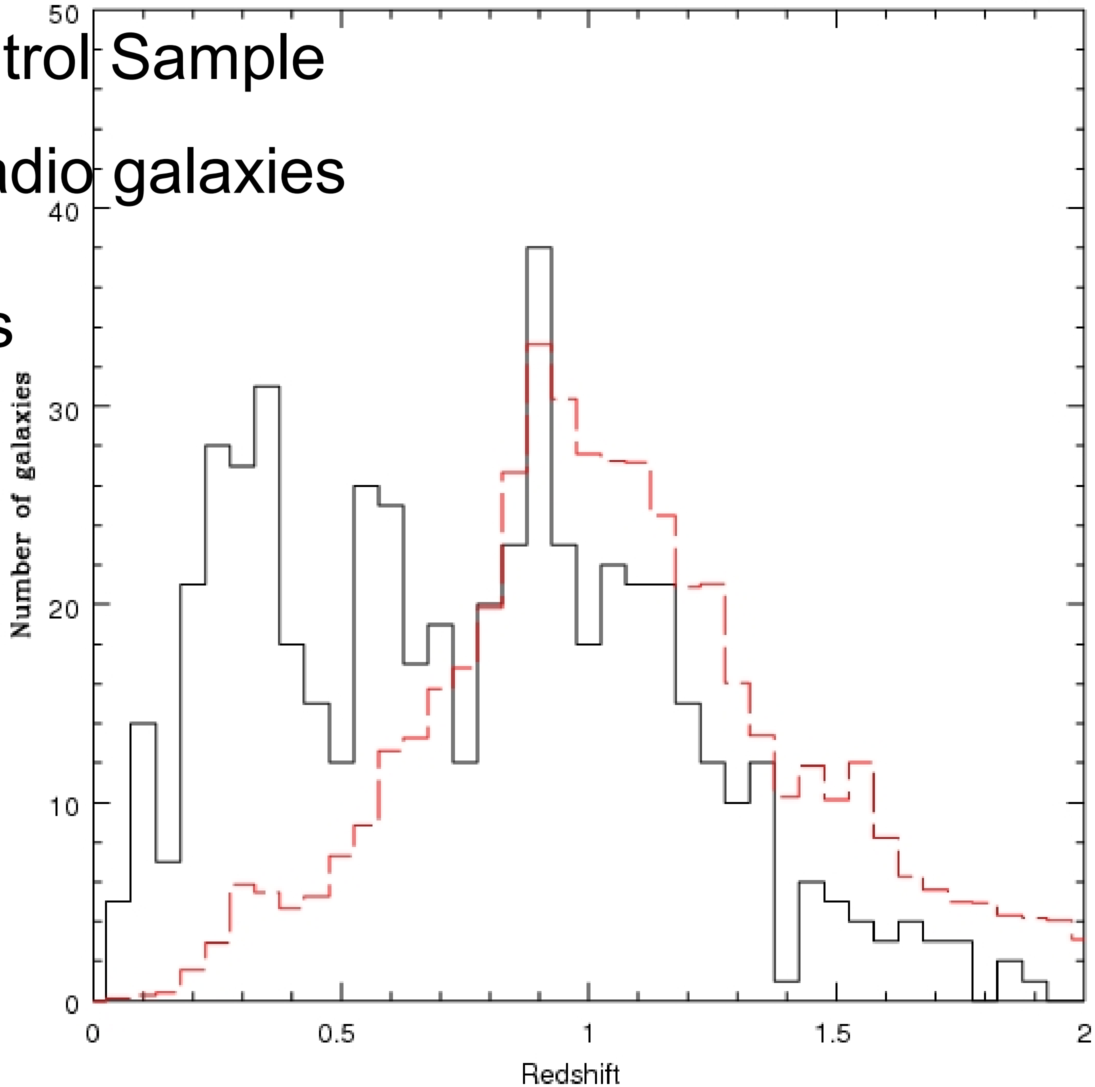

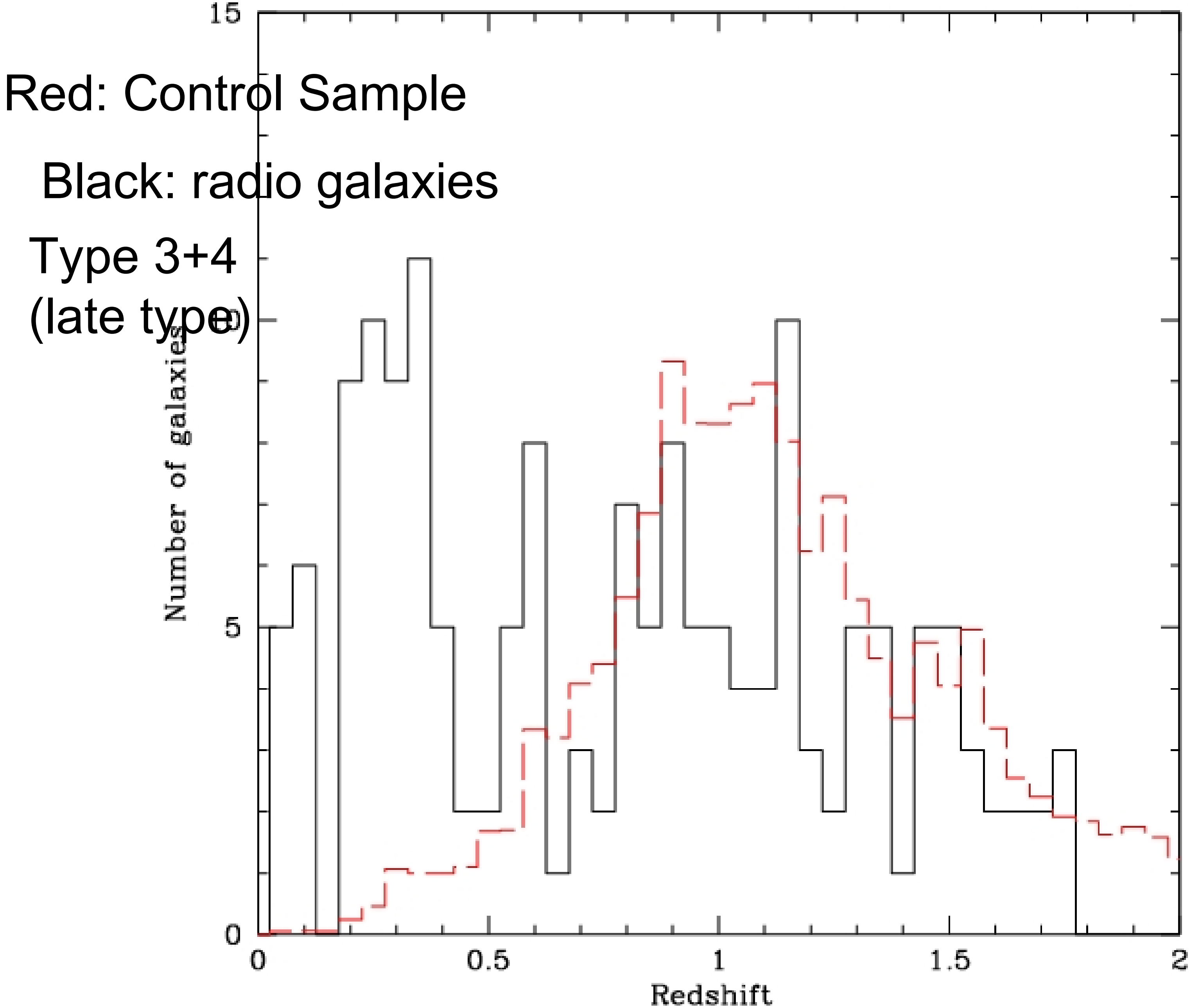
Red: Control Sample
Black: radio galaxies
Type 3+4
(late type)
Number of galaxies
Redshift
15
10
5
0
0
0.5
1
1.5
2

Star Formation “functions”

Red:Control Sample
Black: Complete Sample

Early type

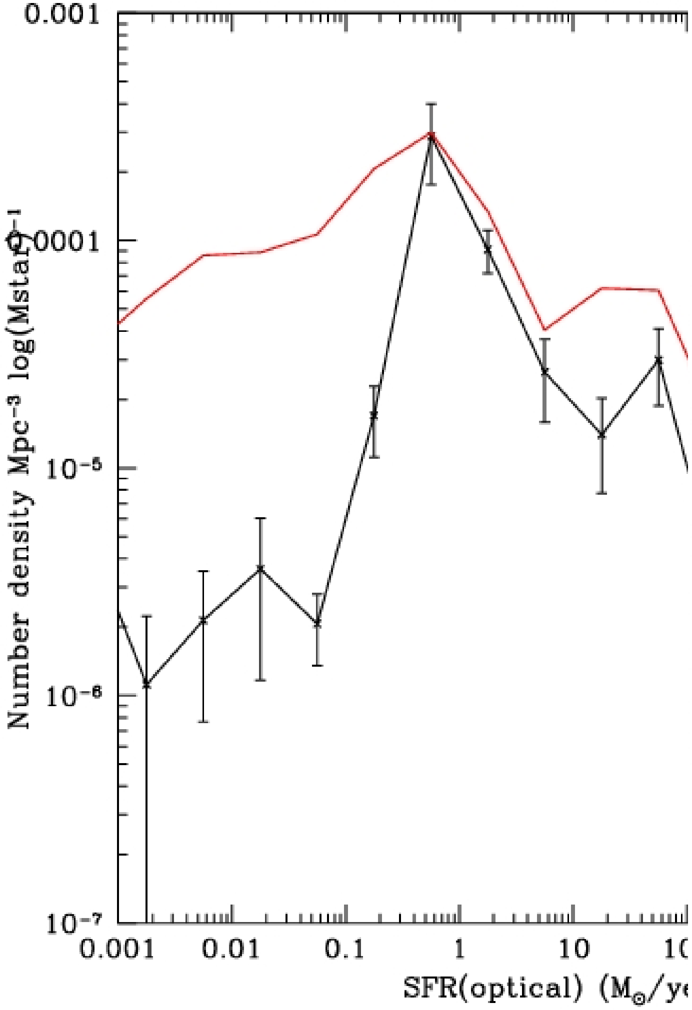

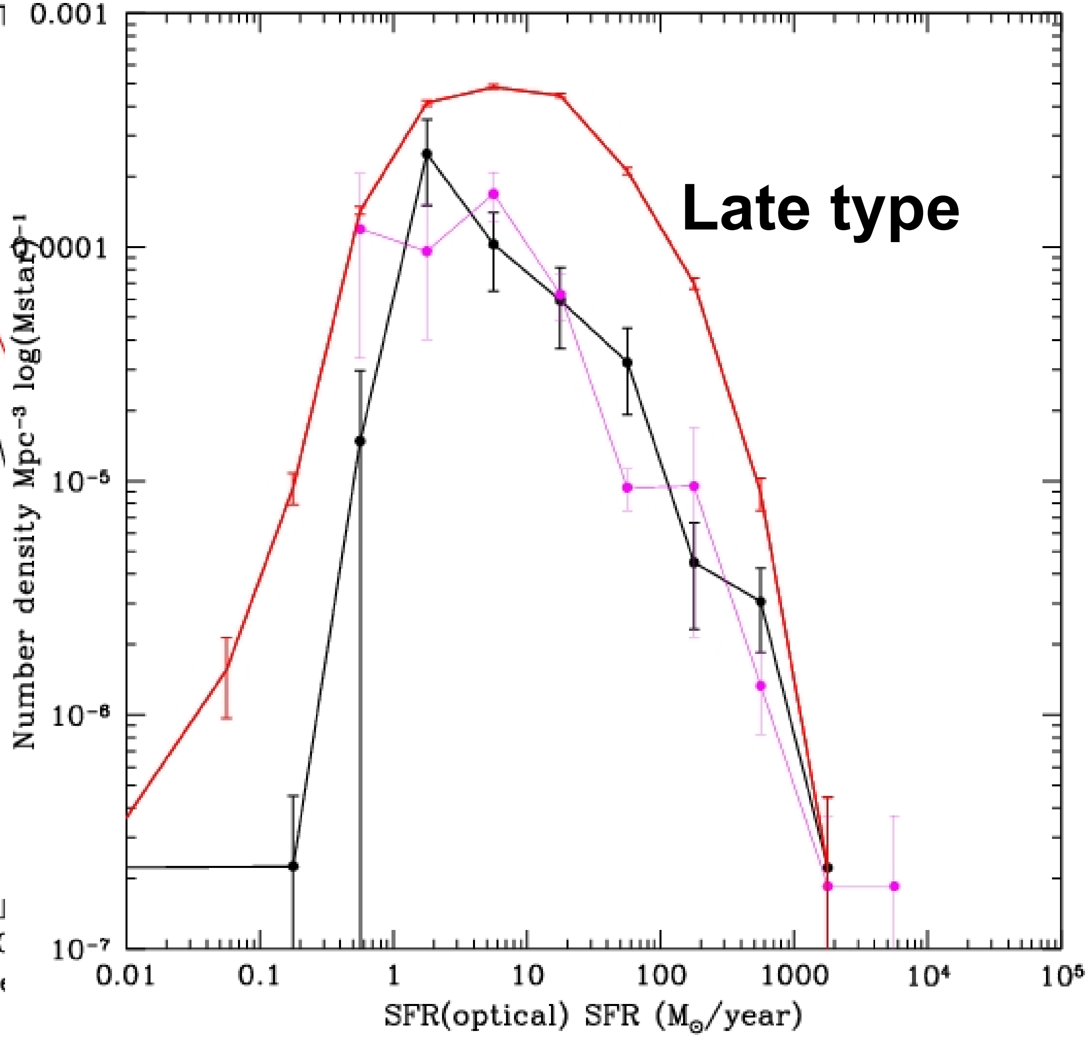

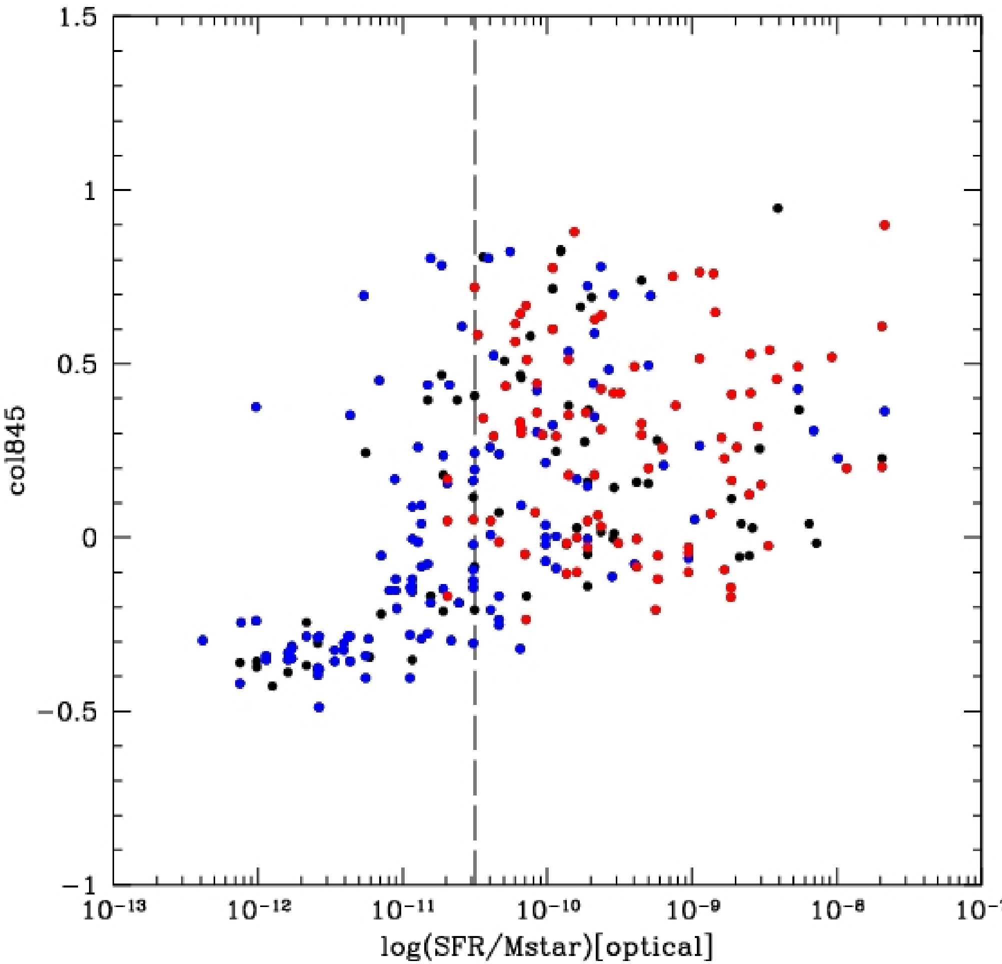

1.5
1
0.5
0
−0.5
−1
col845
10−13
10−12
10−11
10−10
10−9
10−8
10−7
log(SFR/Mstar)[optical]